<table>
<tr><td>1. Report No.
SPR-1759</td><td>2. Government Accession No.
N/A</td><td colspan="2">3. Recipient's Catalog No.
N/A</td></tr>
<tr><td colspan="2" rowspan="2">4. Title and Subtitle
Identify Mapping Techniques of Invasive Plant Species Within the MDOT Right-of-Way</td><td colspan="2">5. Report Date
10/06/2025</td></tr>
<tr><td colspan="2">6. Performing Organization Code
N/A</td></tr>
<tr><td colspan="2">7. Author(s)
Richard Dobson https://orcid.org/0000-0002-5699-154X, Colin Brooks PhD, https://orcid.org/0000-0003-4544-2569, Abby Jenkins, Sam Berger, Dorthea Vander Bilt, Chris Cook, and Rebecca Lowe</td><td colspan="2">8. Performing Organization Report No.
N/A</td></tr>
<tr><td colspan="2" rowspan="2">9. Performing Organization Name and Address
Michigan Technological University
1400 Townsend Drive
Houghton, Michigan 49931</td><td colspan="2">10. Work Unit No.
N/A</td></tr>
<tr><td colspan="2">11. Contract or Grant No.
Contract #2022-0432 Z2</td></tr>
<tr><td colspan="2" rowspan="2">12. Sponsoring Agency Name and Address
Michigan Department of Transportation (MDOT)
Research Administration
8885 Ricks Road
P.O. Box 33049
Lansing, Michigan 48909</td><td colspan="2">13. Type of Report and Period Covered
Final Report, 10/11/2023 – 9/30/2025</td></tr>
<tr><td colspan="2">14. Sponsoring Agency Code
N/A</td></tr>
<tr><td colspan="4">15. Supplementary Notes
Conducted in cooperation with the U.S. Department of Transportation, Federal Highway Administration. MDOT research reports are available at www.michigan.gov/mdotresearch.
N/A</td></tr>
<tr><td colspan="4">16. Abstract
Invasive species can be detrimental to our communities and environment as they can cause economic or environmental harm, including harm to human, animal, or plant health. These species thrive in transportation corridors which can be used to spread into new areas. This project focused on mapping four invasive plant species common reed (Phragmites australis), Japanese knotweed (Fallopia japonica), wild parsnip (Pastinaca sativa), and leafy spurge (Euphorbia esula). The selection of these species was made based on the researchers' previous experience with mapping invasive species and recommendations from MDOT. Mapping guidelines were developed for each species which includes, drone collection parameters, necessary data layers, classification methodologies, and accuracies of the mapping methods.</td></tr>
<tr><td colspan="2">17. Key Words
Drones, Invasive Plants, Mapping, Classification, Remote Sensing, Rights-of-Way</td><td colspan="2">18. Distribution Statement
No restrictions. This document is also available to the public through the Michigan Department of Transportation.</td></tr>
<tr><td>19. Security Classif. (of this report)
Unclassified</td><td>20. Security Classif. (of this page)
Unclassified</td><td>21. No. of Pages
135</td><td>22. Price
N/A</td></tr>
</table>

Form DOT F 1700.7 (8-72) Reproduction of completed page authorized www.mtri.org

Identifying Mapping Techniques of Invasive Plant Species Within Michigan Department of Transportation (MDOT) Right-of-Ways

Final Report, No. SPR-1759

Prepared by:

Richard J. Dobson, Colin Brooks, Abby Jenkins, Sam Berger, Dorthea Vander Bilt, Chris Cook, and Rebecca Lowe

Project Manager:
Carla Ahlschwede
Michigan Department of Transportation
6333 Lansing Road
Lansing, MI 48917

Research Manager:
André Clover, P.E.
Michigan Department of Transportation
8885 Ricks Road
Lansing, MI 48917

Table of Contents

1. Executive Summary

This report describes the accomplishments of the "Identify Mapping Techniques of Invasive Plant Species Within the MDOT Right-of-Way" research project, contract number 2022-0432. Invasive species can be detrimental to our communities and environment as they can cause economic or environmental harm, including harm to human, animal, or plant health. In addition, invasive species are notoriously difficult to manage due to their ability to rapidly spread and outcompete native species, particularly in disturbed areas. This displacement of native species is ultimately harmful to Michigan's flora and fauna, and all residents who depend upon and appreciate access to the state's natural resources. Invasive species thriving in transportation corridors are also detrimental to road safety and infrastructure and can be used in these corridors to spread. This project was focused on identifying effective mapping methods for MDOT to delineate and manage invasive plant species within Michigan's right-of-ways.

The project focused on the detection of four invasive plant species: common reed (*Phragmites australis),* Japanese knotweed (*Fallopia japonica*), wild parsnip (*Pastinaca sativa*), and leafy spurge (*Euphorbia esula*). The selection of these species was made based on the researchers' previous experience with mapping invasive species and recommendations from MDOT. These species are found across the state and represent a range of invasive species which pose a threat to natural ecosystems, livestock, and people. Throughout this project, the research team conducted data collections at more than 10 sites across the state including locations in both the Upper and Lower Peninsulas. Several sites were visited multiple times between 2024 and 2025 field seasons to track changes in plant phenology and understand the optimal times for identifying and mapping through remote sensing techniques.

A major component of this research was identifying which remote sensing and classification methods would be best for MDOT to implement. MDOT currently has a DJI Mavic 3M multispectral drone and access to ArcGIS Pro GIS software, so the researcher team focused on methodologies which utilized these assets. As each of the four focal invasive species have different phenological or physical characteristics that can be leveraged for identification, the research team assessed various combinations of remote sensing layers including RGB optical imagery, multispectral imagery, digital elevation model (DEM), and normalized difference vegetation index (NDVI) for their usefulness in classification. ArcGIS Pro offers a variety of classification methodologies which were also tested across the remote sensing combinations for each of the species. Methodologies identified from literature review and from research teams remote sensing expertise were assessed to determine classification recommendations for MDOT implementation.

2. Background

Invasive species can be very detrimental to our economic and ecological systems by destabilizing infrastructure and natural communities, impeding visibility and mobility, and exposing humans and animals to toxic compounds. By nature, these species are also notoriously difficult to manage due to their aggressive ability to rapidly spread and outcompete native species, particularly in disturbed or cleared areas such as along roadways. This displacement of native species is harmful to Michigan's flora and fauna, and all residents who depend upon or appreciate access to the state's natural resources. Michigan’s economy, which depends upon agriculture, logging, hunting, and tourism, necessitates well-maintained natural habitats, safe grazing and croplands, and reliable transportation corridors connecting them. Many problematic invasive plant species thrive in wide-open rights-of-way (ROWs) along transportation corridors maintained by the Michigan Department of Transportation (MDOT). Tall and rapidly growing invasive species change road conditions through limiting visibility and dense root systems can alter drainage patterns or clog waterways. Some species also produce compounds toxic to animals and humans that pose safety concerns and have economic implications if they spread into active fields. MDOT is required to perform control of invasive species if they pose safety concerns to the traveling public, cause operational or maintenance related difficulties, or are regulated by government entities.

A number of recent federal (1999’s Executive Order (E.O.) 13112: “Invasive Species”, 2016’s E.O. 13751: “Safeguarding the Nation From the Impacts of Invasive Species”) and state (e.g., Michigan's Natural Resources and Environmental Protection Act (NREPA)) environmental regulations have sought to create definitions and standards for the control of invasive plant species. For example, occurrence of the non-native genotype of tall reed *Phragmites australis* (common reed) and *Fallopia japonica* (Japanese knotweed) are recognized by NREPA as invasive in Michigan, with common reed listed as ‘restricted’ and Japanese knotweed as ‘prohibited’ due to their relative establishment and availability of known treatment methods for these species. While these designations alone do not necessitate plant removal, MDOT is required to perform control of these species if they pose a safety concern to the traveling public, cause operational or maintenance related difficulties, or are regulated for treatment by governmental entities.

MDOT manages more than 9,600 miles of road corridors and has surveyed thousands of miles of state and federal roads throughout Michigan for invasive plant species in the ROW environments. However, the threat of invasive species is constantly growing and changing with the introduction of new invasive species, as well as the spreading from existing invasive species populations. Early detection, tracking, and remediation to control these problematic invasive species is essential for the maintenance of these ROWs by MDOT.

Within Michigan’s ROW, four invasive plant species of focus were selected to reflect MDOT’s priorities, due to the scale and urgency of their current or potential impacts, as well as the species potential for being remotely sensed through characteristics such as texture, height, and color. These species were: common reed (*Phragmites australis*), Japanese knotweed (*Fallopia japonica*), wild parsnip (*Pastinaca sativa*), and leafy spurge (*Euphorbia esula*). Tall and rapidly growing species, such as Phragmites and Japanese knotweed, can quickly change or limit road, sign, or other infrastructure visibility within a right-of-way. Other species, such as wild parsnip and leafy spurge, are highly toxic and pose threats to humans and animals if allowed to spread. This project will focus on identifying these invasive species and provide guidance to MDOT on implementing mapping methodologies for internal monitoring and management.

2.1 Objectives

The objectives of this research project, as described in the project Statement of Work, were to:

1. Provide a review of current academic literature on mapping of invasive species—such as Japanese knotweed, leafy spurge, wild parsnip, and Phragmites.

2. Provide a brief summary of remote mapping alternatives for one or more species (such as remote sensing, drone photography, etc).
3. Demonstrate one or more mapping alternatives.
4. Demonstrate accuracy of mapping methods in objective 3 (including comparison of field observations with remote observations).
5. Provide recommendations on mapping methods based on 1) Accuracy of Method, 2) Availability of Technology/Ease of Access, and 3) Other factors deemed appropriate by the research team.

2.2 Tasks

Task 1: Identify One or More Species to Review and Map Remotely

The research team investigated the potential to remotely map the following invasive species which MDOT had expressed interest in: Phragmites, Japanese knotweed, wild parsnip, Kocia, leafy spurge, and/or sweet clover. Our team has the most experience with identifying Japanese knotweed and Phragmites, as demonstrated with our previous and ongoing research (Brooks et al., 2021 and Vander Bilt et al., 2023). Wild parsnip and leafy spurge both have toxic compounds when touched or ingested, leading to increased statewide concern. Therefore, these four species were anticipated to be the primary focus for demonstrating identification and mapping techniques in MDOT right-of-ways. The project team used input from MDOT, the scientific literature, and built upon our own experiences with satellite and drone-based mapping of invasive plants to aid in the identification of the selected species for mapping.

Task 2: Identify One or More Remote Techniques

Invasive species mapping can be achieved through several techniques. Remote sensing platforms include the use of drones which can capture imagery with a ground sample distance (GSD) of less than 0.5 in (1.3 cm), aerial imagery with a GSD of up to 6 in (15 cm), and satellites with a GSD of up to 12 in (31 cm). These platforms provide a range of opportunities to collect the remote sensing data required for balancing sensor, GSD, timeliness of collect, and amount of area required to be mapped. This task is aimed at identifying which remote sensing is most appropriate for MDOT to use for mapping the target species identified in Task 1.

Task 3: Brief Literature Review

A brief review of existing literature, research, extension materials, and other relevant sources was performed (Appendix A). The literature review documented current research in mapping techniques for the invasive species selected in Tasks 1 and 2. A description of different sensors, platforms, and resolutions that are likely to help MDOT meet its invasive plant mapping needs on a practical basis for regular use was included. The results of this review will help guide the research team on data collection and analysis of the selected invasive species in Tasks 5 and 6.

Task 4: Identify Physical Locations for Research

The research team was familiar with selecting study sites from known locations of these invasive plants through our previous mapping projects. Tools such as the Midwest Invasive Species Information Network (MISIN), the Early Detection and Distribution Mapping System (EDDMaps), and the plants section of the USGS Nonindigenous Aquatic Species (NAS) databases provided invasive species distribution and density data. The research team worked closely with MDOT on identifying priority locations such as already invaded sections of specific trunkline corridors that the agency may want to focus on, not all of which may be in existing databases.

The research team met with MDOT early in the project to identify the priority areas for the mapping efforts. This project included study sites located throughout southeastern Michigan, Traverse City, Indian River, Mackinaw City, Houghton, Menominee, and Rudyard. A variety of study sites were selected along Michigan trunkline roads in both rural and urban areas.

Task 5: Data Collection

Data collections were conducted in both 2024 and 2025 through drone data collections. For 2024, the research team was able to collect imagery of invasive species from May to October, enabling the capture of the optimal time periods to identify each of the species. For Southeastern Michigan, the following times were optimal. Leafy spurge is best identified in May and early June, wild parsnip is best identified in July and August, Phragmites is best identified late summer and fall, and Japanese knotweed is best identified in the fall.

For 2025, the research team began monthly field visits to the Hamburg / Pinckney M-36 corridor as it contained all four of our target species. The monthly visits allied the field team to track the development of the species through the growing season to aid in refining identification techniques and windows when these species could be mapped. The monthly visits were conducted from March through September during the first week of each month.

Task 6: Data Analysis

Task 6 focused on the developing classification methods which MDOT could implement. The research team has extensive experience with performing image classification for a variety of different sensors and applications but they may not all be appropriate for the target species or MDOT to implement. A focus of this task was to work with the remote sensing techniques and classification software available to MDOT staff. This would be RGB and multispectral imagery from the DJI Mavic 3M drone and classification tools available in ArcGIS Pro. Accuracies for each of the methods were summarized and the most appropriate methods were identified and documented by species.

3. Work Performed

3.1 Task 1: Identify One or More Species to Review and Map Remotely

The research team selected four target species for this project and they include: Phragmites, Japanese knotweed, wild parsnip, and leafy spurge. These were selected based on input from MDOT along with the team's previous experience with identifying species. Figure 1 shows all four of the species and the differences in color, structure, and other characteristics.

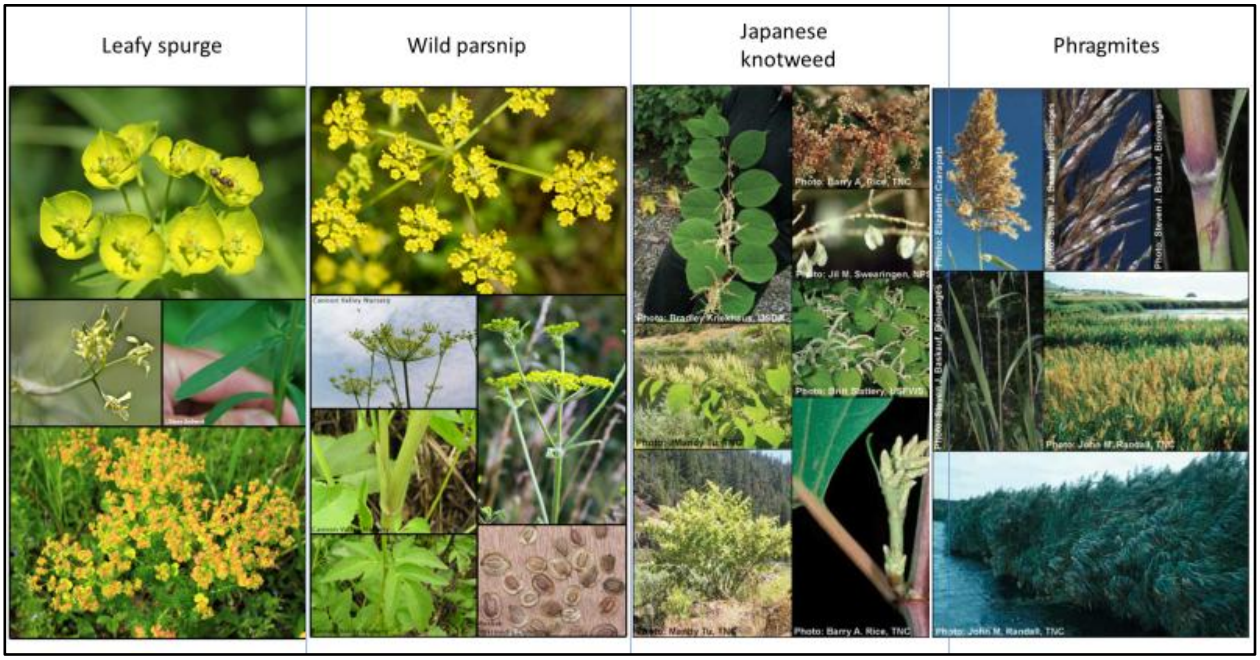

Figure 1: *All target species of the project.*

Phragmites was selected as the project team has extensive experience in mapping this species in previous projects, rapid growth, difficulty to remove, and impacts to transportation infrastructure. Previous work had focused on utilizing satellite and drone-based imagery for mapping Phragmites throughout the Great Lakes Basin. This included using early projects using PALSAR (Synthetic Aperture Radar - SAR) with a ground sample distance (GSD) of 10 m (32.8 ft) for creating maps with a minimum mapping unit of 0.2 ha. Later drones were used to combine RGB optical camera and Near Infrared (NIR) camera to create maps with a GSD of 5 cm (2 in). All of the previous projects relied on the distinctive height and bushy flower heads which create unique features for mapping.

Similarly, Japanese knotweed was selected based on the project team's previous experience with mapping this species, rapid growth, difficulty to remove, and impacts to transportation infrastructure. Previous work had focused on using PlanetScope imagery with a 3m (9.8 ft) GSD. A distinctive feature of Japanese knotweed is that in the fall the stems turn a bright red color and it maintains this color long after other vegetation has lost its leaves. This enables easily identifiable patches late in the season which can be mapped from high resolution satellite, aerial, or drone platforms.

Unlike Phragmites and Japanese knotweed, the project team did not have any previous mapping experience with wild parsnip or leafy spurge. These two species were selected as they are of great interest to MDOT as they are not only invasive but also create risks to livestock and people with their toxic sap. These species do have distinguishing features which allow for mapping through remote sensing techniques. Wild parsnip forms tall flower heads with yellow flowers in midsummer which turn bright orange in late summer. Leafy spurge form distinctive yellow-green bracts in the late spring that are easily identifiable from other plants and flowers blooming during that time period.

3.2 Task 2: Identify One or More Remote Techniques

Invasive plants can be identified with mapping techniques utilizing remote sensing data from satellite imagery, manned aircraft, and uncrewed aerial systems (UAS) or drones. The spectral resolution of the data, such as optical (red-green-blue) or multispectral imagery which includes additional infrared bands, can be leveraged to distinguish species from each other based on their spectral properties. Spatial resolution, determined by the actual size of one pixel in imagery, can be scaled to identify species based on their size or patch size, texture, pattern, or structure. We proposed to use primarily UAS platforms with RGB and multispectral sensors onboard to image species and use machine learning algorithms like Random Forests to conduct object- and pixel-based classifications of the sites identified.

To map the four invasive species in rights-of-way, UAS optical and multispectral imagery from the DJI Mavic 3 Enterprise Multispectral drone was used alongside supervised classification techniques. The multispectral bands are Green (560nm), Red (650nm), Red Edge (730nm), and Near IR (860nm). Drone images were processed into orthophotos, which were then interpreted by a team member with field information, then classified using ArcGIS Pro image classification tools and algorithms. These methods included testing object- and pixel-based classification techniques, stacking imagery layers to run through the classifier, and running different algorithms for the machine learning process.

3.3 Task 3: Brief Literature Review

An efficient and detailed literature review was performed to help inform the research team on the state of the art for mapping our target species. The research team reviewed 104 journal articles, papers, and publications covering the characteristics of the four target species, available remote sensing platforms and classification methods, and specifically, the remote sensing and classification methods previously used to detect each of our target species. This information helped guide the research team on which remote sensing data and algorithms would be the most effective to compare. The literature review was submitted on July 1st, 2024 along with all cited journal articles. The following is a brief summary of the material covered.

Brief Review of Remote Sensing Platforms

Satellites have been traditionally used for mapping starting with the first data collections from NASA's Landsat-1 in 1972. Many more Earth observation satellites carrying a variety of sensors and ranging in spatial, spectral, radiometric and temporal resolution have been launched since. Passive sensor satellites vary in their onboard sensors and data that they collect but can include the capture of optical (red-green-blue bands), thermal, multispectral (3-36 bands), and hyperspectral (36+ bands) imagery. Multispectral and hyperspectral imagery are useful for distinguishing vegetation types based on cellular level interactions with leaf chlorophyll and water content that can lead to distinct spectral signatures for plants. Additionally, active sensors such as radar, multi-frequency synthetic aperture radar (SAR) and light detection and ranging (LiDAR), emit pulses of energy at different wavelengths which can detect feature characteristics such as structure or moisture. Satellites allow for large area mapping with ground sample distances of up to 0.5 m (1.6 ft) or better with some new platforms. The proliferation of small satellite constellations also offers the opportunity for improved revisit times of daily or multiple times per day.

Drones have become increasingly used for mapping and research purposes since the early 2000's. Flying at lower altitudes and oftentimes with narrower fields of view, this results in higher resolution of imagery to be captured, or increased GSD on the resulting maps. For this reason, many studies have explored comparing UAS and satellite imagery for remote sensing of vegetation or using only drone imagery. Furthermore, the high resolution of UAS data is more desirable in some situations because imagery captured will have lower GSD and therefore produce higher accuracy classifications. The tradeoff with this improved GSD of other platforms is that drones are often reduced to mapping smaller areas when compared to manned aircraft or satellites. Drones can also be flexibly deployed as needed multiple times a year, if the drone platform and pilot are available. Some larger drones can also be deployed with a wide variety of interchangeable sensors including high resolution RGB cameras (> 36 megapixels), thermal, multispectral, and hyperspectral.

Brief Review of Classification Methods

While human image interpretation and mapping is possible for all four target species, it is oftentimes very time consuming. Computer based classification methods are able to classify large areas without requiring excessive human involvement. Typically, the models need to be set up with the appropriate data layers (i.e. multispectral image, DEM, NDVI layers) and parameters set for the classification. Additionally for supervised classification there is an additional step to create polygons of known locations of the target species for the model to train on. Unsupervised classification methods will automatically cluster like pixels and this step is not required.

The two main types of classifiers available are pixel based and object based. For pixel based classification, when classifying an image each individual pixel is assessed for its similarity to the pixels associated with the training dataset. These types of classifiers often produce maps that are more speckled in appearance as the individual pixels are classified. Object based classification by contrast parses imagery into semi-homogeneous "objects" using spatial and similarity-based segmentation algorithms prior to classification. There are both benefits and drawbacks to the use of OBIA relative to pixel-based classification. First, the integration of similar neighboring pixels into objects reduces the speckled appearance of a classification. More importantly these objects and their associated properties can provide additional spatial (e.g., position, adjacency and distance to other classes), textural (e.g., color and shadow, color mixtures), and contextual (e.g., shape, size, found within) information useful for classification purposes which are not available for pixel based classification. One drawback to object based classification is the requirement of a large amount of computer memory for the calculation of relationships between objects, which increases with the addition of more spectral bands and improved image resolution.

Brief Review of Methods Used for Each Target Species

An important section of the literature review was a review of the latest methods used for mapping each of the four target species. For each species the remote sensing method and classification methods were documented along with the accuracies achieved. This informed the research team on the most practical and accurate methods to test for implementation for MDOT. Some species like Phragmites have a large number of published articles on mapping methods whereas wild parsnip has very limited publications covering mapping techniques.

Common Reed (Phragmites australis) - Invasive Form (Genotype)

Phragmites is prevalent in many wetland ecosystems, but is often found in wet, low-lying areas like roadside ditches. This can mean that the species can be found in mixed ecosystems or in monoculture stands, depending on the landscape. Several studies showed the use of satellite imagery from Landsat, WorldView 2 and 3, and Sentinel-2 to map areas of Phragmites. Since Phragmites form large dense monocultures, satellite imagery is useful for mapping large patches. The eight-band WorldView imagery with object-based classification had the greatest overall accuracy when identifying the species, which was 93.2%, compared to 90.8% for the four-band object-based classification accuracy. The pixel-based classifications were considerably lower in accuracy. A multi-date multi-sensor mapping approach combining satellite based synthetic aperture radar (SAR) with the multispectral has been used for detection of Phragmites with a 94% overall accuracy and 84% user's accuracy for Phragmites using the Random Forest classification method in the software R (Bourgeau-Chavez et al., 2015).

UAS has also been used for mapping Phragmites, particularly in small areas or low density, using a combination of optical and near-infrared bands. Brooks et al., 2021 demonstrated a four class mapping approach in Trimble eCognition with RGB, NIR, DEM, Visible Atmospherically Resistant Index (VARI), and NDVI data layers. The high resolution optical classifications achieved 91.7% overall accuracy. This method was able to capture Phragmites stands of 0.1 ha (0.25 acres) where the satellite methods above could map Phragmites stands of 0.2 ha (0.5 acres) or larger.

Japanese Knotweed (Fallopia japonica)

Since its dispersal as an invasive species, researchers around the globe have been looking into ways to accurately map Japanese knotweed, including the application of remote sensing technology. Studies have frequently listed UAS-collected, or other aerial imagery with high spatial resolution as the most effective methods but some studies have also found success using satellite imagery.

A 2020 study used Sentinel-2, which has a GSD of 10 meters and a revisit time of every 5 days, for classification of Japanese knotweed (Smerdu et al., 2020). Multispectral imagery was used for Support Vector Machine (SVM) classification. This methodology concluded with the orthophoto classification resulting in an 83% accuracy (Smerdu et al., 2020).

Strictly UAV-based approaches to detecting knotweed, such as in Michez et al., 2016 set out to define an easily reproducible methodological framework for mapping three different species: Impatiens glandulifera, Heracleum mantegazzianum, and Japanese knotweed (Fallopia sachalinensis, Fallopia japonica and hybrids). This study used a Gatewing X100 UAS with two pre-calibrated Ricoh GR3 cameras (10 megapixel; focal length of 6 mm), researchers performed a total of seven flights, and utilized a 75% overlap on all imagery taken. The orthophotos were then processed in eCognition with the supervised classification processes based on the RF algorithm and were used to identify invasive plant species segments versus non-invasive plant species by applying 20% of the training sets to 80% of the evaluations sets to determine accuracy. Unfortunately, the accuracies that were achieved by this study were not high enough for operational application, being only 68%.

Leafy Spurge (Euphorbia esula)

The persistent invasive leafy spurge is often identified with multispectral or hyperspectral imagery, especially in spring when the bracts appear. One of the most cited studies for identification of leafy spurge was done in Theodore Roosevelt National Park in 1999. Ground-level and plant spectral data, 325-2500 nm with a GER2600 spectrometer, was collected along with differential GPS locations with a Trimble GPS Unit. Four flight lines, with four scenes, were gathered from the high-altitude Airborne Visible and Infrared Imaging Spectrometer (AVIRIS) (O'Neill, 2000). Spectral measurements were made from approximately one meter above the vegetation, producing a 0.40 m diameter GSD. The Principal Components Analysis (PCA) and Spectral Angle Mapper (SAM) algorithms were performed in ENVI and applied to the field spectra. AVIRIS image processing was conducted in ENVI, except for the calibration to reflectance. The calibration to reflectance was processed in a modified version of MODTRAN, calibration site field spectra, and Perl scripts (O'Neill, 2000).

Another study from 2005 supported the use of HyMap (126 bands between 0.45 μm and 2.5 μm with a pixel size of 3.5 m and bandwidths ranging from 15 μm in the visible and near infrared to 20 μm in the shortwave infrared) hyperspectral imagery that was classified with a Mixture Tuned Matched Filtering (MTMF) algorithm to detect small infestations in southeastern Idaho. The MNF transformed reflectance data was classified using the MTMF algorithm (Glenn, 2005). The accuracy of the hyperspectral sensors in detecting leafy spurge was 70% producer's accuracy and 84% user's accuracy, even for small infestations in a riparian or steppe environment. Methods were considered repeatable if the leafy spurge cover was over 40% per 3.5 pixel (Glenn, 2005).

Wild Parsnip (Pastinaca sativa)

Identifying wild parsnip has been challenging due to the small size and common yellow colored flower. Not many studies have focused on identification of wild parsnip with remote sensing, and of those that have had limited success with differentiating wild parsnip from other species. The study that had the most success was Liu et al., 2021 which used an object-based classification that provided an overall accuracy of 95.2% with a SVM classifier. Imagery was captured by a drone through an RGB camera. The study found that the workflow of masking out large vegetation and using the object-based SVM classifier with 0.02 m (7.9 in) GSD RGB imagery worked the best for classifying wild parsnip as long as other small, yellow colored flowers were not in the area of interest.

3.4 Task 4: Identify Field Locations

Field Site Selection

Field focus locations for collecting drone footage and related field data of the targeted invasive species were selected after reviewing invasive species distribution from data collected by the Michigan Department of Transportation (MDOT) and the Midwest Invasive Species Network (MISIN). MDOT staff member Todd Rowley, Transportation Maintenance Coordinator, shared a long-term MDOT dataset of invasive species along ROWs gathered using Field Maps and Natural Features Inventory. This MDOT "invasive weed" dataset (Shapefile / GIS layer) provided the locations (polylines) of known invasive species from the past ten years as well as the data collector, the date collected, the stand depth, and the most recent spray (herbicide) date.

The second dataset, the Midwest Invasive Species Network (MISIN), hosts invasive species observations from 2001 to 2024 including sampling parameters such as the observers named, observations verification,, the scientific and common names of the species observed, the identification date, the latitude and longitude, site specific comments, and a description of the object area size (few to acres), and object area density (sparse, patchy, dense, monoculture). The density values were helpful in selecting specific studies with high enough densities for the invasive species to be detected with remote sensing. Fall of 2024, the Keweenaw Invasive Species Management Area (KISMA) coordinator Sigrid Resh supplied us with additional invasive knotweed sites and treatment data they have been monitoring around the Keweenaw Peninsula for the past 7 years. This supplemental data allowed for the imaging of large knotweed stands that were senescing in the Houghton/Hancock area, which we are often traveling to the university for other work, this makes for a convenient location to study.

The MDOT and MISIN datasets were aggregated and invasive species data refined in ESRI ArcGIS Pro Version 3.3.2. The field data were filtered to the target invasive species (wild parsnip, leafy spurge, Japanese knotweed, and Phragmites) and reduced to only observations within a 500 ft. buffer distance along all MDOT roads (Interstate highways, U.S. Highways, and M-numbered state highways) to represent invasive species found in the ROW (Figure 2). The target species distribution within the simulated ROW was then used to identify clusters that could be potential focal field locations throughout the state (Figure 3).

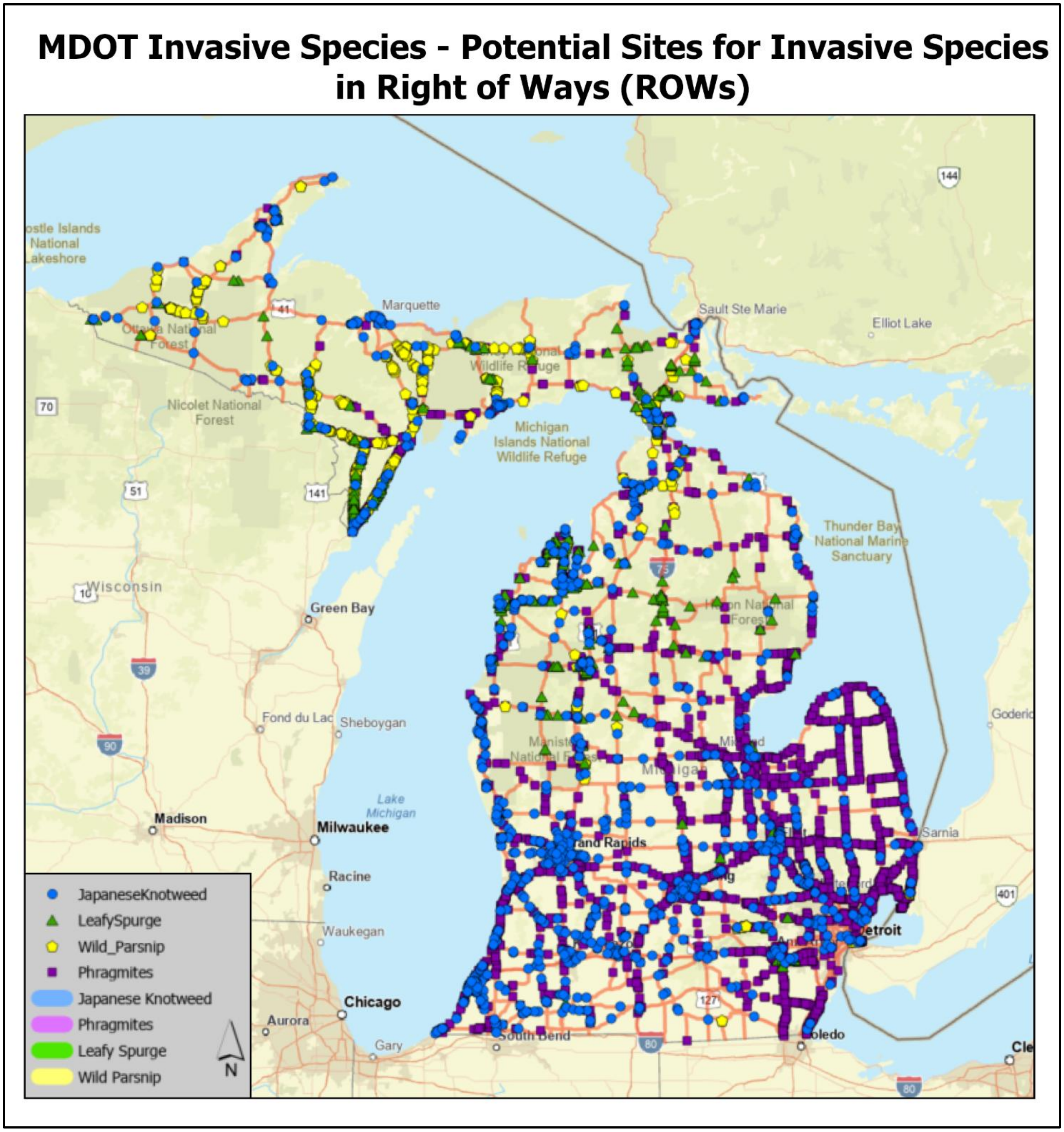

Figure 2: *Target species in MDOT ROWs (500' buffer) for the State of Michigan (MDOT and MISIN data).*

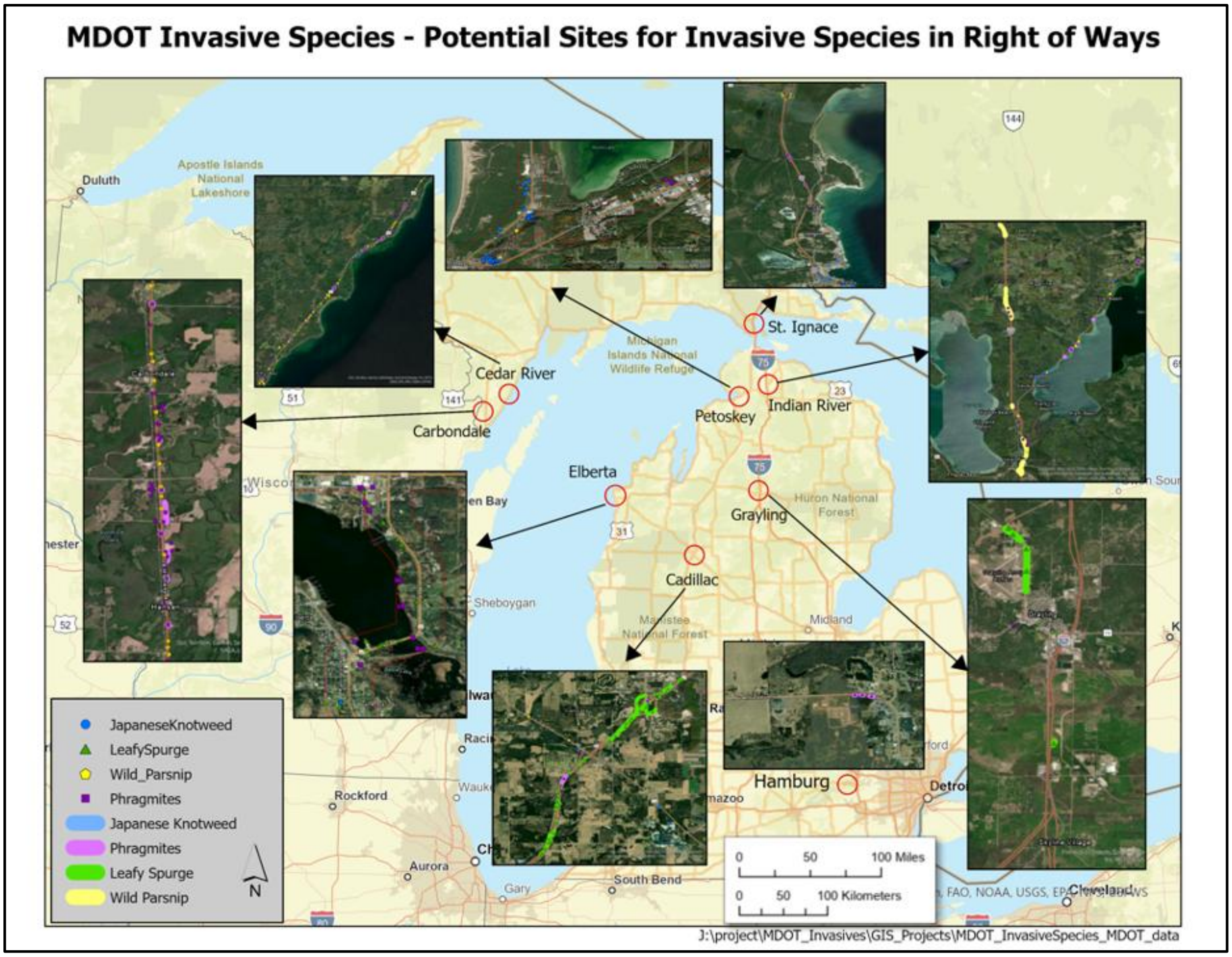

Figure 3: *Potential sites for the target species in MDOT ROWs based on the MDOT and MISIN data close to state roads; site selection was further winnowed down from the collective data.*

These areas were reviewed with MDOT staff and several supplemental focal locations were recommended, such as I-75 near Grayling for wild parsnip and Rudyard in the Upper Peninsula for leafy spurge. Six final focal field locations were selected based on the following criteria: the ability to find all four species in the area allowing for efficient data collection and maximizing imagery utility, a high number of GIS species records which would increase the likelihood of the species present and ability to build robust training data, the density of the targeted species to increase the likelihood of species detection and differentiability of different patch sizes, and their proximity to state roads which would allow for access and assessment of ROW invasions. These chosen focal areas for UAS work with counties were (Figure 4):

1. M36 Pinckney/Hamburg (Livingston and Washtenaw)
2. Cadillac (Wexford, Missaukee, Osceola, Mecosta)
3. Traverse City (Leelanau, Benzie, Grand Traverse)
4. Northern Lower Peninsula, Indian River, and Grayling (Emmet, Cheboygan, Otsego, Crawford)
5. Eastern Upper Peninsula (Mackinac and Chippewa)
6. Southwestern Upper Peninsula (Menominee, Dickenson)

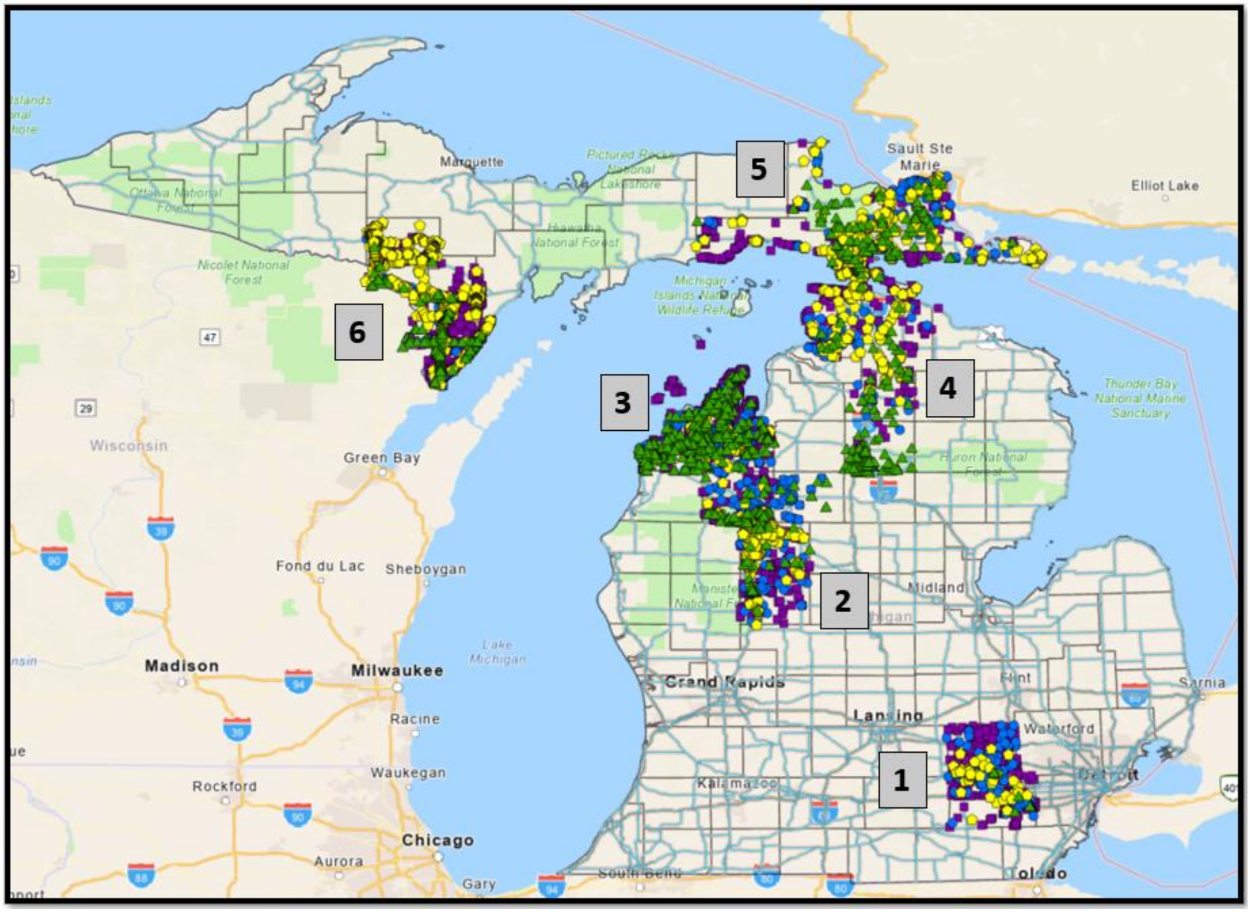

Figure 4: *Zones (by counties) picked for focusing invasive species drone work in the right of ways on MDOT roads using MDOT and MISIN data.*

These larger focal regions were then further narrowed down to very specific locations in those regions based upon more in-depth information, specifically, the date of observation, who observed the species, how close to the road, and the patch density. Each of the zones were visited during the 2024 field season at least once. The timing of the visits was scheduled in an attempt to capture the target species at their peak identifiable window for sensing. This would be times where they are flowering or are otherwise distinctive from the surrounding vegetation. Two additional sites were also visited towards the end of the 2024 field season with recommendations from Todd Rowley at MDOT (Rudyard with leafy Spurge and Hamburg with Japanese knotweed) and Sigrid Resh at KISMA (Houghton with Japanese knotweed).

For the 2025 field season the team focused on capturing leafy spurge in Zone 5 (Rudyard) and Wild Parsnip in Zone 4 (Indian River) while they were at their peak identifiable window. The research team also focused on capturing all four species monthly as they developed through the season. Zone 1 - Hamburg / Pinckney was selected for this as it is close to the office, contains all four species, and the species are all adjacent to the road.

Zone 1: M-36 Pinckney/Hamburg

<u>Species in Zone 1</u> - Leafy spurge, wild parsnip, Phragmites, and Japanese knotweed (Figure 5).

<u>Selection Rationale</u> - The focused area in Zone 1 between Pickney and Hamburg along M-36 was chosen because the location provided easy access for field study during a day trip from the MTRI office in Ann Arbor, MI, and would be a good test site for establishing field methods. Not all target species were well represented in southeastern Michigan, but the Pickney corridor provided all four species within twenty miles and were found within the ROW's (Figure 6).

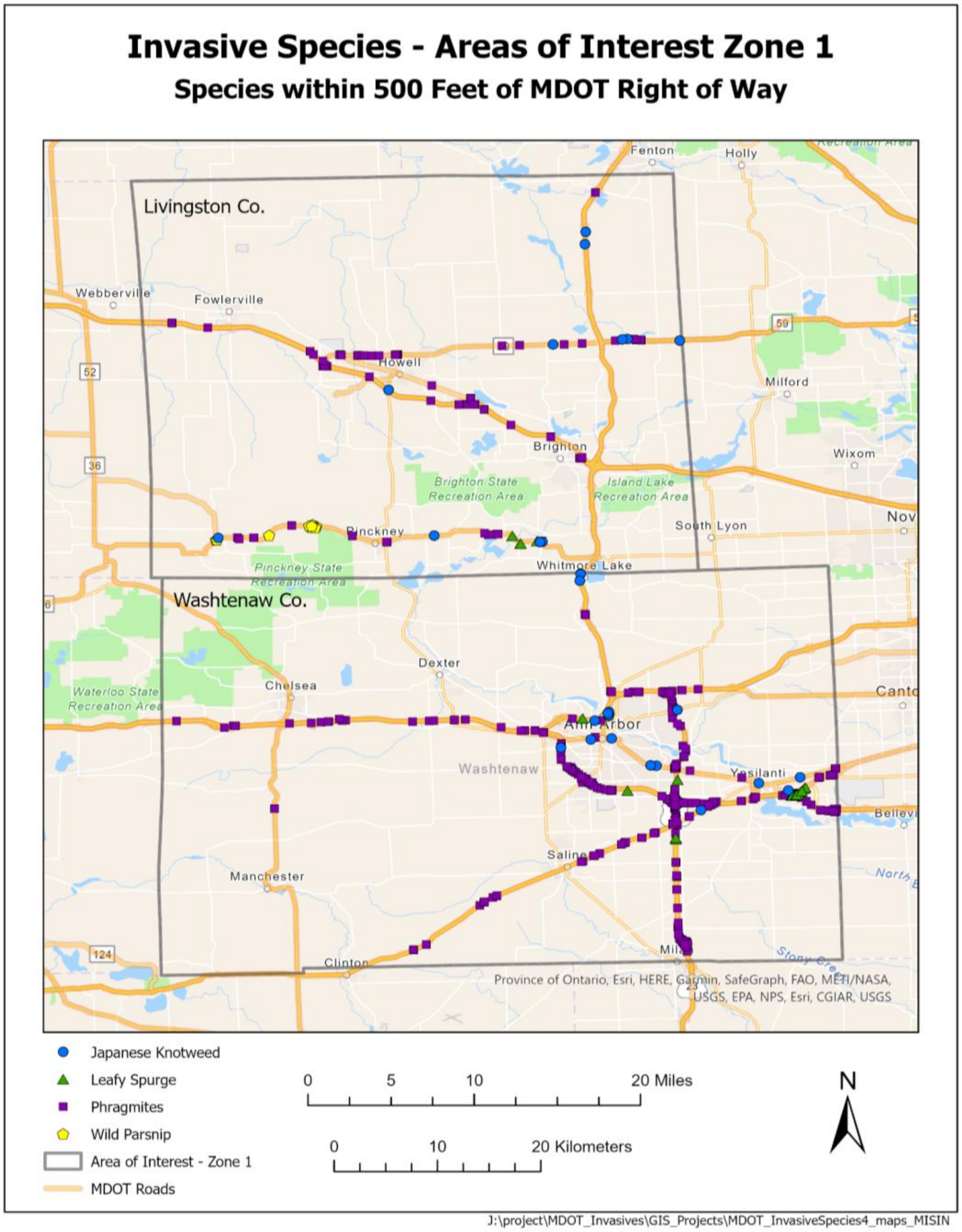

Figure 5: *Zone 1 - Pinckney/Hamburg area in Livingston and Washtenaw Counties - picked for invasive species drone work in the right of ways on MDOT roads (MISIN data).*

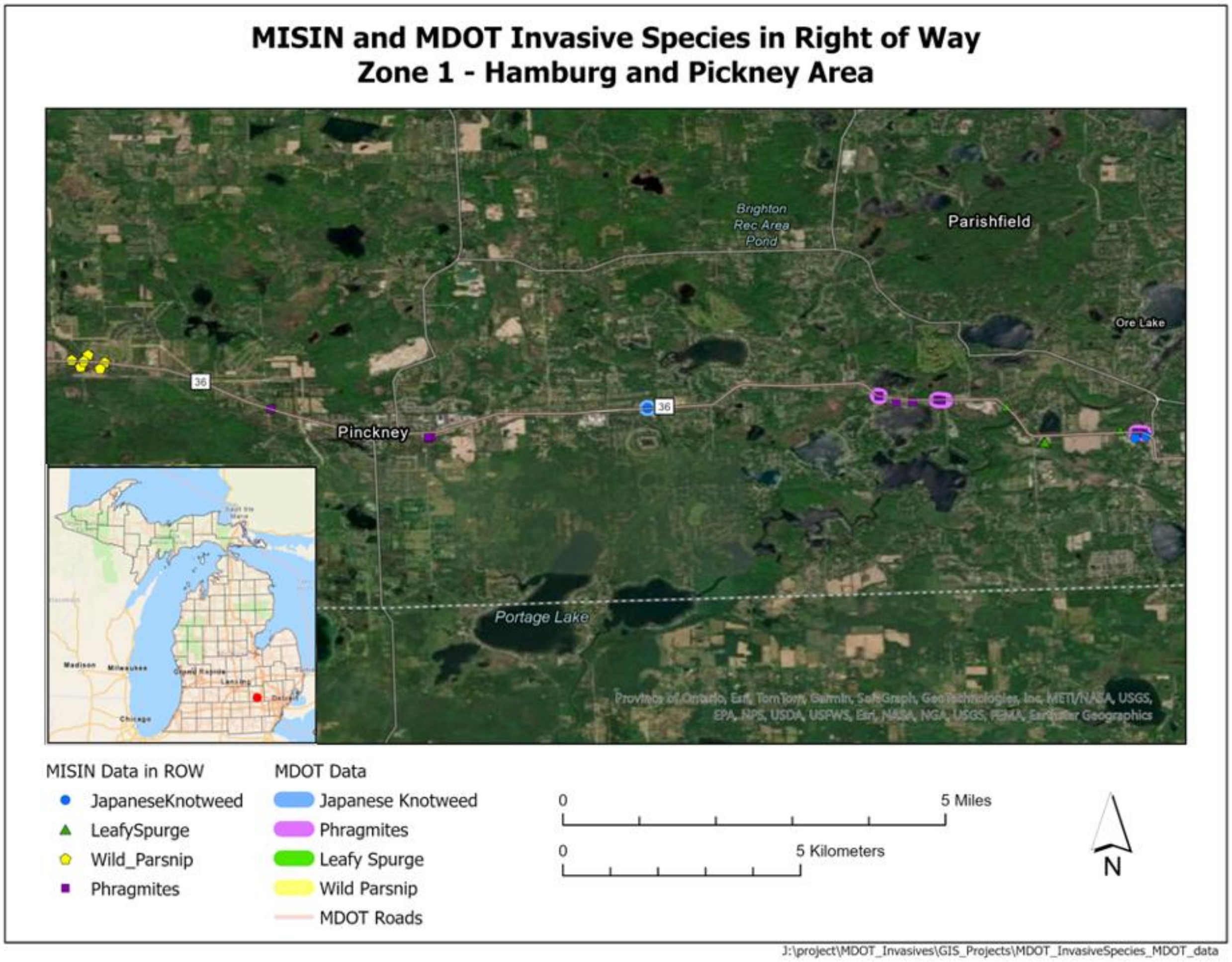

Figure 6: *Focused area of Zone 1 with leafy spurge, wild parsnip, Phragmites, and Japanese knotweed located along M-36 (MDOT and MISIN data).*

Zone 2: Cadillac

<u>Species in Zone 2</u> - Leafy spurge, wild parsnip, Phragmites, and Japanese knotweed (Figure 7).

<u>Selection Rationale</u> - The focused area in Zone 2 near Cadillac, at the junction of M115 and M131 (Figure 8), was originally chosen because every species was represented; however, many of the locations were not found within the 500' roadway buffer. Wild parsnip was the best species represented here and we had other choice locations/zones with being in the northern zones later in the field season when wild parsnip is easier to locate. This proved true with the I-75 sites near Indian River and near M-28 in the Upper Peninsula.

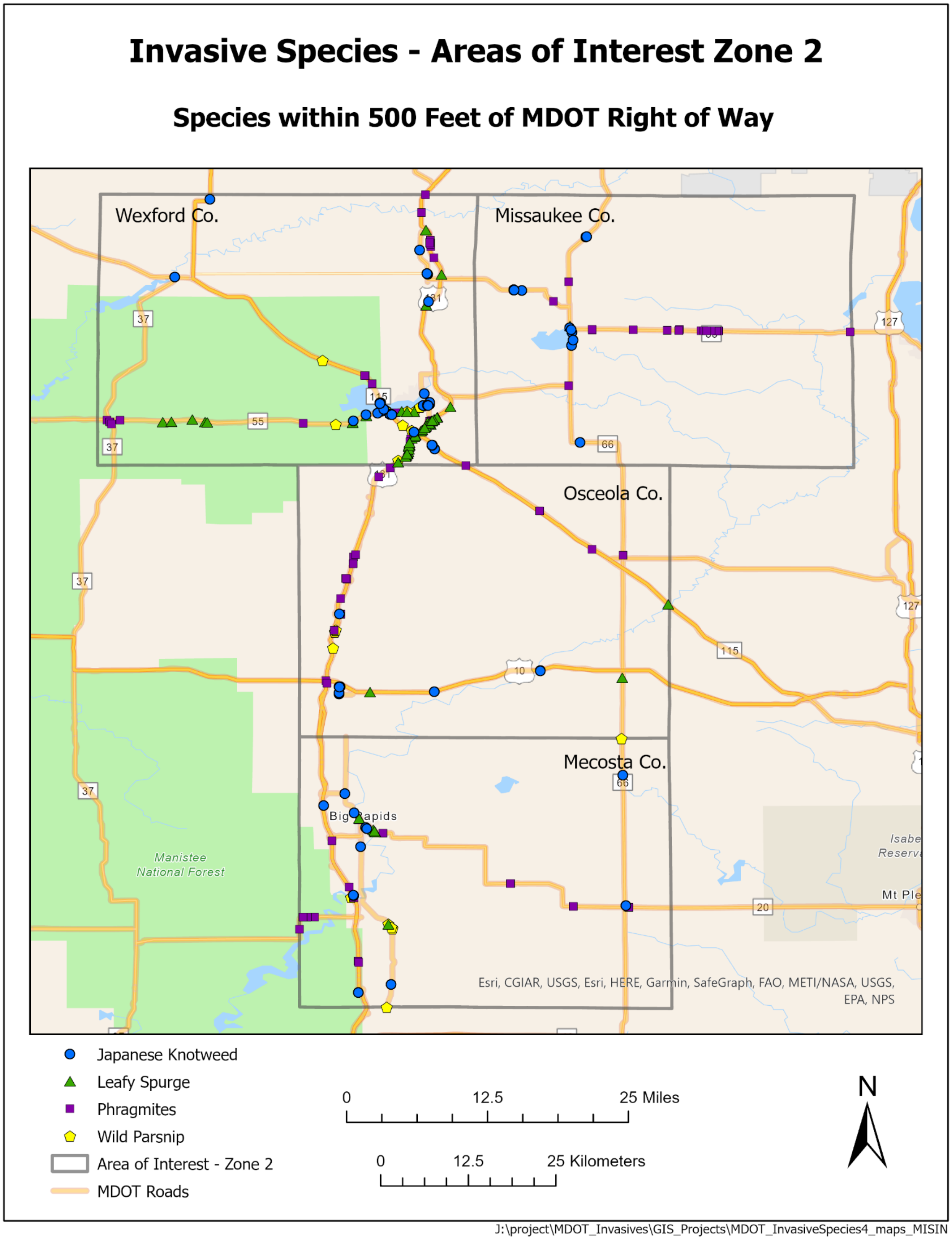

Figure 7: *Zone 2 - Wexford, Missaukee, Osceola, and Mecosta Counties - picked for invasive species drone work in the right of ways on MDOT roads (MISIN data).*

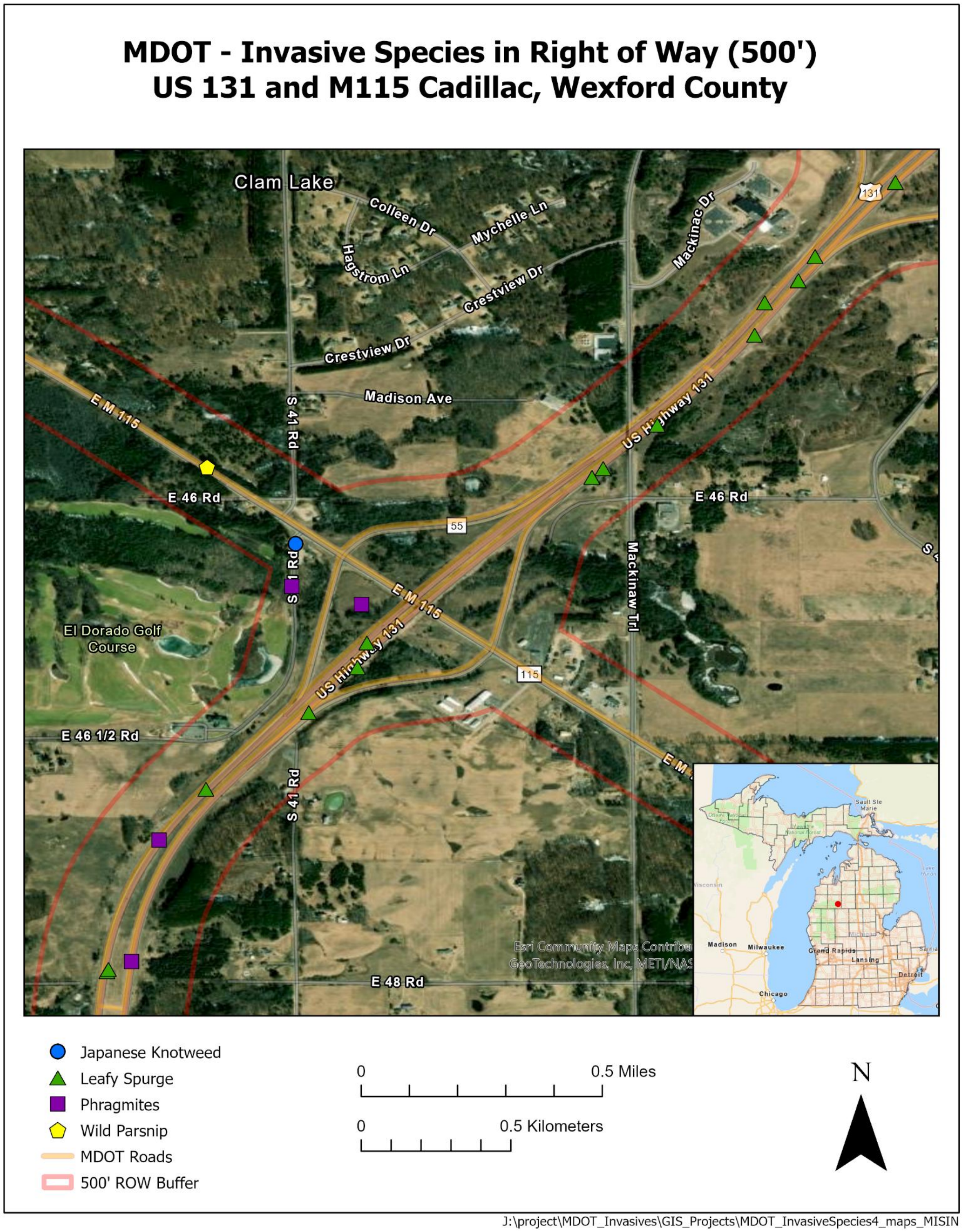

Figure 8: *Focused area of Zone 2 with leafy spurge, wild parsnip, Phragmites, and Japanese knotweed located along M-131 and M-115 (MISIN data).*

Zone 3: Traverse City

Species in Zone 3 - Leafy spurge, wild parsnip, Phragmites, and Japanese knotweed (Figure 9).

Selection Rationale - The focused area in Zone 3 near Elberta (Figure 10) and Suttons Bay along M022 was originally chosen because every species was represented. Of the two areas chosen, Suttons Bay had Japanese knotweed in denser patches based upon MISIN's invasive species reports (Figure 11).

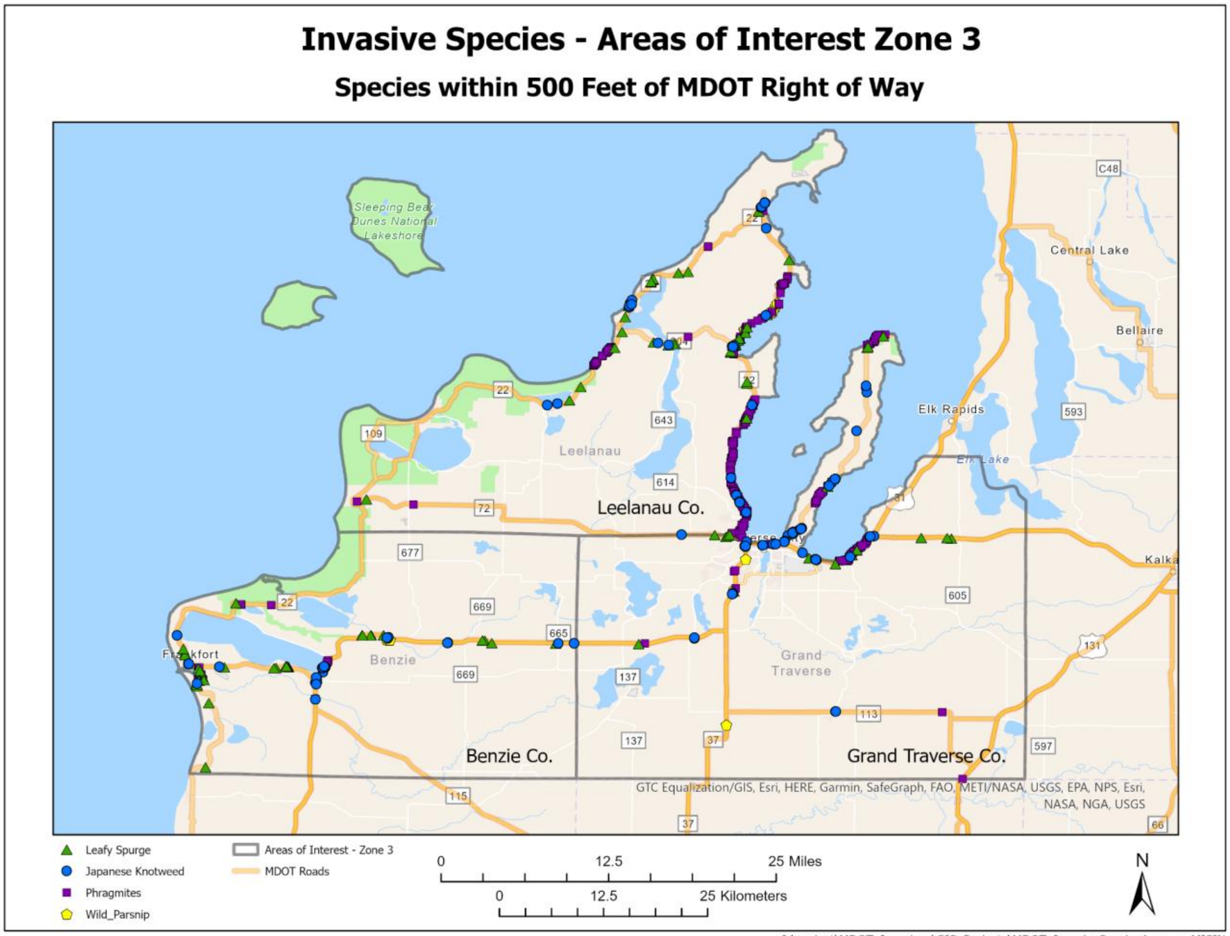

J:\project\MDOT_Invasives\GIS_Projects\MDOT_InvasiveSpecies4_maps_MISIN

Figure 9: *Zone 3 - Leelanau, Benzie, and Grand Traverse Counties - picked for invasive species drone work in the right of ways on MDOT roads (MISIN data).*

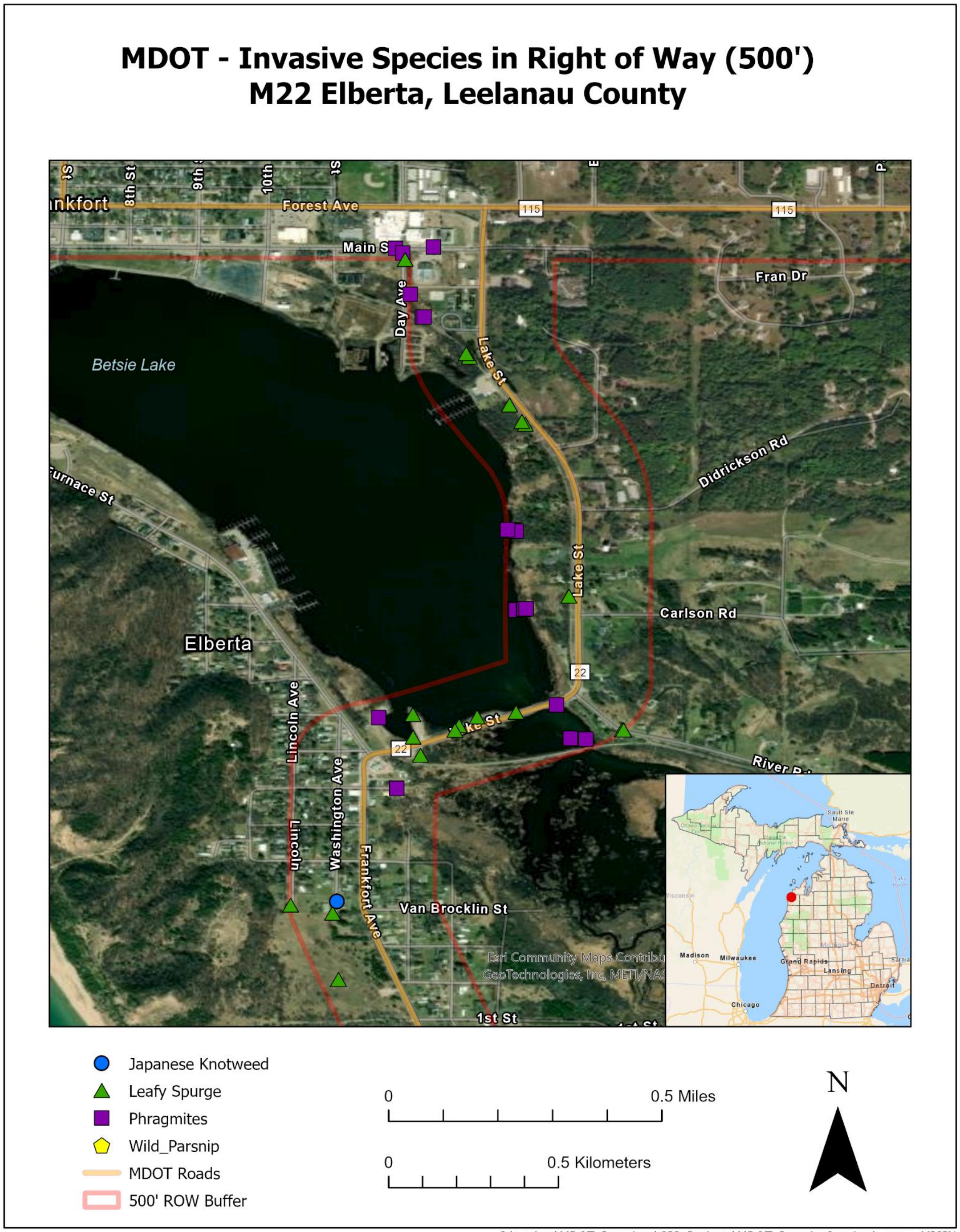

J:\project\MDOT_Invasives\GIS_Projects\MDOT_InvasiveSpecies4_maps_MISIN

Figure 10: *Focused area of Zone 3 with leafy spurge, wild parsnip, Phragmites, and Japanese knotweed located along M22 near Elberta (MISIN data).*

Figure 11: *Focused area of Zone 3 with leafy spurge, wild parsnip, Phragmites, and Japanese knotweed located along M22 near Suttons Bay (MISIN data).*

Zone 4: Northern L.P. (Indian River and Grayling)

Species in Zone 4 - leafy spurge, wild parsnip, Phragmites, and Japanese knotweed (Figure 12).

Selection Rationale - The two focus areas in Zone 4 were Petosky for Japanese knotweed (Figure 13) and wild parsnip near Topinabee (Figure 14). Later in the summer and moving into fall, both Japanese knotweed and wild parsnip are easiest to find due to the deepening red of the branches of the knotweed and the white flowers at the ends of the stems reaching up and the height of wild parsnip and yellow/green flowers that cluster to look like multiple umbrellas off of the stems. Just south of Indian River, abundant with wild parsnip was found along I-75 and was easily imaged with the drone in early fall when the plant was fully bloomed with large leaves (Figure 15). The area south of Mackinaw City was too far off the right of way and not considered needed with the multiple sites north and south of Mackinaw City (Figure 16).

Figure 12: *Zone 4 - Emmet, Cheboygan, Otsego, and Crawford Counties - picked for invasive species drone work in the right of ways on MDOT roads (MISIN data).*

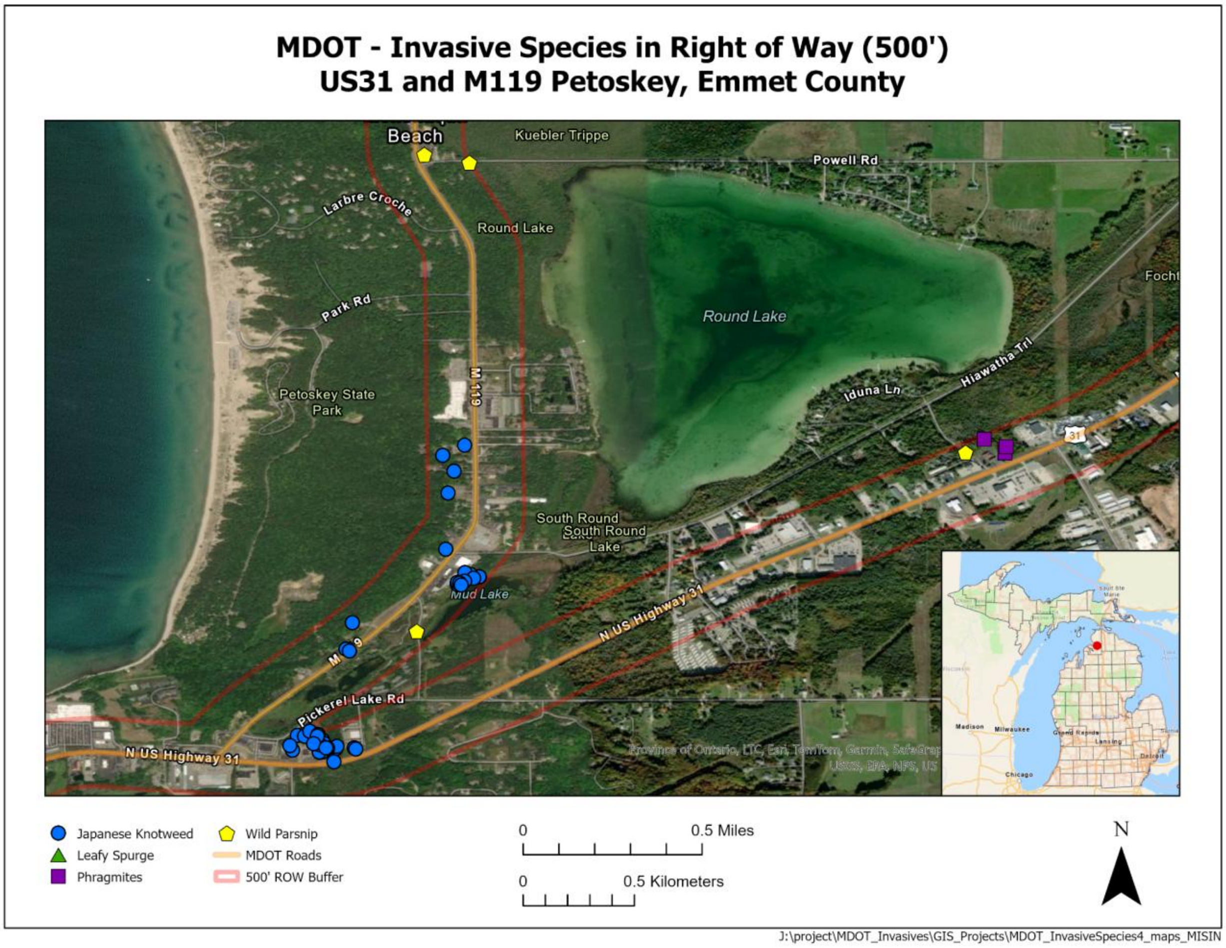

Figure 13: *Focused area of Zone 4 with leafy spurge, wild parsnip, Phragmites, and Japanese knotweed located along US31 and M119 near Petoskey (MISIN data).*

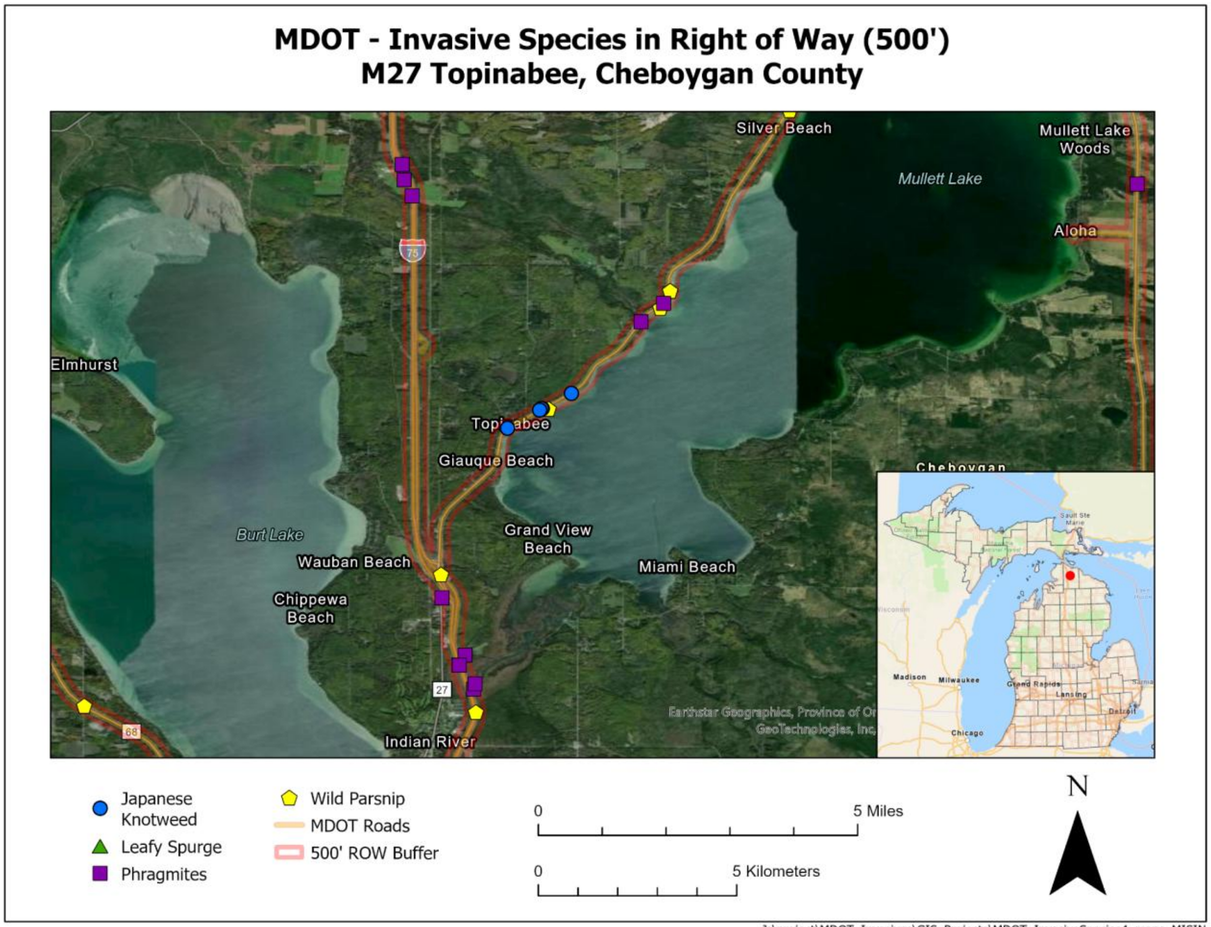

J:\project\MDOT_Invasives\GIS_Projects\MDOT_InvasiveSpecies4_maps_MISIN

Figure 14*: Focused area of Zone 4 with leafy spurge, wild parsnip, Phragmites, and Japanese knotweed located along M27 near Topinabee (MISIN data).*

Figure 15: *Focused area of Zone 4 with leafy spurge, wild parsnip, Phragmites, and Japanese knotweed located along I-75 near Grayling (MISIN data).*

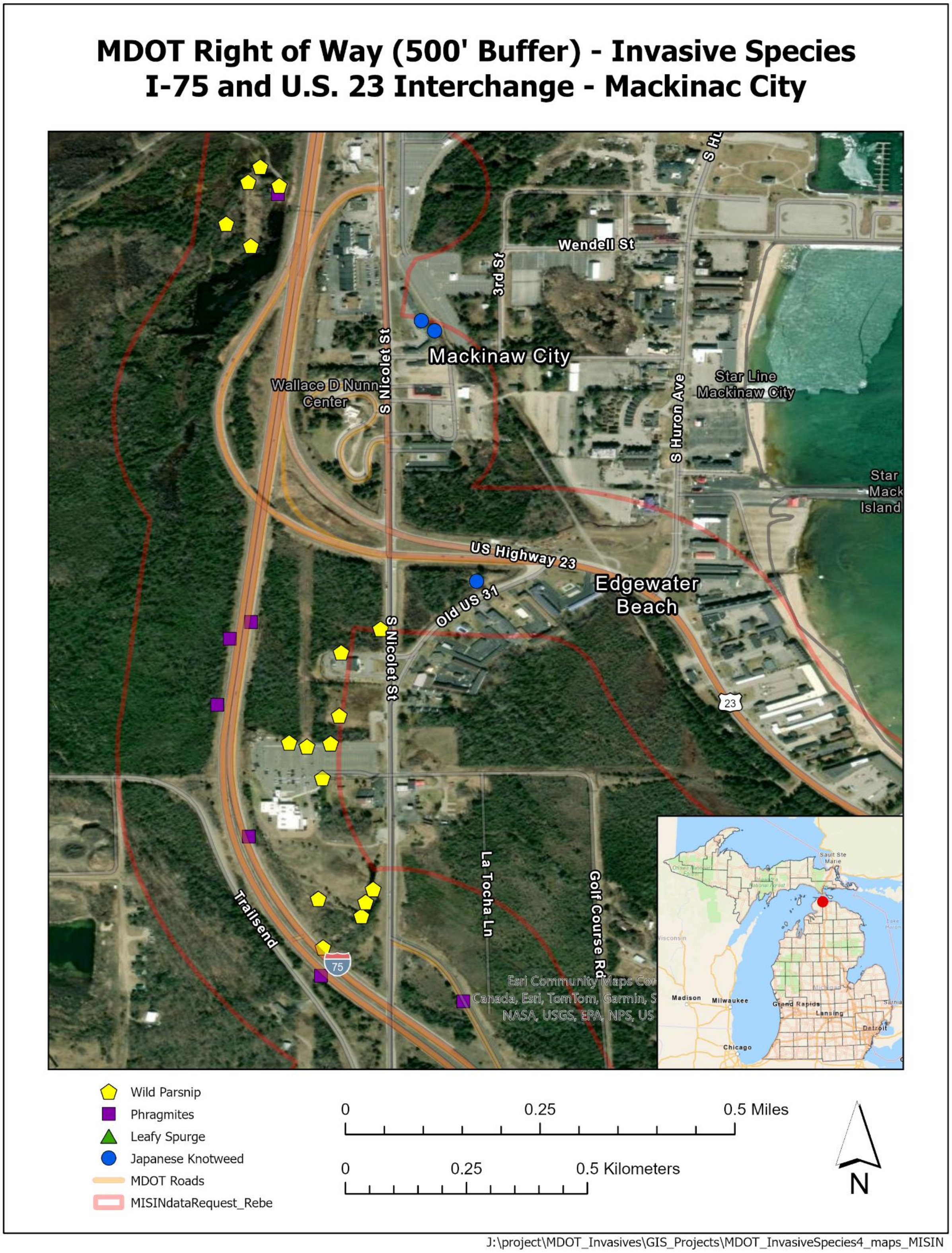

Figure 16: *Focused area of Zone 4 with leafy spurge, wild parsnip, Phragmites, and Japanese knotweed located along I-75 and US23 near Mackinaw City (MISIN data).*

Zone 5: Eastern Upper Peninsula

Species in Zone 5 - leafy spurge, wild parsnip, Phragmites, and Japanese knotweed (Figure 17).

Selection Rationale - The two focus areas in Zone 5 were St. Ignace for all of the targeted species (Figure 18) and Sault Ste Marie for Japanese knotweed as that was later in the field season (Figure 19).

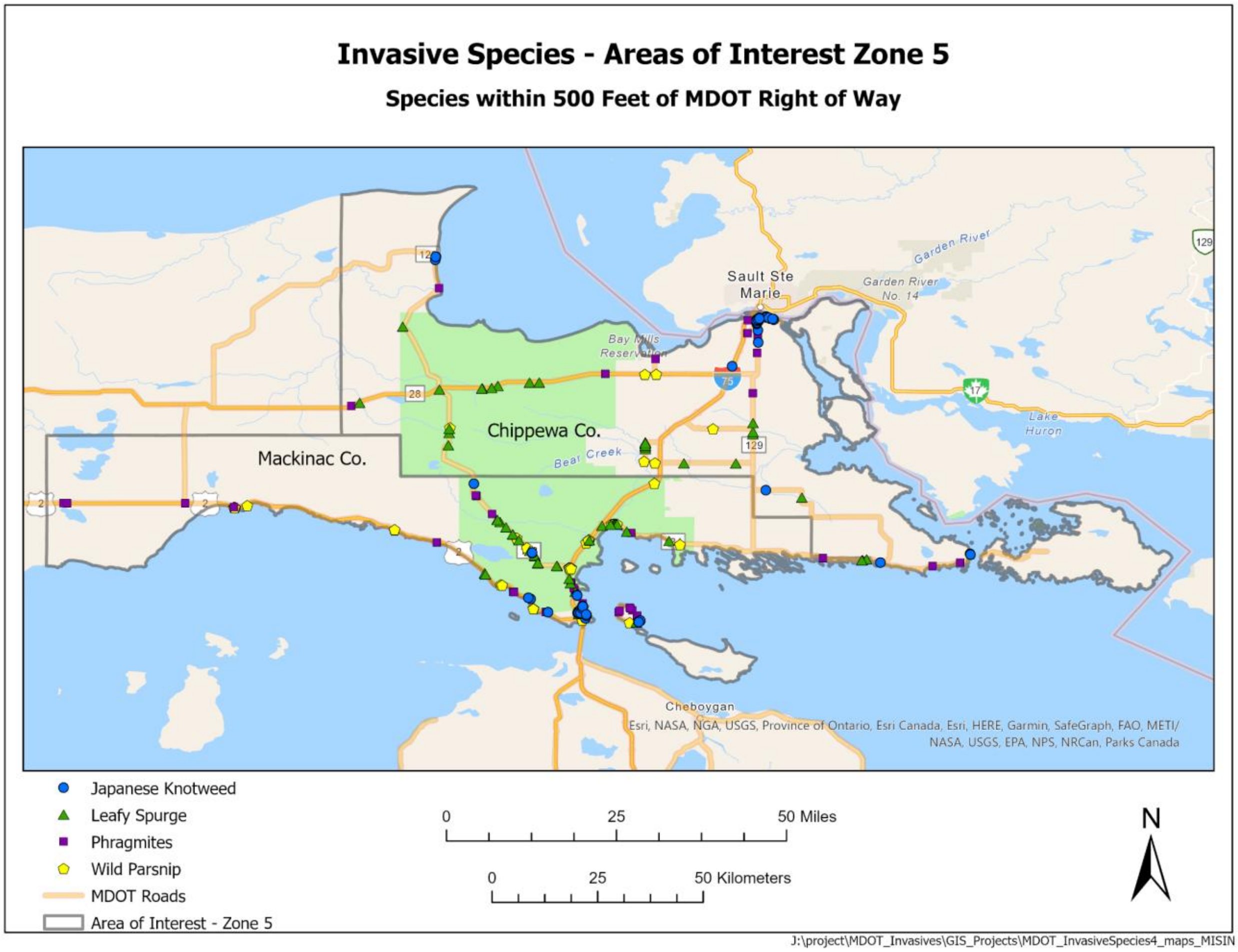

Figure 17: *Zone 5 - Mackinac and Chippewa Counties - picked for invasive species drone work in the right of ways on MDOT roads (MISIN data).*

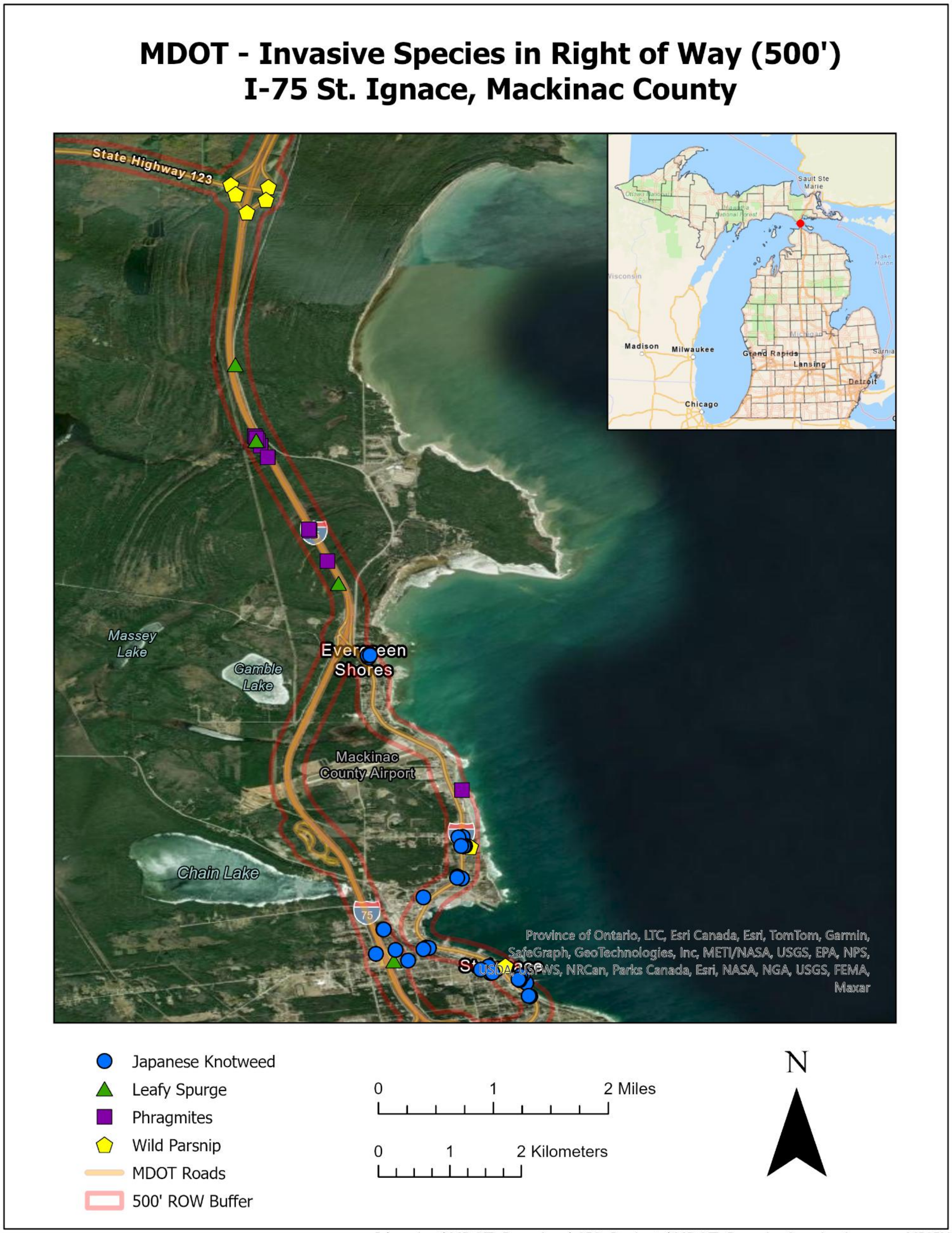

J:\project\MDOT_Invasives\GIS_Projects\MDOT_InvasiveSpecies4_maps_MISIN

Figure 18: *Focused area of Zone 5 with leafy spurge, wild parsnip, Phragmites, and Japanese knotweed located along I-75 near St. Ignace (MISIN data).*

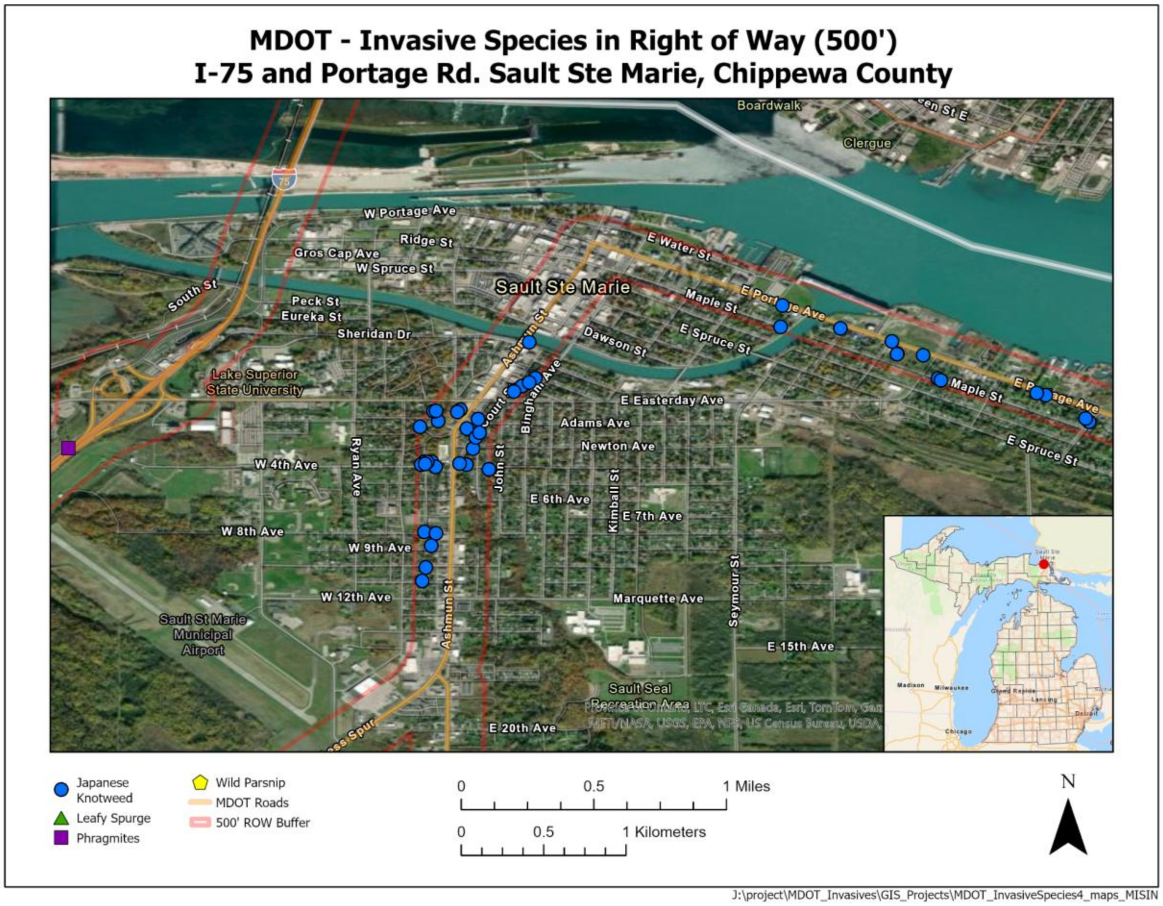

Figure 19: *Focused area of Zone 5 with leafy spurge, wild parsnip, Phragmites, and Japanese knotweed located along I-75 and Portage Rd. in Sault Ste. Marie (MISIN data).*

Zone 6: Southwestern U.P. (Menominee County and Dickinson County)

<u>Species in Zone 6</u> - leafy spurge, wild parsnip, Phragmites, and Japanese knotweed (Figure 20).

<u>Selection Rationale</u> - The two focus areas in Zone 6 were Arthur Bay (Figure 21) and Carbondale (Figure 22) that all of the targeted species were present and easily accessible.

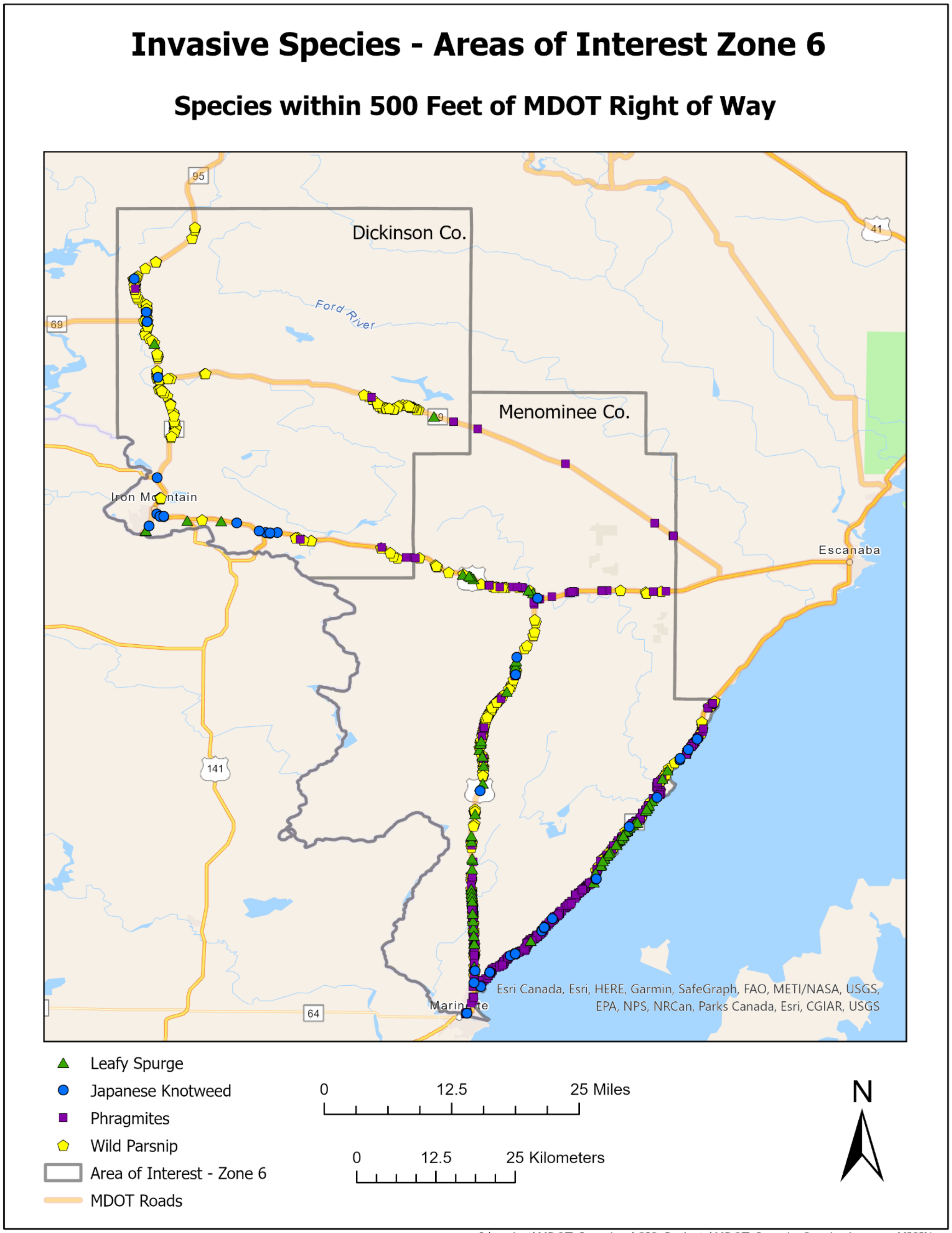

J:\project\MDOT_Invasives\GIS_Projects\MDOT_InvasiveSpecies4_maps_MISIN

Figure 20: *Zone 6 - Eastern U.P. - Dickinson and Menominee Counties - picked for invasive species drone work in the right of ways on MDOT roads (MISIN data).*

Figure 21: *Focused area of Zone 6 with leafy spurge, wild parsnip, Phragmites, and Japanese knotweed located along M35 near Cedar River (MISIN data).*

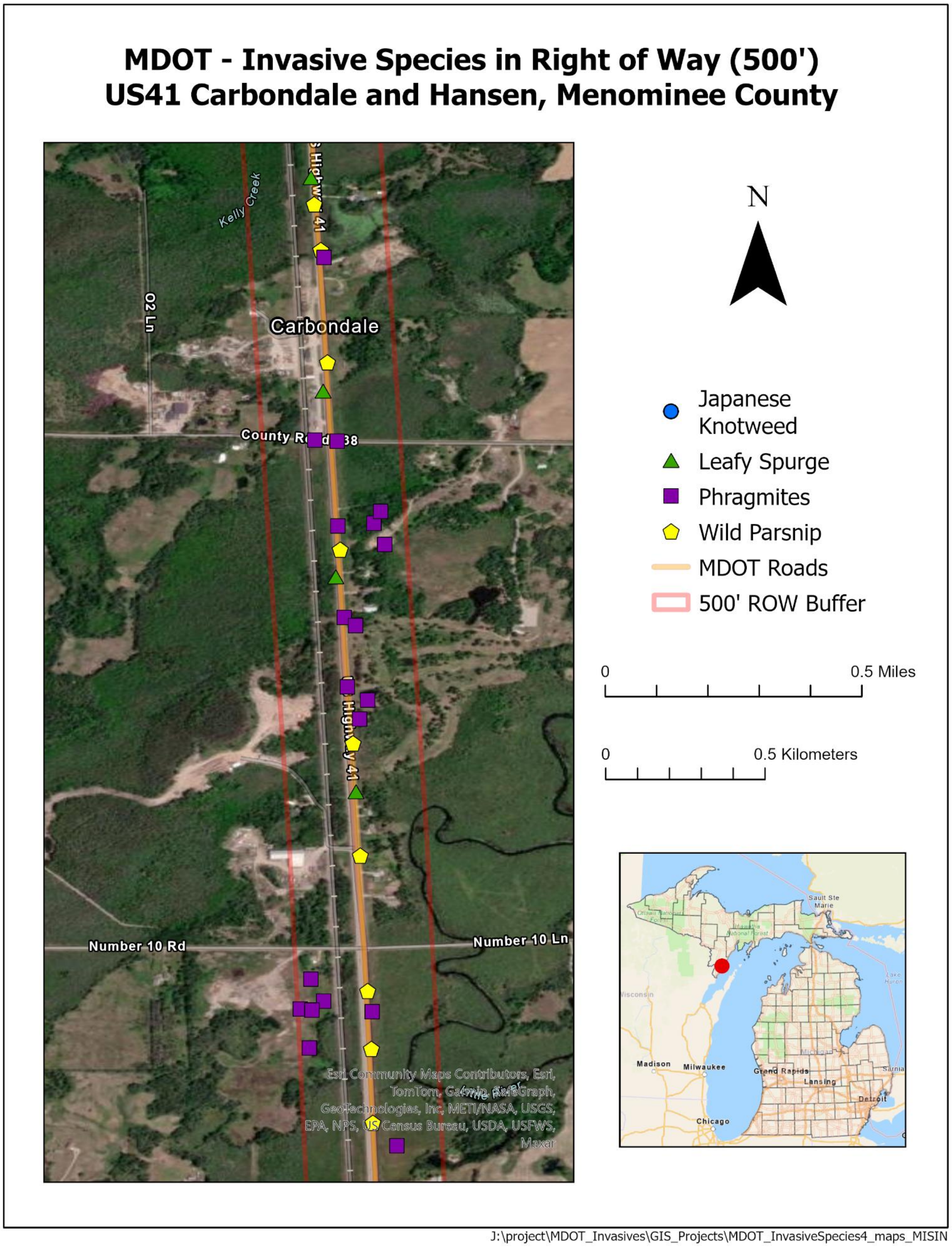

Figure 22: *Focused area of Zone 6 with leafy spurge, wild parsnip, Phragmites, and Japanese knotweed located along US41 near Carbondale (MISIN data).*

Additional Site 1: Lansing (MTRI)

<u>Species found:</u> Japanese knotweed (Figure 23).

<u>Selection Rationale</u> - Another site for Japanese knotweed was needed for the late season examples when the stems transition to a red color and are obvious in UAS imagery. Lansing had a large quantity of Japanese knotweed reported in MISIN and is a day field trip from MTRI. A large stance of the knotweed was located at the northwest corner of Abbot Rd. and East Lake Lansing Rd.

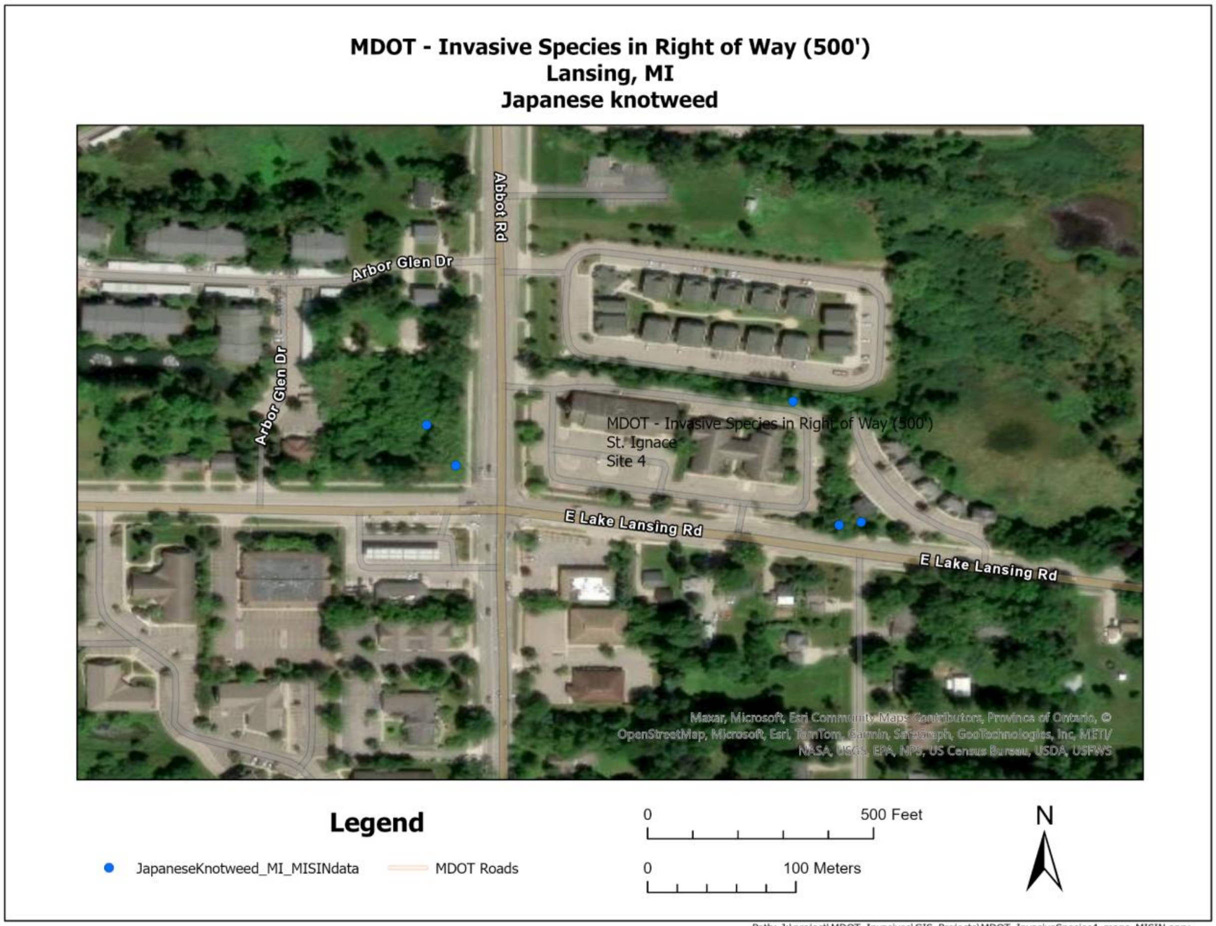

Figure 23: *Additional site 1 - Japanese knotweed near Abbot Rd. Park in Lansing (MISIN).*

Additional Site 2: Keweenaw Peninsula (KISMA)

<u>Species found in Hancock Area</u> - Japanese knotweed (Figure 24).

<u>Selection Rationale</u> - The local KISMA, which our team has previously worked with, had several recent records of Japanese knotweed being in the area, and since we had limited sites with any significant knotweed, we added this site.

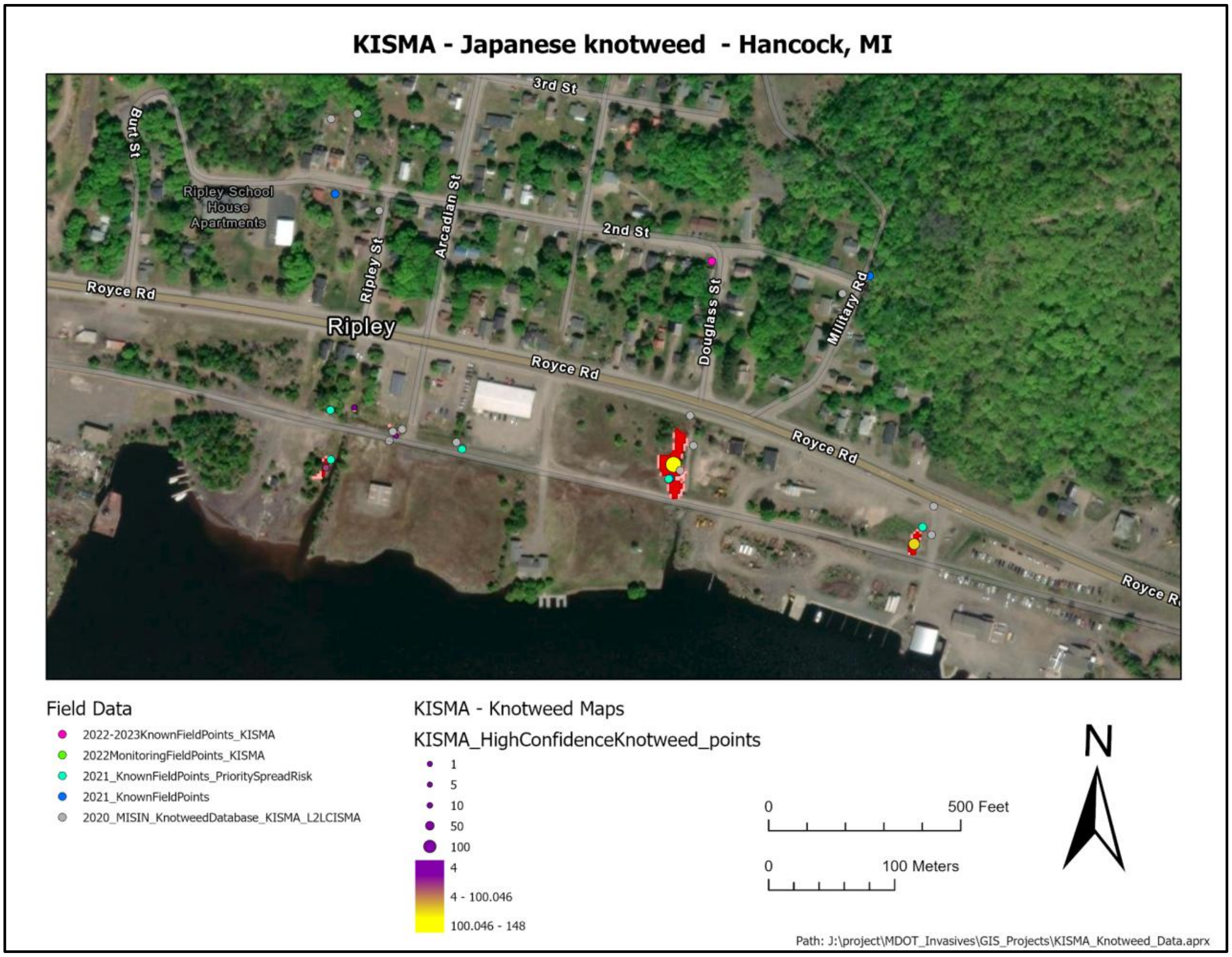

Figure 24: *Additional site 2 - Japanese knotweed located east of Hancock (KISMA data, https://mtu.maps.arcgis.com/apps/webappviewer/index.html?id=8c6e81da66f1404b990c19deae4086ce).*

3.5 Task 5: Data Collection

Data Collection Methodology

The data collection for this project was carried out in two primary phases. The first involved aerial surveys of the target areas using a pre-programmed flight plan executed with a DJI Mavic 3M. Flight parameters were adjusted to ensure adequate image overlap in both forward and side directions, allowing for high-quality orthomosaic generation and consistent spatial coverage. The second phase consisted of on-the-ground vegetation surveys conducted within the same areas. These surveys provided a detailed understanding of the local ecological composition and served as a source of ground truth data for validating the accuracy of the image classification results. Figure 25 is a blank vegetation survey field form that the team developed for ground validation surveys to relate observations to aerial imagery and classification. The research team conducted data collections to locate and collect imagery on all four species. Table 1 is a summary of all the locations surveyed with more detailed descriptions of each after.

MDOT Invasives in ROW Validation and Training Field Data

Location Name:		Date/Time:	
Site ID (MTRI or MISIN):		Observers:	
Waypoint ID:		Waypoint Lat:	
GPS Time:		Waypoint Long:	
GPS Unit #:		datum WGS84, decimal degrees	
Camera #:		Photo #s: (N, E, S, W, Nadir)	
ite Access Notes:			
Other Site Notes:			

INVASIVE SPECIES

Species (circle): Phragmites (P), Japanese Knotweed (JK), Leafy spurge (LS), Wild Parsnip (WP), Other: ________

Phenology: seedling/emergent sprout vegetative (fully leafed) flowering seeding dormant dead

Estimated Area: individual/few/several 1000sq/ft (half tennis court) 1000sq/ft to 1/2 acre 1/2-1 ac >1 acre

Estimated Density: sparse patchy dense (40% area) monoculture (100% of area)

1 x 1 meter plot

Unique ______ Distribution = E (even), C (center), Pe (peripheral)

As needed, record live (L) and/or dead (D) Record height of 3 samples if over 10% of plot

	% Cover	Height (cm) of 3 samples	Distribution	Picture #s
Species 1 (dom)				
Species 2				
Species 3				
Species 4				
Species 5				
Species 6				

Species notes or classifications:

Figure 25: *Blank vegetation survey form.*

Table 1: *Summary table of all the field sites visited for this project.*

Date	Zone	Location	Species & Notes	Drone Flight Altitudes
May 23, 2024	1	*Pinckney / Hamburg*	Wild parsnip (leafy), leafy spurge (flowering), Phragmites (leafy and flowering)	130 ft (wildparsnip), 300ft (Phragmites), 100ft, 200ft, & 300ft (Japanese knotweed & leafy spurge)

Date	Zone	Location	Species & Notes	Drone Flight Altitudes
July 11, 2024	1	*Pinckney / Hamburg*	Wild parsnip (flowering), leafy spurge (seeding), Phragmites (leafy), Japanese knotweed (leafy)	75ft, 100ft, 200ft (all species)
August 7, 2024	6	*Menominee*	Wild parsnip (seeding), leafy spurge (flowering), Phragmites (leafy and flowering)	100ft & 200ft (all species)
August 8, 2024	4	*Indian River*	Wild parsnip (flowering)	100ft & 200ft
September 18, 2024	3	*Traverse City*	Japanese knotweed (flowering), wild parsnip (seeding)	100ft & 200ft (both species)
September 19, 2024	3	*Petosky*	Japanese knotweed (flowering)	100ft & 200ft
September 19, 2024	5	*Rudyard*	wildparsnip (seeding)	100ft & 200ft
September 20	4	*Mackinaw City*	Japanese knotweed (flowering)	100ft & 200ft
October 9, 2024	N/A	*Lansing*	Japanese knotweed (flowering)	150ft & 200ft
October 9, 2024	1	*Pinckney / Hamburg*	Japanese knotweed (flowering)	150ft & 200ft
October 29, 2025	N/A	*Houghton / Hancock*	Japanese knotweed (flowering or senesced depending on which side of the river)	100ft
April 1, 2025	1	*Pinckney / Hamburg*	leafy spurge (emergent), Japanese knotweed (senesced)	150 ft (both species)
May 9, 2025	1	*Pinckney / Hamburg*	Wild parsnip (leafy), leafy spurge (flowering), Phragmites (leafy), Japanese knotweed (leafy)	150 ft (all species)
May 28, 2025	1	*Ann Arbor*	leafy spurge (flowering)	100 ft

Date	Zone	Location	Species & Notes	Drone Flight Altitudes
June 6, 2025	1	*Pinckney / Hamburg*	Wild parsnip (leafy), leafy spurge (flowering), Phragmites (leafy), Japanese knotweed (leafy)	150 ft (all species)
June 19, 2025	5	*Rudyard*	leafy spurge (flowering), Wild parsnip (leafy)	150ft (both species)
June 20, 2025	4	*Indian River*	Wild parsnip (leafy)	150ft
July 28, 2025	4	*Indian River*	Wild parsnip (leafy)	150ft

Field Season 2024

This section will review the data collection performed for the 2024 field season.

May 23rd, 2024 - Zone 1: Pinckney / Hamburg

The research team went on an exploratory trip to the Hamburg/Pinckney corridor highlighted in focus Zone 1 (Figure 26). The purpose of the trip was to familiarize the team with our target species and complete a preliminary assessment on the viability of detecting these species from the air with UAS technology. An additional goal for the team was to collect aerial imagery of any species that leadership believed to be good enough for later analysis. Ultimately, throughout the day all four of the target species were identified in this corridor. While some species such as wild parsnip were still leafing out for the season (Figure 27), others such as leafy spurge were reaching the peak of their flowering season in southeast Michigan (Figure 28).

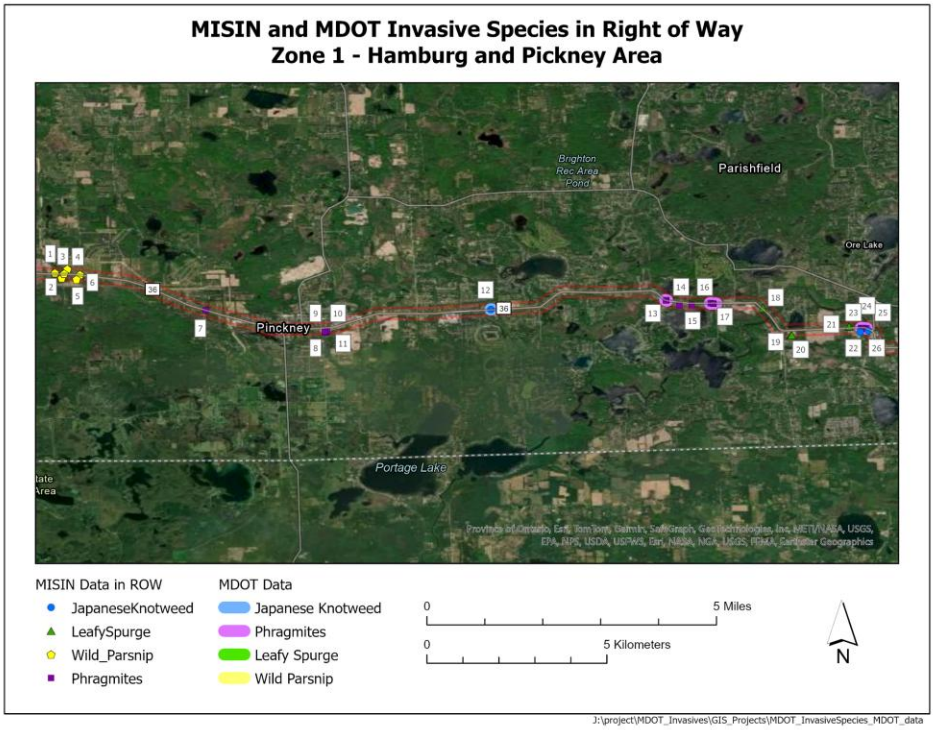

Figure 26: *Hamburg/Pinckney site map.*

Figure 27: *Leafing* wild parsnip*.*

Figure 28: *Flowering leafy spurge.*

The team visited 10 locations along the over 10 mile stretch of M-36 and performed 8 drone flights over areas of interest which contained a target species. All four of the species of interest were found and data was collected on all. The data collection proved to be highly important to the team's first year observations, being the only site with all species present within one single road corridor. By revisiting this site at later dates, the team was able to track the phenological changes in target species closely. This proved to be an invaluable measurement for informing the schedule of future data collections.

July 11th, 2024 - Zone 1: Pinckney / Hamburg

As the Pinkney / Hamburg sites proved valuable, this was the first revisit that the team scheduled. The intention for this trip was to track the phenological changes of species in proven locations and gather higher accuracy aerial imagery from the best sites located on the first visit. The main highlight for this trip was the discovery that the wild parsnip sites had gone to flower (Figure 29). With the highly distinct yellow flowers sitting upon a tall stalk, it made for easy discovery even from the air.

Figure 29: *Wild parsnip in bloom.*

While the sites represented by Phragmites and Japanese knotweed didn't have any significant changes in their phenology, the sites with leafy spurge proved the opposite. While the flowers remained present, the yellow/green pigmentation that was characteristic in their earlier bloom had faded to a darker green as the flowers had gone to seed (Figure 30). This made detection by UAS more difficult compared to the characteristics of the inflorescence seen in May. Data gathered during this trip informed the decision to make a more significant data collection soon after.

Figure 30: *Leafy spurge bracts having lost pigment and gone to seed.*

August 8th, 2024 - Zone 6: Menominee

As informed by the Hamburg / Pinckney data collection in July, it was determined that early August would be a good time to collect more sites where wild parsnip and leafy spurge may be present. While leafy spurge had gone to seed in southeastern Michigan, the hope was that both species would be in bloom further north. Zone 6 was chosen as this target, as it had reports of the target species in close proximity to one another. Three sites were chosen after a period of in person investigation, one on M-35 and two on US-41. The first of these sites was the sole site on M-35. While this site was not the best example for any one species, it contained three of our target species, only lacking Japanese knotweed. It was at this site however, that our researchers discovered a very interesting detail about wild parsnip. While its stalks and yellow flowers make it a prime target in the midst of its bloom, these examples found here showed an equally if not more distinct feature. When the flowers begin to go to seed, the whole stalk will change to a dark rusty brown (Figure 31). This is significant, as it stands out from its surroundings exceptionally well.

Figure 31: *Seeding wild parsnip is a distinctive brown which stands out from the other green vegetation.*

The first of the sites on US-41 was quite similar to the site on M-35, as it also had decent amounts of the rusty brown wild parsnip, and a small amount of leafy spurge that seems to have been cut back once or twice, as it seemed to be very early in its life cycle. The second site on US-41 was a very good find. Not only did this site have a large monoculture of Phragmites, it also had large patches of leafy spurge that were just past peak bloom (Figure 32-33). This made for an excellent opportunity to get both in a single area.

Figure 32: *US-41 South leafy spurge patch.*

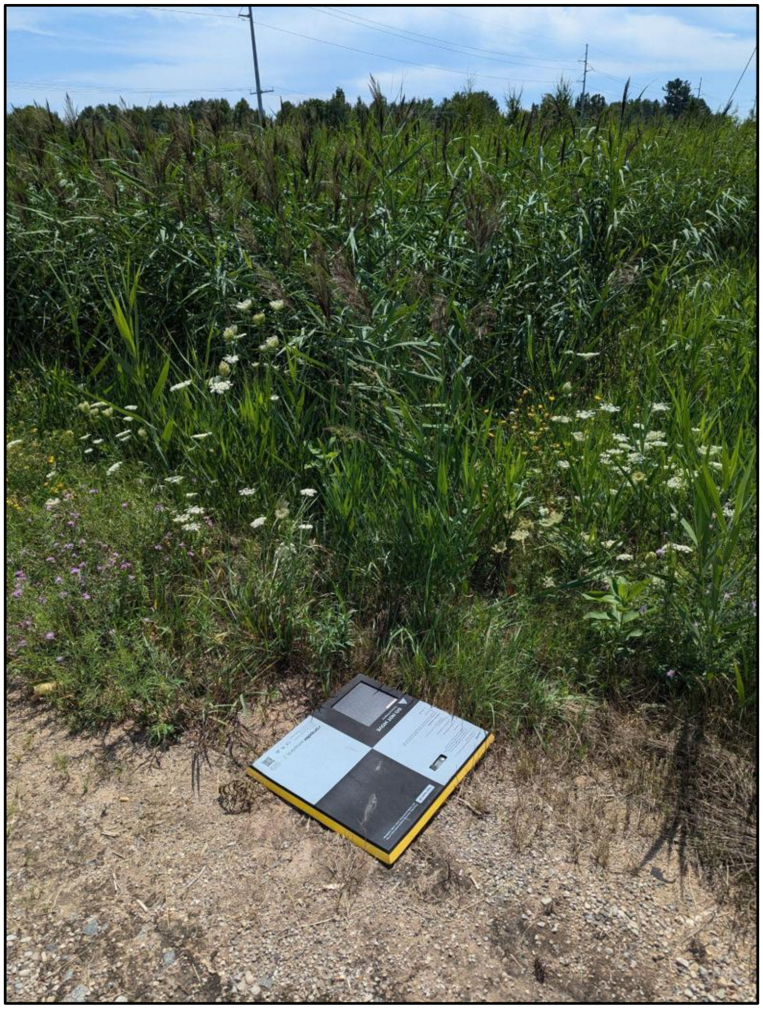

Figure 33: *US-41 South Phragmites patch.*

August 9th, 2024 - Zone 4: Indian River

While traveling to Menominee our field team came across an ideal site along the I-75 corridor through Indian River. This site was ideal in showing a characteristic growth pattern of wild parsnip (Figure 34). It was self-evident to our researchers that the species began to dominate the area after it had become disturbed, likely when it was mowed back for the season. Because of this, the species grew in a hedge-like pattern lining the road for a significant stretch. As the collection in Menominee was finished in a timely manner, the team resolved to stop for this stretch on the way back to the institute. This site proved to be another very valuable area to gather data, however, as the plants were past their prime flowering stage, the team decided it would be valuable to revisit this site in year two of fieldwork.

Figure 34: *Wild parsnip row along I-75 South.*

September 18, 2024 - Zone 3: Traverse City

As the season began to change, our researchers moved on to Zones 3 and 5. This attempt was motivated by gathering data on a wider range of our target species. Zone 3 in particular did not yield many great sites. The wild parsnip was even further along in its life cycle than it had been on the previous trip and was beginning to blend in with other species beginning their senescence. One site here gave us pause however, was declared a victory regardless. This site had a bush of Japanese knotweed, and it was in a fully flowering state. Figure 35 shows a patch of flowering Japanese knotweed found along US-31 in Beulah, MI. Five drone flights were performed over two sites at different altitudes to help the team investigate what the optimal flying altitude would be for classification.

Figure 35: *Flowering Japanese knotweed (white flowers in center of the image) mixed in with other vegetation.*

September 19, 2024 - Zone 3: Petoskey / Rudyard I-75

Moving northeast from Zone 3, the team traveled through Petoskey, finding another good example of Japanese knotweed in its flowering state (Figure 36). After collections at that site, the team moved north to fully explore Zone 5. While the Sault Ste. Marie area proved to be less valuable than anticipated, a couple of sites around Rudyard seemed to show significant promise for both wild parsnip and leafy spurge, but this visit was too late in the season for classification (Figure 37). These sites were documented with both an aerial survey and vegetation survey completed, and the team resolved to make a return trip earlier in the next field season. Five drone flights were performed between a site near Mudd Lake in Petoskey and Rudyard.

Figure 36: *Large patch of flowering Japanese knotweed found at Mudd Lake in Petoskey also showing bright red stalks which would become more distinctive later in the season.*

Figure 37: *Vegetation survey plot taken in Rudyard showing numerous wild parsnip flower stalks that have turned dark brown which would be difficult to distinguish through remote sensing classification.*

September 20, 2024 - Zone 4: Mackinaw City

As there were numerous sightings of our target species around the St. Ignace and Mackinaw City area, the team decided to investigate these areas before heading back to the office. While the search effort was put in, the weather and species were not cooperating. In the end, one site was documented in Mackinaw City (Figure 38). This site had a bush of Japanese knotweed, and it was near the end of its flowering state.

Figure 38: *Flowering Japanese knotweed in Mackinaw City Public Schools Park.*

October 9, 2024 - Additional Site 1: Lansing

As the field season came to a close, our researchers began to discuss what priorities needed to be explored before we could call the field season a success. While there were sites associated with all four of our target species at this point, our team felt the need to gather more concrete examples of late season Japanese knotweed. Past studies regarding this species suggested that the best time to collect imagery for analysis would be after the plant loses its leaves. That left the team with only a single season to collect data on this species. Therefore, the team planned a trip to the greater Lansing area to explore historical sightings reported in the MISIN database. While the species was less abundant than anticipated, a significant amount of imagery was obtained of the target species. Unfortunately, the target species was still in bloom at the time of visiting, so the characteristic red stalks were still obscured (Figure 39).

Figure 39: *Flowering Japanese knotweed in Lansing.*

October 28, 2024 - Additional Site 2: Houghton

With one final opportunity to collect late season Japanese knotweed the research team traveled to Houghton to survey known locations which have been documented by a colleague at Michigan Tech University. The university has a strong forestry department, with local invasive species management experts being employed there. With the help of our local expert, we were able to locate and document multiple areas with large infestations, including multiple phenological stages in close proximity to one another. This trip proved to be exactly the kind of data our researchers needed to substantiate our methodology with Japanese knotweed. Figure 40 shows Japanese knotweed in the late season distinctive reddish-brown color after the leaves have fallen, found in Ripley, MI which is almost directly across Portage Lake from Michigan Tech University. By contrast, Figure 41 shows an example of a large patch of Japanese knotweed that is on MTU’s campus which is directly adjacent to the waterway which still has bright green leaves.

Figure 40: *Japanese knotweed showing the distinctive red branches after the leaves have fallen.*

Figure 41: *Drone image of the large patch of Japanese knotweed which is still green amongst other vegetation that had already begun to senesce.*

Field Season 2025

This section will review the data collection performed for the 2025 field season.

May 28, 2025 - Zone 1: Ann Arbor

A drone collection was performed on M-14 near Ann Arbor to capture leafy spurge which was growing in the center median of the freeway. There were multiple patches along a 0.5 mile (0.8 km) stretch west of the Joy Rd. overpass. The DJI Mavic 3M was flown at an altitude of 100 ft and captured 315 images during a single 11 minute flight. Figure 42 shows an example of a single image captured by the drone as it flew over the center median. The leafy spurge was in full bloom and very distinctive from the surrounding vegetation with its yellow-green bracts.

Figure 42: *DJI Mavic 3M image of a patch of leafy spurge in the center median of M-14 near Ann Arbor.*

June 19, 2025 – Zone 5: Rudyard

The team traveled to Rudyard to survey leafy spurge along the M-48 corridor. The leafy spurge appeared to be at peak blooming and is roughly a month behind the peak for downstate blooming. The team collected two segments along M-48 with the first being a 1-mile segment between S

Mackinac Trail and S Centerline Rd west of Exit 373 for I-75 (Figure 43). This segment was flown at an altitude of 100ft (30.5m) and required two flights and 47 minutes to complete. Figure 44 shows a large patch of leafy spurge along M-48 as captured in the drone imagery.

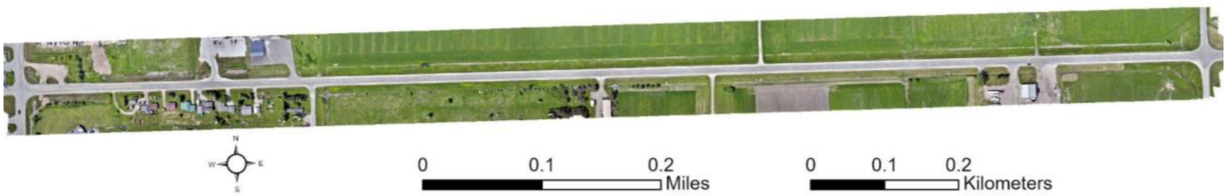

Figure 43: *A one-mile corridor of M-48 which was collected in Rudyard, MI to identify leafy spurge.*

Figure 44: *Large patch of leafy spurge along M-48 as seen from drone imagery.*

The second segment was a nearly half mile segment south of Rudyard. Unlike the northern stretch of M-48, this site didn't have the extensive dense patches of leafy spurge. Leafy spurge was more sparsely scattered along the side of the road as shown in Figure 45.

Figure 45: *Sparse leafy spurge along M-48 at the southern site.*

This second segment also contained a patch of wild lupine (*Lupinus perennis*) at the intersection of M-48 and S Mackinac Trail. It is sparsely populated in a roughly 0.25 acre (0.1 ha) patch on the west side of M-48. Figure 46 shows the wild lupine as seen from an oblique drone image. Two drone flights were performed at this southern site, one at 100 ft (30.5 m) to be similar to the other Rudyard site and the second flight was done at 75 ft (22.9 m) for a higher GSD in the imagery. The lower altitude was not able to be flown at the northern site due to taller trees near the road and focusing on collecting a larger corridor.

Figure 46: *Wild lupine along M-48 south of Rudyard.*

June 20, 2025 – Zone 4: Indian River

On the return trip the team collected along the I-75 S segment which was previously collected on August 9th, 2024 which had significant wild parsnip patches. This was still early in the season for using remote sensing methods as it was roughly the same height as the grasses and the flower stalks have yet to develop. This stop was still valuable to track the development of the wild parsnip as the team is planning for a midsummer data collection. Figure 47 shows the wild parsnip and grass at about the same height and difficult to distinguish through remote sensing techniques. A single drone flight was performed to capture the same area previously captured during the July 2024 data collection.

Figure 47: *Image captured alongside I-75 south bound lanes showing wild parsnip mixed with grass.*

July 28, 2025 – Zone 4: Indian River

A final data collection was performed at the I-75 SB Indian River site to capture changes in the wild parsnip between 2024 and 2025. There was a significantly reduced amount of wild parsnip at the site when compared to the previous data collected from August 2024. Figure 48 shows the change in the extent of wild parsnip at the site. In August 2024 the wild parsnip was dense and formed a continuous strip along the right-of-way (dark orange/brown color as it is going to seed) while in July 2025 there were only individual plants scattered along the same extent.

Figure 48: *Comparison of the extent of wild parsnip between 2024 and 2025 data collects along I-75 near Indian River.*

2025 Monthly Revisits to Zone 1: Pinckney / Hamburg

As part of the 2025 field season the team selected the Hamburg / Pinckney corridor to perform monthly monitoring of the development of the four target species. The surveys began in April and continued until September to track the development progress of the species and to identify more precisely when they would be most easily identified through our remote sensing techniques.

Wild Parsnip

The monthly development of wild parsnip is shown in Figure 49.

Figure 49: *The development of wild parsnip through the season.*

Phragmites

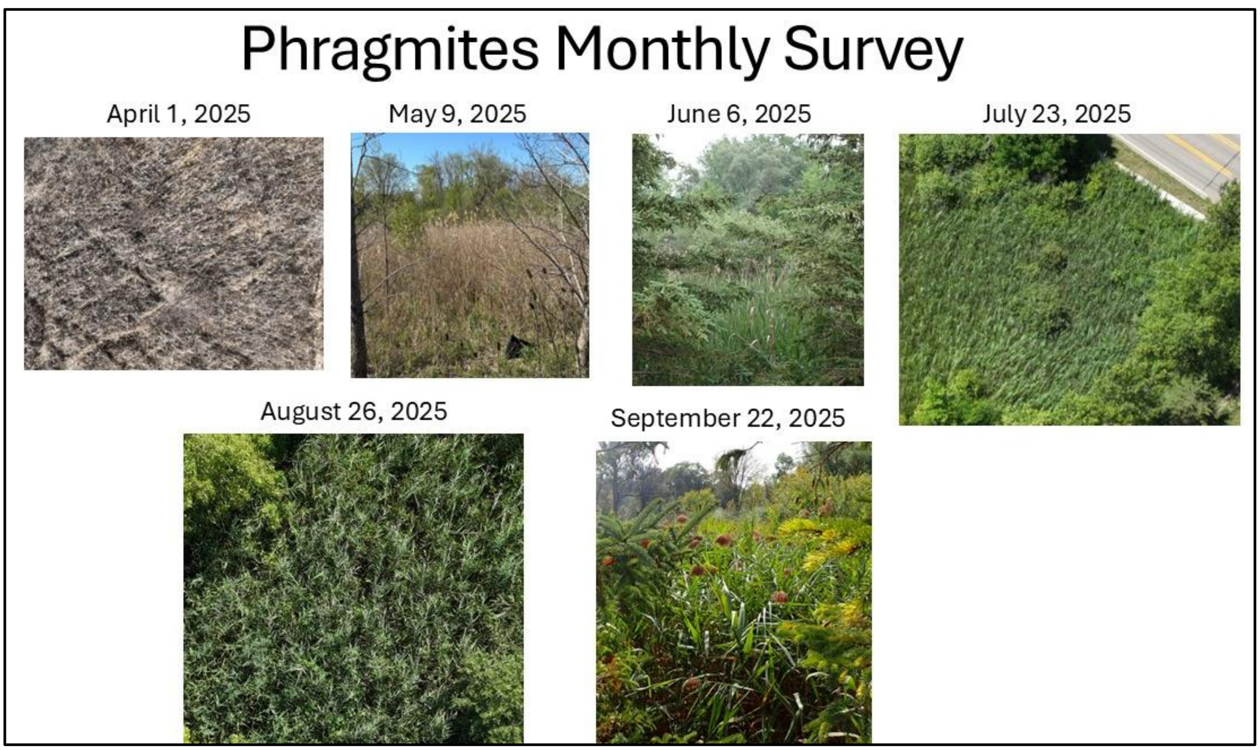

Figure 50: *The development of Phragmites through the season.*

Japanese Knotweed

Figure 51: *The development of Japanese knotweed through the season.*

Leafy Spurge

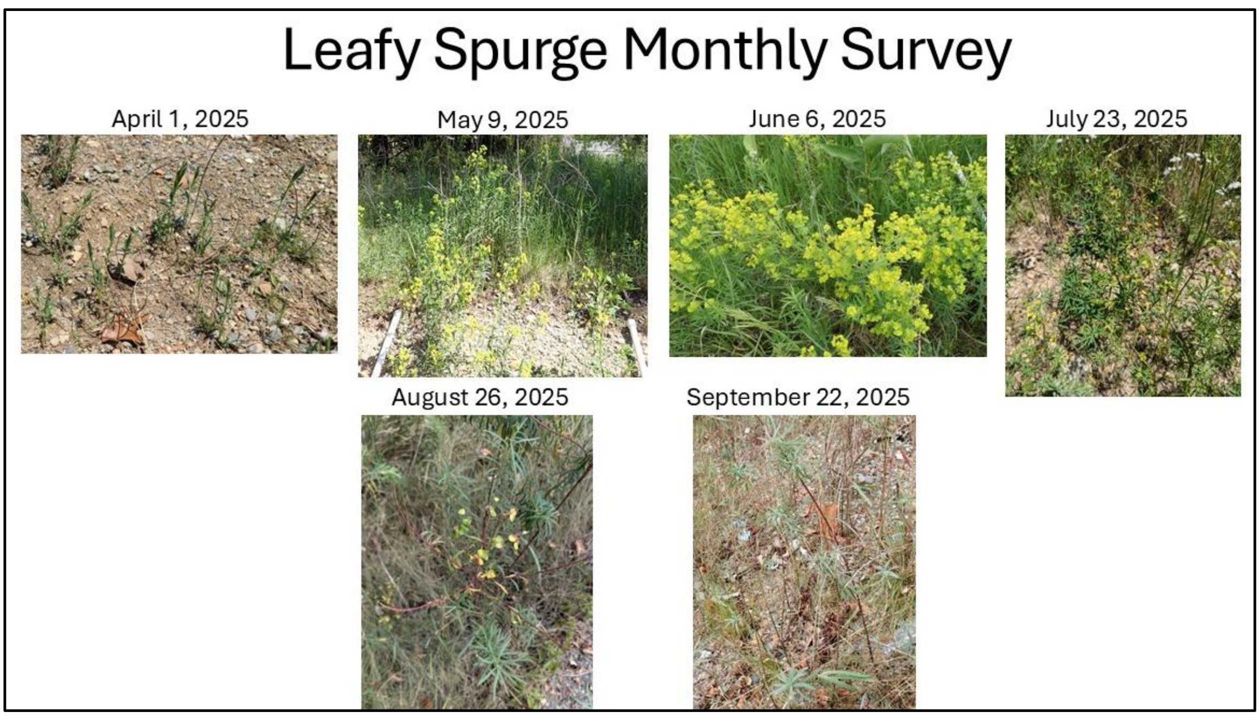

Figure 52: *The development of leafy spurge through the season.*

3.6 Task 6: Data Analysis

The research team used UAS optical and multispectral imagery from the DJI Mavic 3 Enterprise Multispectral drone to identify invasive species in MDOT right-of-ways. The four target species were surveyed at multiple locations across the state, where both on-the-ground vegetation surveys and UAS flights were conducted to support the classification process. First, the UAS imagery was processed into orthophotos and DEMs using 3D photogrammetry software. These layers were the input for supervised classification. ArcGIS Pro was used for most classifications, both object- and pixel-based, as it is available to MDOT staff. eCognition was also tested for object-based classification early in the project. Training data were created for each site in the Training Samples Manager. For the pixel-based methods, polygons were drawn for each desired class and for object-based methods, segments were selected from the segmentation layer generated in ArcGIS Pro by the Segmentation tool, based on class. These were then input with the imagery into the classifier or Classify tool. All classifications in ArcGIS follow the same classification workflow shown in Figure 53.

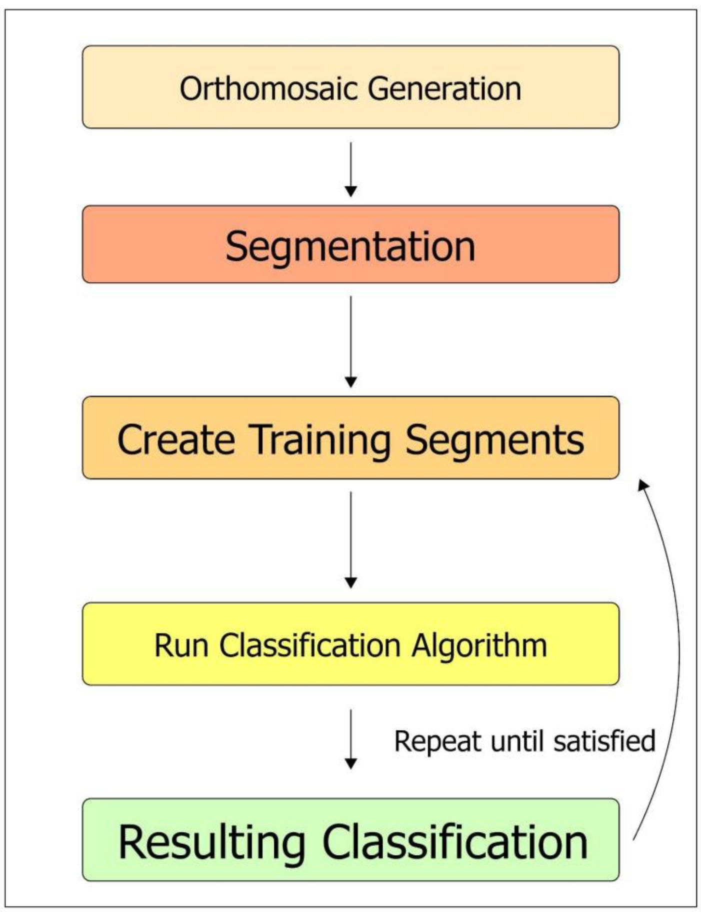

Figure 53: *Image Classification Flowchart*

In ArcGIS Pro, the classification toolset allows the user a selection of multiple algorithms, including Random Forest, Support Vector Machine, K-Nearest Neighbor, and ISO-cluster. For each site, classifications were run on both RGB and multispectral imagery to identify four target species. After the initial classification, outputs were visually assessed for accuracy, and the training data was adjusted iteratively when necessary. In cases where object-based classification was used, segmentation played a key role in shaping the outcome. Segment size and shape were adjusted based on the characteristics of each site and species—since some species are smaller or more sparsely distributed, the segmentation parameters needed to be flexible to reflect meaningful class differences. Figure 54 shows the process of object-based classification where the process starts with data layers, image segmentation, and then a final classification if produced.

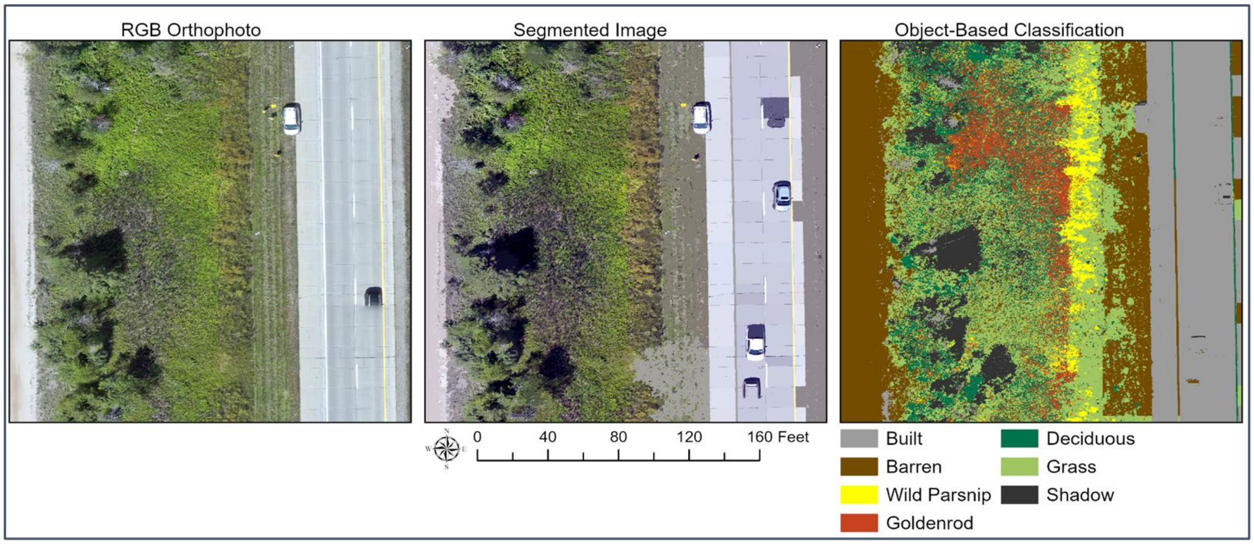

Figure 54: *Object-based classification in ArcGIS Pro going from input layers to segmentation and the final classification, created in ArcGIS Pro.*

Building on these classification workflows, we systematically tested a range of band combinations to identify the most effective inputs for image classification of our target species (Figure 55). Our data sources included standard RGB imagery, four-band multispectral (MS) imagery, NDVI layers, and digital elevation models (DEMs). Rather than relying on a single composite, we explored multiple configurations such as RGB alone, RGB combined with NDVI, MS paired with NDVI, and full image stacks incorporating all four data types. Across most sites, the full stack that included RGB, MS, NDVI, and DEM consistently produced the most accurate results, providing a richer spectral and contextual foundation for classification. However, the addition of DEM data was not universally beneficial. In some cases, particularly in areas with minimal variation in vegetation heights, it introduced confusion or reduced accuracy.

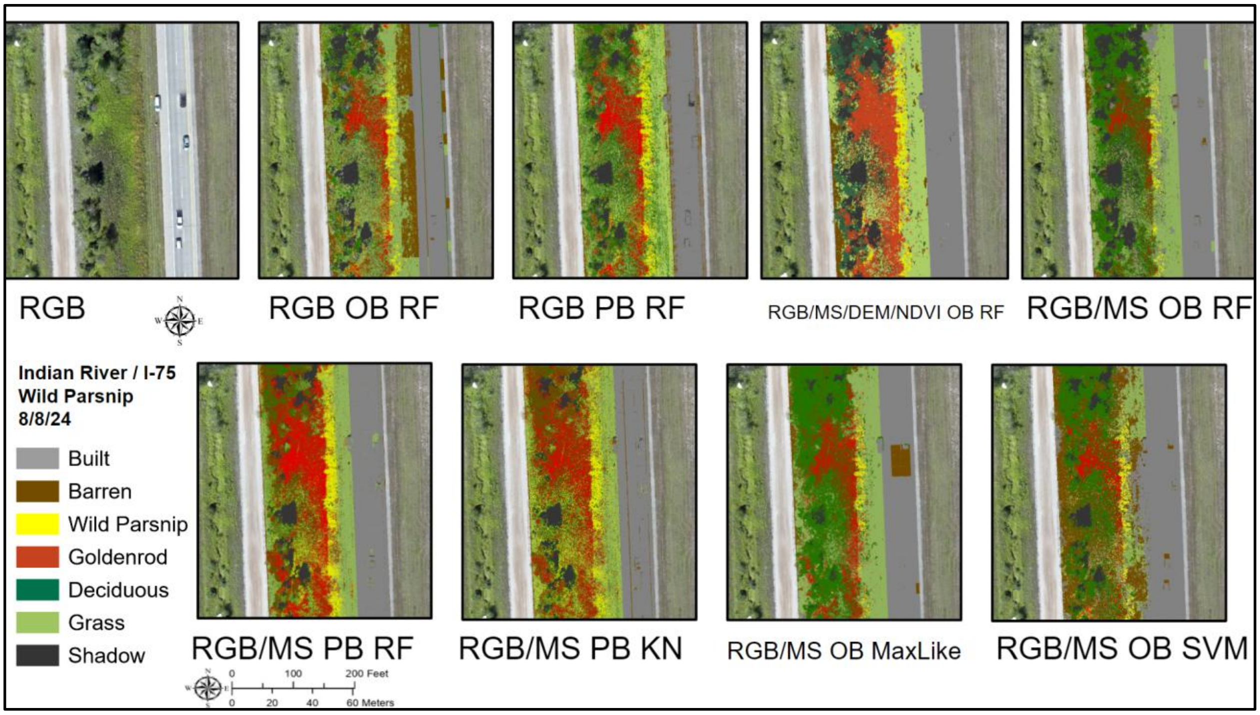

Figure 55: *Sample results of different band and classification selections. Section A shows a comparison of the same classifier (object based Random Forest) with different remote sensing data composites. Section B shows a subset of the composites with the pixel based Random Forests, and Section C shows a sample of other classification methods (Support Vector Machine and Max Likelihood) using object based and RGB/MS for comparison.*

We also evaluated the performance of several classification algorithms including Random Forest (RF), Support Vector Machine (SVM), K-Nearest Neighbor (KNN), and Maximum Likelihood (ML) across the different input combinations (Figure 55). RF and SVM typically yielded the highest classification accuracy, especially when used with multispectral and NDVI-enhanced imagery. KNN was less effective in regions with subtle differences between classes, while ML performed best in more uniform landscapes. This comprehensive approach allowed us to refine our classification strategy and better understand which combinations of spectral inputs and algorithms are most effective for ecological image analysis.

In cases where object-based classification was applied, the quality of segmentation became a critical factor. Segmentation quality was influenced by three main factors: spatial resolution, spectral resolution, and the minimum allowable size of image segments. Spatial resolution determines the ground area represented by each pixel and affects the level of detail visible in the segmentation. Higher resolutions help capture fine-scale features, but in heterogeneous areas, they can also introduce unnecessary noise. Spectral resolution, or the number and width of spectral bands, helps differentiate species based on reflectance differences; especially valuable when structurally similar plants are spectrally distinct. Lastly, setting a minimum segment size helps eliminate small, non-informative segments, ensuring that each segment contains enough information to support reliable classification while still capturing relevant ecological features.

Random Forest was the default algorithm used for most classifications as it typically performs well, while the other methods were tested at selected sites as detailed below. Overall, classification accuracy and quality were shaped by the interaction of the algorithm, the segmentation parameters, and whether a pixel-based or object-based approach was used. To assess performance, accuracy assessments were conducted to quantify how well each classification matched ground-truth data. Figure 56 shows four different classifications for Japanese knotweed in Houghton, MI. Random Forest produced the most accurate results with an overall accuracy of 93.6%. Other methods tested were Maximum Likelihood (49.1%), K Nearest Neighbor (52.7%), and SVM (55.7%).

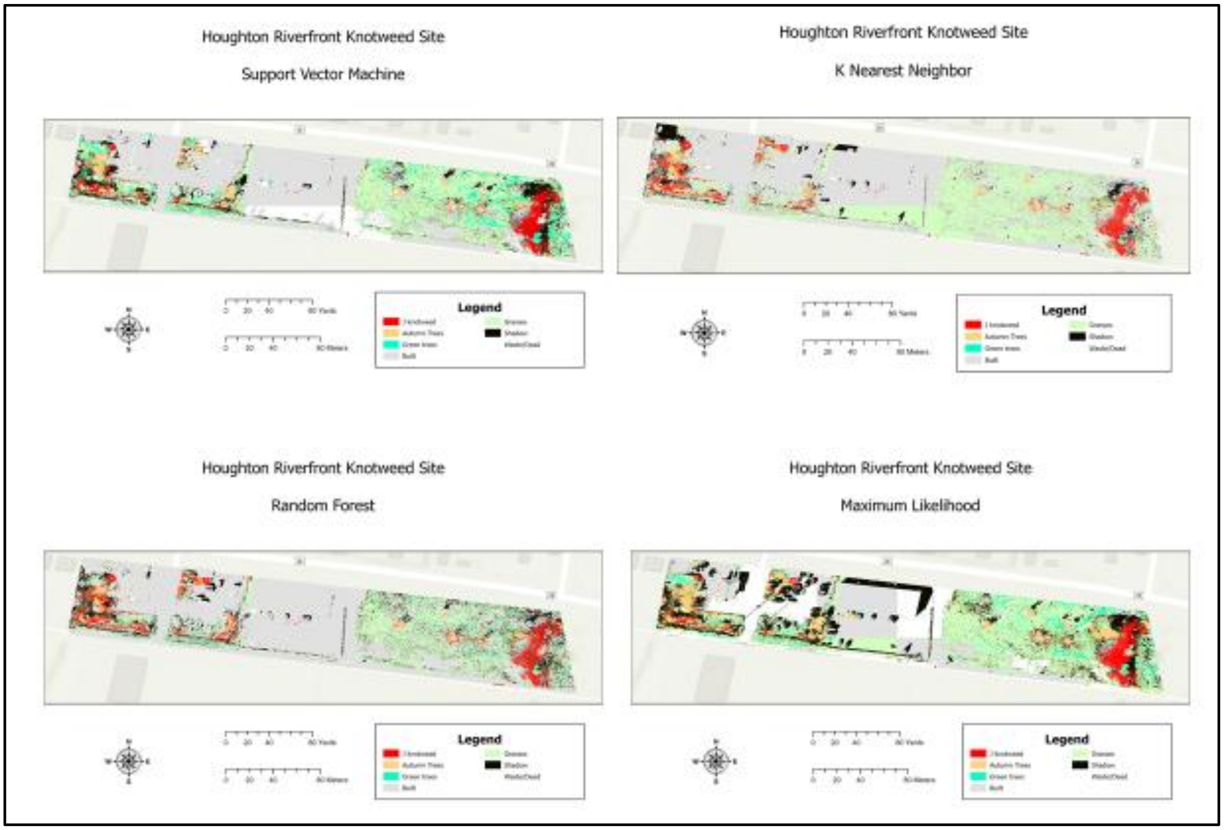

Figure 56: *Four classification methods used to test for mapping Japanese knotweed in Houghton, MI showing the differences between them.*

Our methods have also shown that going back to sites of invasive species along right-of-ways can also help track changes over time, such as determining growth patterns. The Japanese knotweed site in Hamburg/Pinckney, MI appeared to have spread beyond the extent of our year one observations. Similarly, changes in density and distribution of Wild Parsnip were noted along the I-75 Indian River site. Figure 57 shows the additional classification which was done after the July 2025 data collection. Table 2 shows the accuracies for each of the new classifications where Random Forest was clearly outperformed the other methods with and accuracy of 71% verses less than 60% for the other three methods.

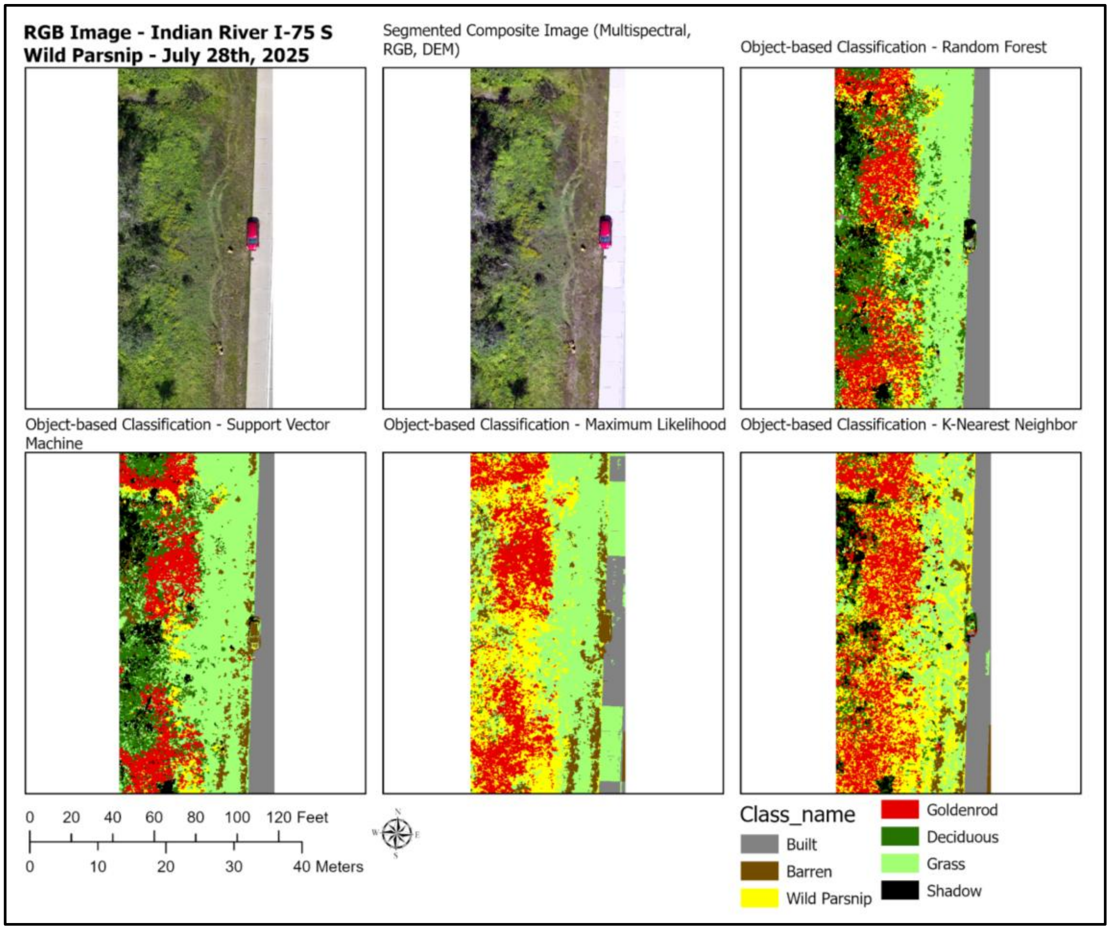

Figure 57: *The July 2025 classifications for wild parsnip in the Indian River area off of I-75 Southbound, including multiple image input combinations, classification methods, and algorithm types.*

Table 2: *Accuracy of the classification methods tested with overall accuracy represented by Kappa.*

	Indian River Wild Parsnip August 2025			
	SVM	RF	KNN	ML
PA	0.5	0.6	1	1
UA	0.5	0.6	0.5	0.307692
Kappa	58.01%	70.82%	48.69%	46.90%

The project team also demonstrated the ability to map a 1-mile corridor along M-48 in Rudyard. Figure 58 shows examples of classifications performed to identify Leafy Spurge in the rights-of-way. Random Forest and SVM have shown to out perform KNN and Maximum Likelihood methods. Random Forest and SVM methods are classified with an accuracy of over 80% (Table 3) while KNN and Maximum Likelihood performed with an accuracy of 50% or less. This is a similar result to the accuracy assessments from classifications performed on data from 2024.

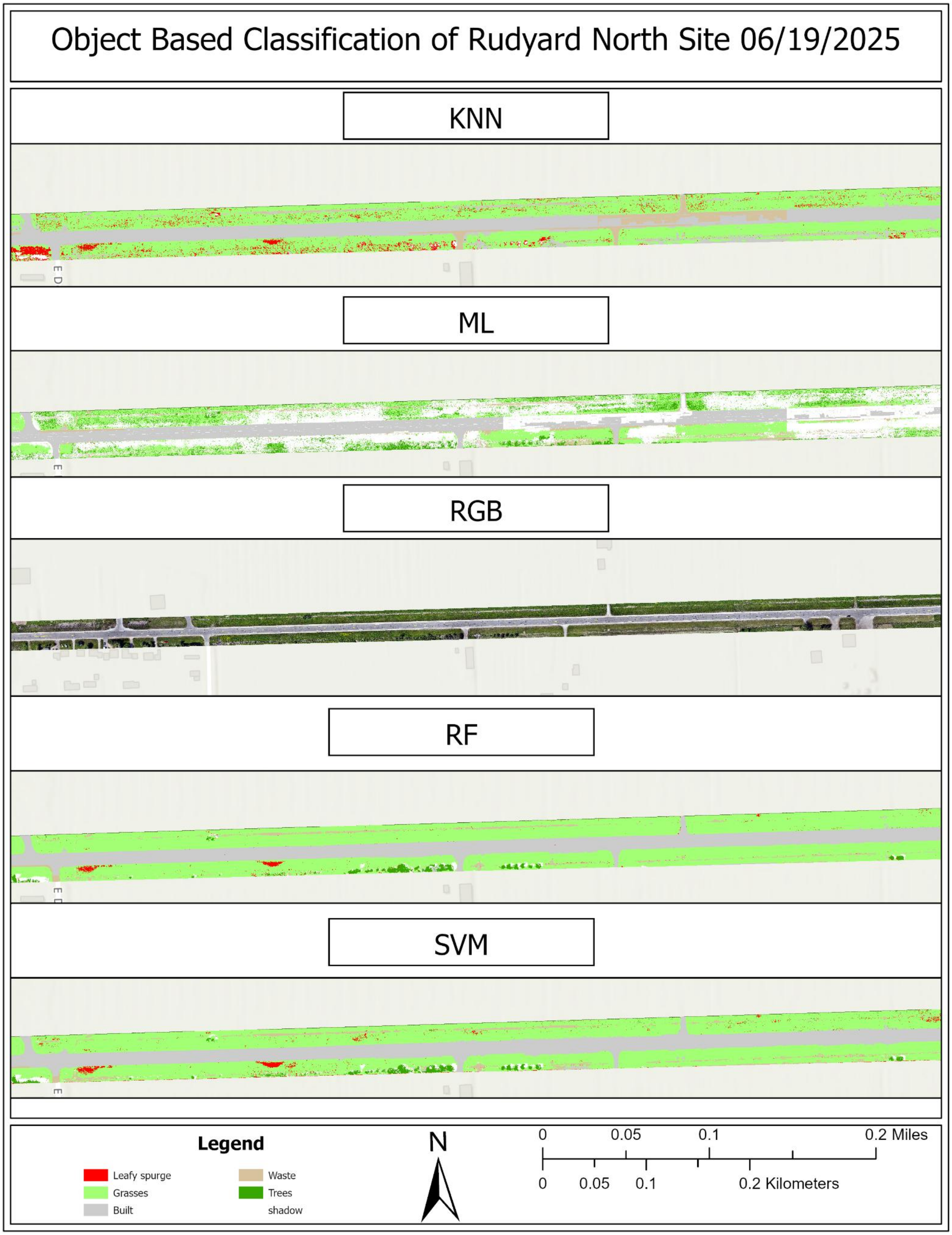

Figure 58: *Leafy spurge classification examples from June 19, 2025 in Rudyard, MI.*

***Table 3**. Accuracy of the classification methods tested with overall accuracy represented by Kappa.*

	Rudyard June 2025			
	SVM	RF	KNN	ML
PA	1	1	1	1
UA	1	1	57.14%	1
Kappa	88.60%	84.68%	41.47%	55.44%

Accuracy Assessment Methods

To evaluate classification performance, accuracy assessments followed the standard procedures outlined by Congalton and Green (2009), which emphasize the use of error matrices (confusion matrices) as the foundation for quantitative analysis. For each classified map, a stratified random sample of reference points was generated, typically based on ground-truth data or high-resolution imagery. These reference points were then compared to the corresponding classified values to determine agreement.

From this comparison, an error matrix was constructed, summarizing the number of correctly and incorrectly classified samples for each class. Using this matrix, several key accuracy metrics were calculated, including overall accuracy, user's accuracy, producer's accuracy, and the Kappa coefficient. Overall accuracy provides a general measure of agreement across all classes, while user's and producer's accuracies highlight commission and omission errors, respectively. The Kappa statistic offers a measure of how much better the classification performed compared to a random assignment, accounting for chance agreement. This approach provides a standardized and repeatable method for evaluating classification results and is widely used in remote sensing to assess the reliability of map products (Figure 59).

Class Value	Built	Barren	Wild Parsnip	Goldenrod	Deciduous	Grass	Shadow	Total	Users Accuracy	Kappa
Built	10	0	0	0	2	0	0	12	83.3%	
Barren	0	2	0	0	0	0	0	2	100.0%	
Wild Parsnip	0	0	1	0	0	0	0	1	100.0%	
Goldenrod	0	0	0	3	0	0	0	3	100.0%	
Deciduous	0	0	0	3	5	3	0	11	45.5%	
Grass	0	0	0	0	1	7	0	8	87.5%	
Shadow	0	0	0	0	0	0	7	7	100.0%	
Total	10	2	1	6	8	10	7	44	0.0%	
Producers Accuracy	100.0%	100.0%	100.0%	50.0%	62.5%	70.0%	100.0%	0.0%	79.5%	
Kappa										74.9%

***Figure 59:** Example of an error matrix from a classification of the Indian River wild parsnip site in 2024.*

4. Mapping Method Recommendations

The project team has performed extensive fieldwork and testing of analysis methods through Tasks 5 and 6. Through Task 5 the team has developed field methods for collecting data using drones. The project team purchased a DJI Mavic 3M to demonstrate utilizing a drone that is easy to deploy and includes integrated multispectral cameras. As MDOT has also purchased a DJI Mavic 3M the project team focused on using this platform to collect imagery of road corridors. This small multispectral platform is easily deployable from roadsides and has a flight time of over 30 minutes which allows for larger areas to be mapped on a single battery. For all target species it is recommended to fly at an altitude of 150 ft (46 m) above the ground. This will provide sufficient GSD for classification while keeping the drone above trees and most power lines.

There are several photogrammetry software available for the processing of the RGB and multispectral imagery from the Mavic 3M. MDOT currently uses Pix4D and Bentley iTwin (formerly Context Capture) for imagery processing and both are capable of processing this imagery. It is recommended by the project team to use Pix4D as the primary imagery processing tool for drone imagery. This is due to its ease of use and it was specifically intended to process standard drone mapping missions with only nadir imagery. Bentley iTwin is more complex and is intended for building 3D models of objects such as bridges and other transportation infrastructure.

For image analysis it is recommended for MDOT to use ArcGIS Pro. While there are other specialized software packages available, ArcGIS Pro with the Image Analyst extension is already available to MDOT staff and it offers a wide range of analysis techniques cited within the literature review. There are five main classifiers available: ISO Cluster, Maximum Likelihood, Random Forest (also known as Random Trees), Support Vector Machine (SVM), and K-Nearest Neighbor. With most of these methods there are options available for both pixel and object-based classification as well as supervised or unsupervised training methods. The research team tested classification methods discovered through the literature review and others on all four target species and below is the recommended methods for each species. The following are the recommended methods for each of the target species.

Leafy Spurge

Among the four focal species, leafy spurge (*Euphorbia esula*) posed the greatest classification difficulty. Initial efforts using RGB imagery and the RF algorithm yielded poor results, largely due to the limited spectral distinction of leafy spurge in the visible spectrum. Although the yellow-green bracts of the plant provide some visual contrast, these features are not reliably captured with RGB data alone.

Subsequent classification trials incorporated a composite image stack consisting of RGB, MS, and NDVI bands, which substantially improved performance. DEM data was also evaluated, though its utility varied by context. In areas with low vegetation density and limited vertical structure, DEM inclusion introduced confusion into the model and did not enhance accuracy. However, in sites with reduced canopy interference, the DEM showed modest improvements, likely due to the subtle elevation differences associated with leafy spurge patches.

Leafy spurge typically grows to a height of approximately one meter and often appears in scattered, patchy distributions, making it difficult to classify unless population density is high. This spatial sparsity, combined with weak spectral contrast in some environments, necessitated a careful tuning of segmentation parameters. Specifically, reducing spatial resolution while enhancing spectral resolution during segmentation improved the model's ability to detect dispersed individuals. Among the classification algorithms tested, KNN, SVM, ML, and RF, RF provided slightly superior results, although SVM also performed well. KNN consistently underperformed, particularly in sparse populations, and showed a tendency to misclassify surrounding vegetation (Figure 60 and Table 4).

Recommended Months: May and June

Recommended Layers: RGB, MS, NDVI, and DEM

Classification Method: Random Forest - Object-based classification

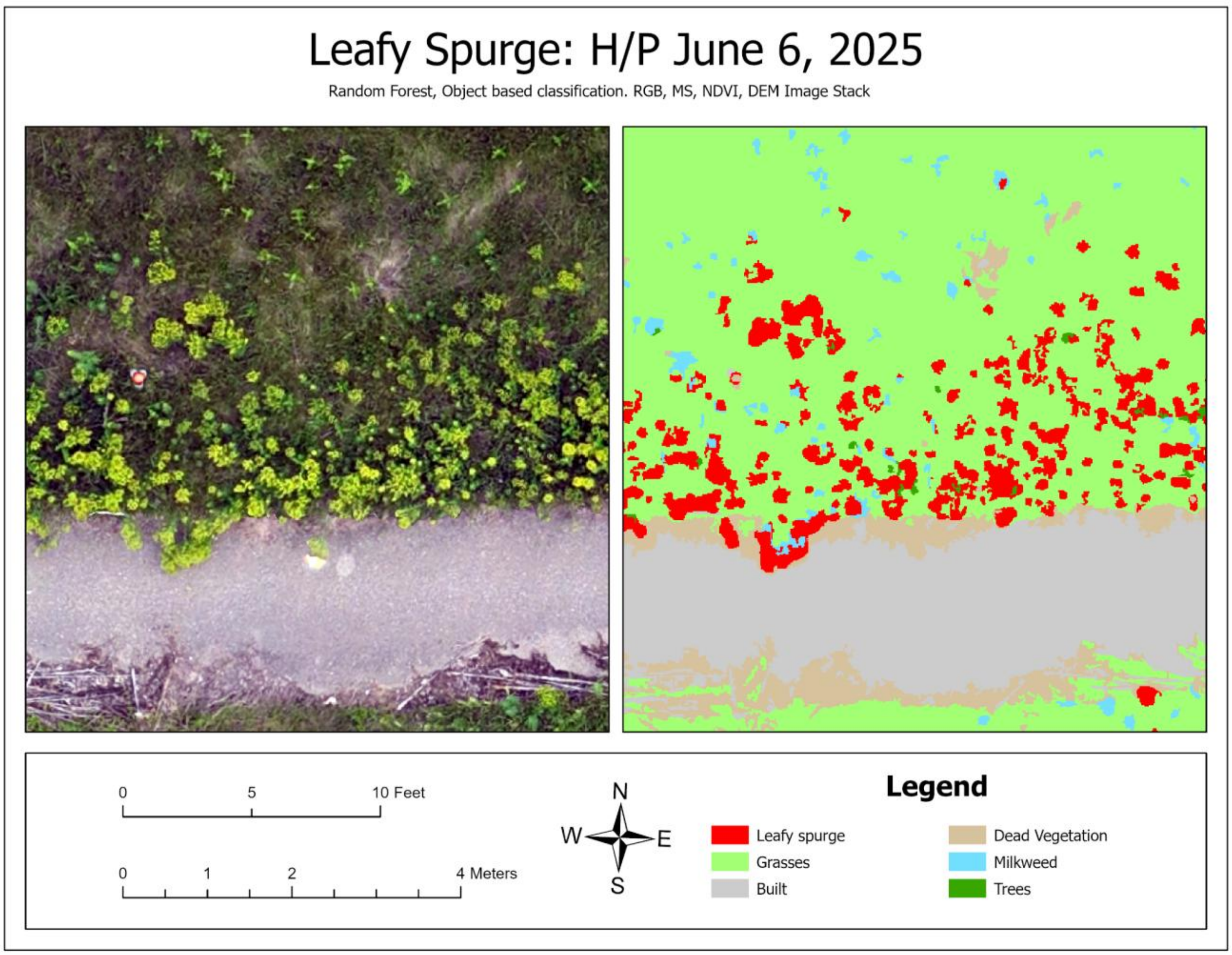

Figure 60: *Leafy spurge classification example, Hamburg/Pinkney 2025.*

Table 4: *Accuracy of the classification methods tested with overall accuracy represented by Kappa.*

	HP 18 Spurge June 2025			
	SVM	RF	KNN	ML
PA	91.05%	79.17%	38.13%	N/A
UA	78.61%	81.77%	45.50%	N/A
Kappa	83.57%	90.83%	35.25%	N/A

Phragmites

Phragmites australis (common reed) proved to be the most reliably detected species in this study. Its tall, dense growth and distinctive spectral signature allowed for consistent classification across multiple sites. Composite image stacks including RGB, MS, NDVI, and DEM data yielded strong performance, with the DEM contributing significantly to model accuracy. The vertical structure of Phragmites, often exceeding nearby vegetation in height, allowed the elevation data to help differentiate it from other plant types, especially in flat, open areas with limited canopy interference.

All classification algorithms tested—KNN, SVM, ML, and RF—successfully identified Phragmites to varying degrees. However, KNN frequently overclassified the species, resulting in inflated coverage and poor user's accuracy. SVM and RF both demonstrated strong performance, with SVM showing an advantage in final accuracy metrics. The effectiveness of Phragmites classification is likely due to its combination of unique structural and spectral characteristics, which align well with the capabilities of object-based classification methods (Figure 61 and Table 5).

Recommended Months: July - September

Recommended Layers: RGB, MS, NDVI, and DEM

Classification Method: SVM - Object-based classification

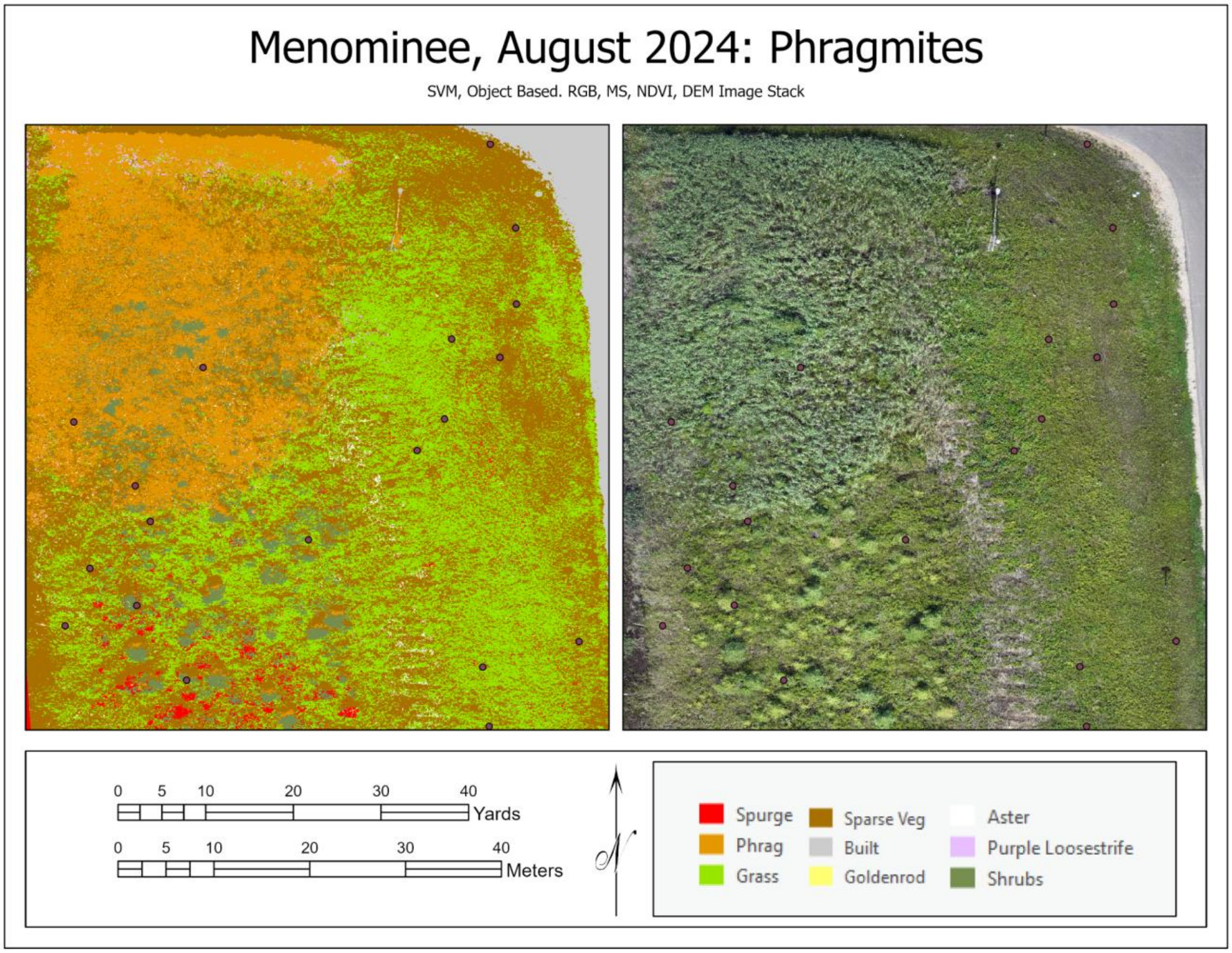

Figure 61: *Classification example of Phragmites.*

Table 5: *Accuracy of the classification methods tested with overall accuracy represented by Kappa.*

	Menominee Phragmites August 2024			
	SVM	RF	KNN	ML
PA	95.12%	78.89%	73.85%	65.29%
UA	96.09%	87.37%	73.61%	67.61%
Kappa	90.39%	79.02%	70.35%	59.29%

Japanese Knotweed

Japanese knotweed (*Fallopia japonica*) was primarily surveyed during the latter part of the 2024 field season, by which point the classification workflow had been refined through earlier analyses. At sites where the species was dominant, particularly those with minimal competing vegetation, classification results were especially strong. Japanese knotweed's distinctive red stems, especially visible during the fall and winter months, contributed to increased spectral separability. In contrast, spring and summer imagery would likely be less effective due to the plant's less distinctive appearance during peak growth.

From the outset, classification utilized a full composite stack of RGB, MS, NDVI, and DEM layers. The absence of substantial vegetative interference at most knotweed locations enhanced classification performance. As with the other species, four algorithms—KNN, SVM, Maximum Likelihood (ML), and RF—were tested. KNN and ML both produced moderate results, with ML performing surprisingly well in this context. SVM delivered robust accuracy, but RF consistently outperformed the other algorithms, suggesting that Japanese knotweed may have a spectral profile particularly well suited to RF classification. Whether this result is site-specific or indicative of a broader trend remains to be determined through additional sampling in future seasons (Figure 62 and Table 6).

Recommended Months: September - Winter season as long as snow free

Recommended Layers: RGB, MS, NDVI, and DEM

Classification Method: SVM - Object-based classification

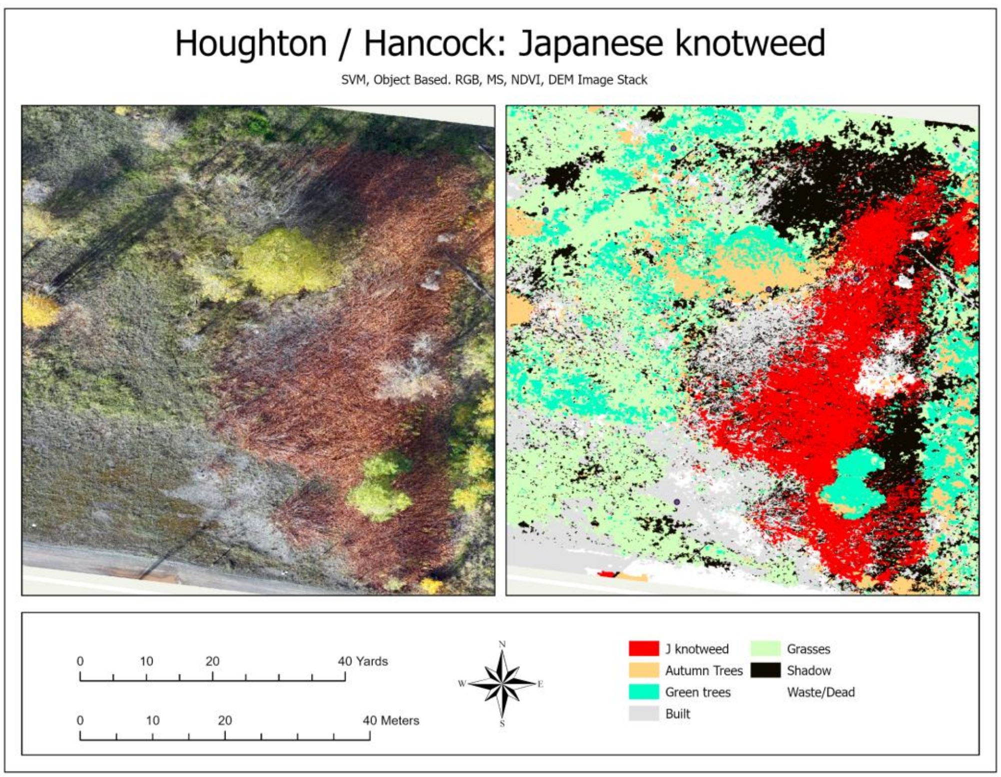

Figure 62: *Example classification of Japanese knotweed.*

Table 6: *Accuracy of the classification methods tested with overall accuracy represented by Kappa.*

	Houghton JP October 2024			
	SVM	RF	KNN	ML
PA	88.89%	75.46%	53.53%	91.57%
UA	89.31%	94.21%	60.14%	90.87%
Kappa	85.55%	71.08%	49.59%	83.92%

Wild Parsnip

Wild parsnip (*Pastinaca sativa*) was classified with multiple machine learning algorithms and image stacks in order to compare accuracies. The species was visibly distinctive at the Indian River site which was within the right-of-way of I-75 Southbound, even though there was goldenrod and typha mixed in. Classes used for the classification were built, barren, wild parsnip, goldenrod, deciduous treed areas, grass, and shadow. The RGB orthophoto, multispectral orthophoto, DEM, and NDVI layers were included in different combinations for the input image stacks. These combinations were RGB only, RGB/MS only and RGB/MS/DEM/NDVI. Creating these stacks was done by ensuring that the layers were georeferenced and using the ArcGIS Pro Composite Images geoprocessing tool. The classifications were created in ArcGIS Pro using the training manager to select polygons within segmented image stack layers for object-based classification, and drawing polygons within pixel groups for each class for the pixel-based classification. Both classification methods were tested and algorithms for the machine learner included Random Forests, Support Vector Machine, Maximum Likelihood, and K-nearest neighbors. From the various combinations of input products, classification methods, and machine learning methods, the best classification by visual inspection was the RGB, MS, DEM, NDVI image stack classified with object-based methods and the Random Forests algorithm. From these classification tests and observations, the recommended method for identifying wild parsnip in right-of-ways is to combine the optical and multispectral bands with the DEM and then add in the NDVI layer derived from the multispectral red and infrared bands, then segment the image stack and train the objects or segments with expert image interpretation. Random Forests performed well for all classification input combinations, so this algorithm is recommended (Figure 63-64 and Table 7-8). Figure 64 and Table 7 show the classification results for the July 2025 Hamburg / Pinckney monthly visit which helped to define the optimal month and classification method.

Recommended Months: July and August

Recommended Layers: RGB, MS, NDVI, and DEM

Classification Method: Random Forest - Object-based classification

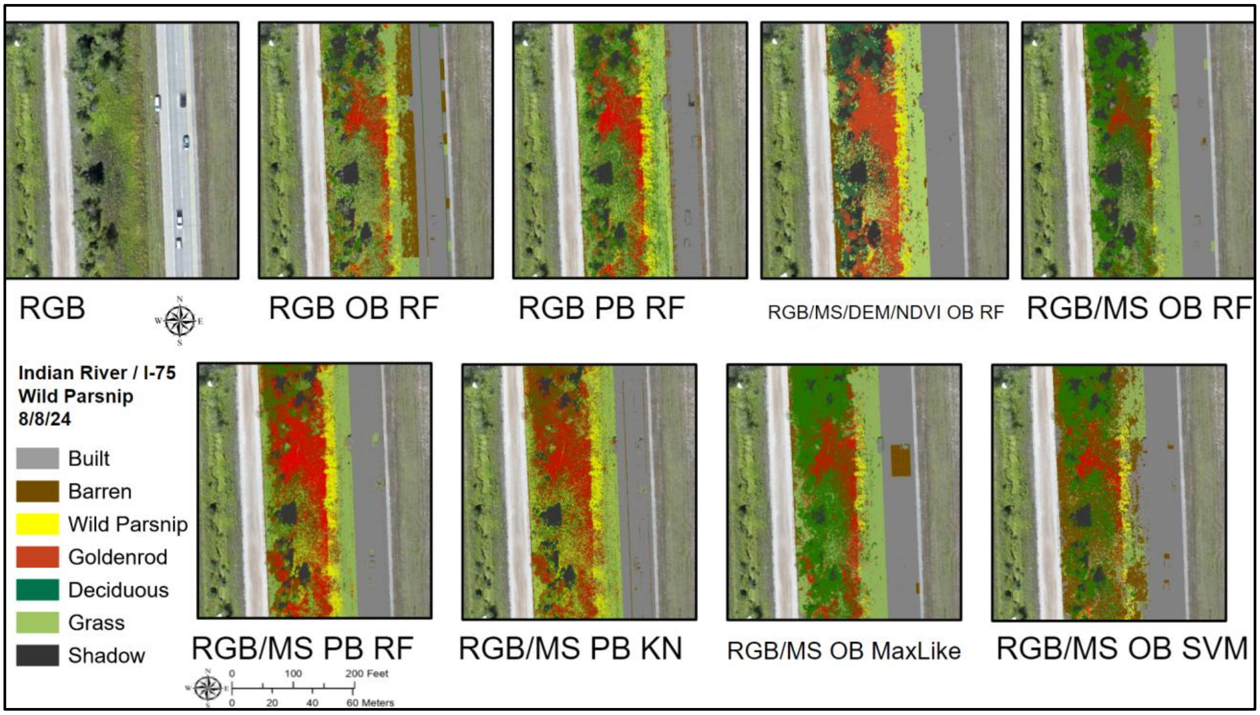

Figure 63: *The August 2024 classifications for wild parsnip in the Indian River area off of I-75 Southbound, including multiple image input combinations, classification methods, and algorithm types.*

Table 7: *Accuracy of the classification methods tested with overall accuracy represented by Kappa.*

	Indian River August 2024	
	Object Based RF	Pixel Based RF
PA	75.67%	83.21%
UA	72.06%	88.04%
Kappa	61.40%	74.87%

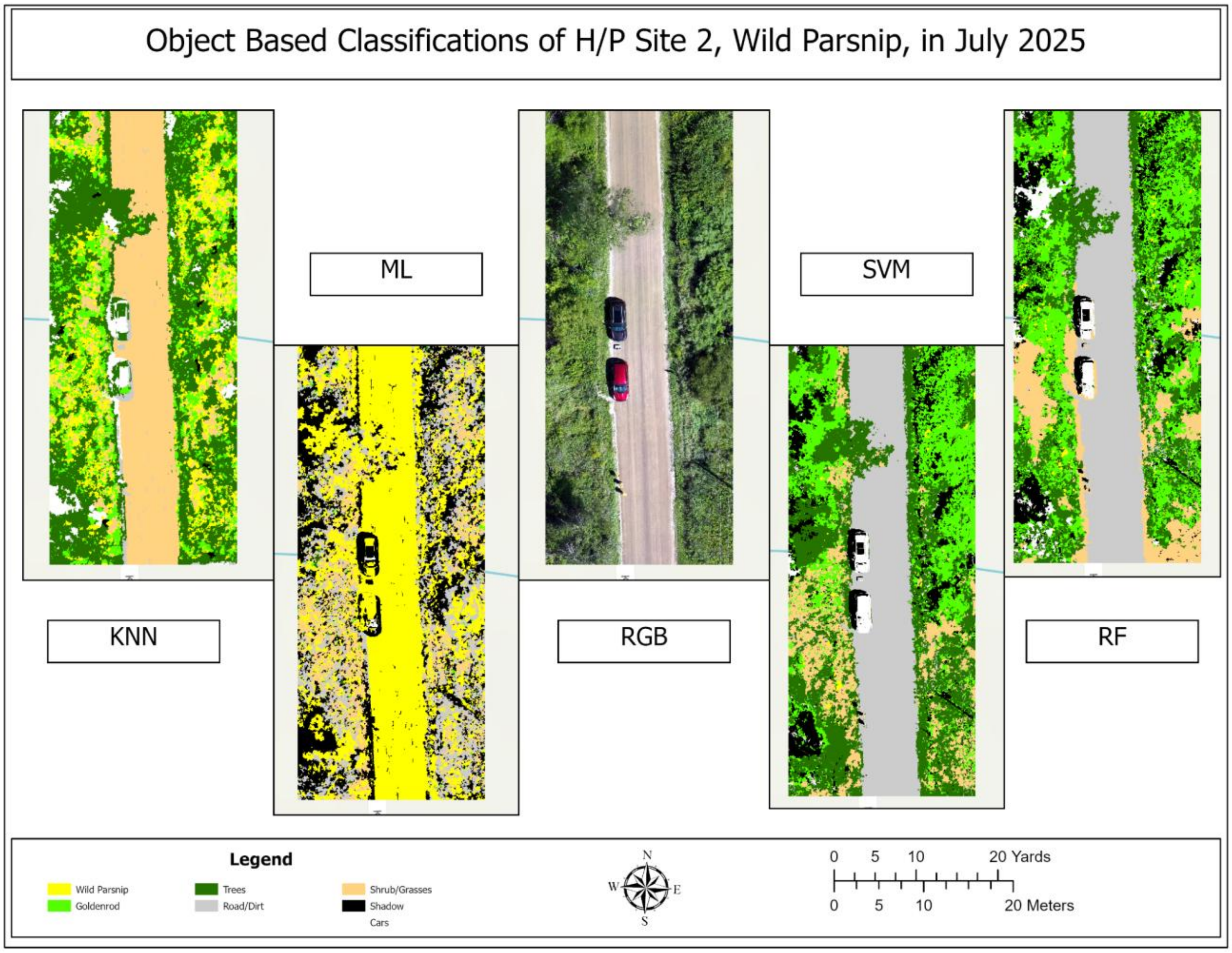

Figure 64: July 2025 *Hamburg/Pinkney example classifications showing the differences in the results between the methods.*

Table 8: *Accuracy of the classification methods tested with overall accuracy represented by Kappa.*

	HP 2 July 2025			
	SVM	RF	KNN	ML
PA	1	50.00%	1	1
UA	1	1	57.14%	28.57%
Kappa	73.90%	74.51%	41.47%	59.52%

5. Conclusions

This research project allowed for the testing of a variety of remote sensing classification methods for identifying and mapping Phragmites, Japanese knotweed, leafy spurge, and wild parsnip. The main goal of this project was to identify and document methods in which MDOT can implement remote sensing based mapping methods into day-to-day workflows. To accomplish this the research team collected UAS-based imagery at a variety of sites across Michigan for all species to compile a variety of site conditions to aid in identifying the best method by species.

While there are several options for remote sensing platforms and sensors, the research team focused on UAS based RGB and multispectral imagery. This is primarily due to the availability of a DJI Mavic 3M to the MDOT team. Other considerations to platform and sensor choice include the higher GSD afforded to UAS when compared to satellite and manned aerial based platforms but also cost and availability. For comparison, the highest GSD multispectral satellite platform (WorldView-4) has a GSD of 12in (31cm) where a DJI Mavic 3M at an altitude of 150ft (46 m) has an RGB GSD of 0.5in (1.3cm) and a multispectral GSD of 0.9in (2.2cm). This has a huge benefit for identifying invasive species which are sparsely populated or smaller in size like leafy spurge. UAS data can also be collected on demand, where other platforms are not as flexible.

The research team also focused on using ArcGIS Pro for classification and mapping of invasive species .Again, this is due to the availability of the software to MDOT staff. Other popular classification software such as Trimble eCognition, ENVI, or R software would be new to MDOT which would require additional cost to purchase or may not be able to be used by MDOT due to other restrictions. Keeping the analysis with ArcGIS Pro also enables easier implementation as MDOT staff are already familiar with the software and will be able to easily incorporate new ArcGIS tools into their workflow.

For all of the target species, it was determined that the best classification results are achieved by using RGB, multispectral, DEM and NDVI layers. These layers are run through the Random Forest classification methodology for best results for mapping Leafy Spurge and Wild Parsnip. For best results for mapping Phragmites and Japanese Knotweed it is recommended to use the SVV classification methodology. The other two classification methods, KNN and Maximum Likelihood, were found to perform with accuracies of 50% or less. Compared to accuracies of 75% or better for Random Forest and SVM, KNN and Maximum Likelihood are not able to produce reliable results.

By using the methods developed through this project MDOT will be able to deploy their own drone team to collect remote sensing data and utilize classification methods for mapping each of the invasive species covered. This implementation will also enable MDOT to track distribution changes within specific areas of their rights-of-way. This is both due to the expansion along the roadway but also for monitoring areas that are actively sprayed to control the spread. These methods will also enable MDOT to identify corridors which may be at risk of having one or more species expand its distribution from neighboring properties and allowing for species identification before large dense patches form.

6. Bibliography

Brooks, Colin, Charlotte Weinstein, Andrew Poley, Amanda Grimm, Nicholas Marion, Laura Bourgeau-Chavez, Dana Hansen, and Kurt Kowalski. “Using Uncrewed Aerial Vehicles for Identifying the Extent of Invasive Phragmites Australis in Treatment Areas Enrolled in an Adaptive Management Program.” Remote Sensing 13, no. 10 (May 12, 2021): 1895. https://doi.org/10.3390/rs13101895.

Bourgeau-Chavez, Laura, Sarah Endres, Michael Battaglia, Mary Miller, Elizabeth Banda, Zachary Laubach, Phyllis Higman, Pat Chow-Fraser, and James Marcaccio. “Development of a Bi-National Great Lakes Coastal Wetland and Land Use Map Using Three-Season PALSAR and Landsat Imagery.” Remote Sensing 7, no. 7 (July 9, 2015): 8655–82. https://doi.org/10.3390/rs70708655.

Congalton, Russell G., and Kass Green. *Assessing the accuracy of remotely sensed data: principles and practices*. CRC press, 2019.

Glenn, Nancy F., Jacob T. Mundt, Keith T. Weber, Timothy S. Prather, Lawrence W. Lass, and Jeffrey Pettingill. “Hyperspectral Data Processing for Repeat Detection of Small Infestations of Leafy Spurge.” Remote Sensing of Environment 95, no. 3 (2005): 399–412. https://doi.org/10.1016/j.rse.2005.01.003.

Michez, Adrien, Hervé Piégay, Lisein Jonathan, Hugues Claessens, and Philippe Lejeune. “Mapping of Riparian Invasive Species with Supervised Classification of Unmanned Aerial System (UAS) Imagery.” International Journal of Applied Earth Observation and Geoinformation 44 (February 2016): 88–94. https://doi.org/10.1016/j.jag.2015.06.014.

Liu, J., M. D. Hossain, and D. Chen. “A PROCEDURE FOR IDENTIFYING INVASIVE WILD PARSNIP PLANTS BASED ON VISIBLE BANDS FROM UAV IMAGES.” The International Archives of the Photogrammetry, Remote Sensing and Spatial Information Sciences XLIII-B1-2021 (June 28, 2021): 173–81. https://doi.org/10.5194/isprs-archives-XLIII-B1-2021-173-2021.

O’Neill, Michael, Susan Ustin, Steve Hager, and Ralph Root. “Mapping The Distribution of Leafy Spurge at Theodore Roosevelt National Park Using Aviris.” NASA, n.d. chrome-extension://efaidnbmnnnibpcajpcglclefindmkaj/https://aviris.jpl.nasa.gov/proceedings/workshops/00_docs/ONeill_web.pdf.

Smerdu, Ana, Urša Kanjir, and Žiga Kokalj. “Automatic Detection of Japanese Knotweed in Urban Areas from Aerial and Satellite Data.” Management of Biological Invasions 11, no. 4 (2020): 661–76. https://doi.org/10.3391/mbi.2020.11.4.03.

Vander Bilt, Dorthea J., Laura L. Bourgeau-Chavez, Colin Brooks, Chris Cook, and Amanda Grimm. "Building a Framework for the Detection, Treatment, and Long-Term Monitoring of Invasive Species in the Great Lakes Utilizing Multitemporal Remote Sensing." In AGU Fall Meeting Abstracts, vol. 2023, no. 1895, pp. B11I-1895. 2023.

7. Appendices

Appendix A

7.1 ESRI ArcGIS Pro Classification Workflow: Step-by-Step

In ArcGIS Pro, there are a few different ways to classify an image. For images with very distinct differences in classes, there is a classification wizard tool, located on the imagery tab of the ribbon, which helps a user to go through all the steps necessary to create a simple object-based classification.

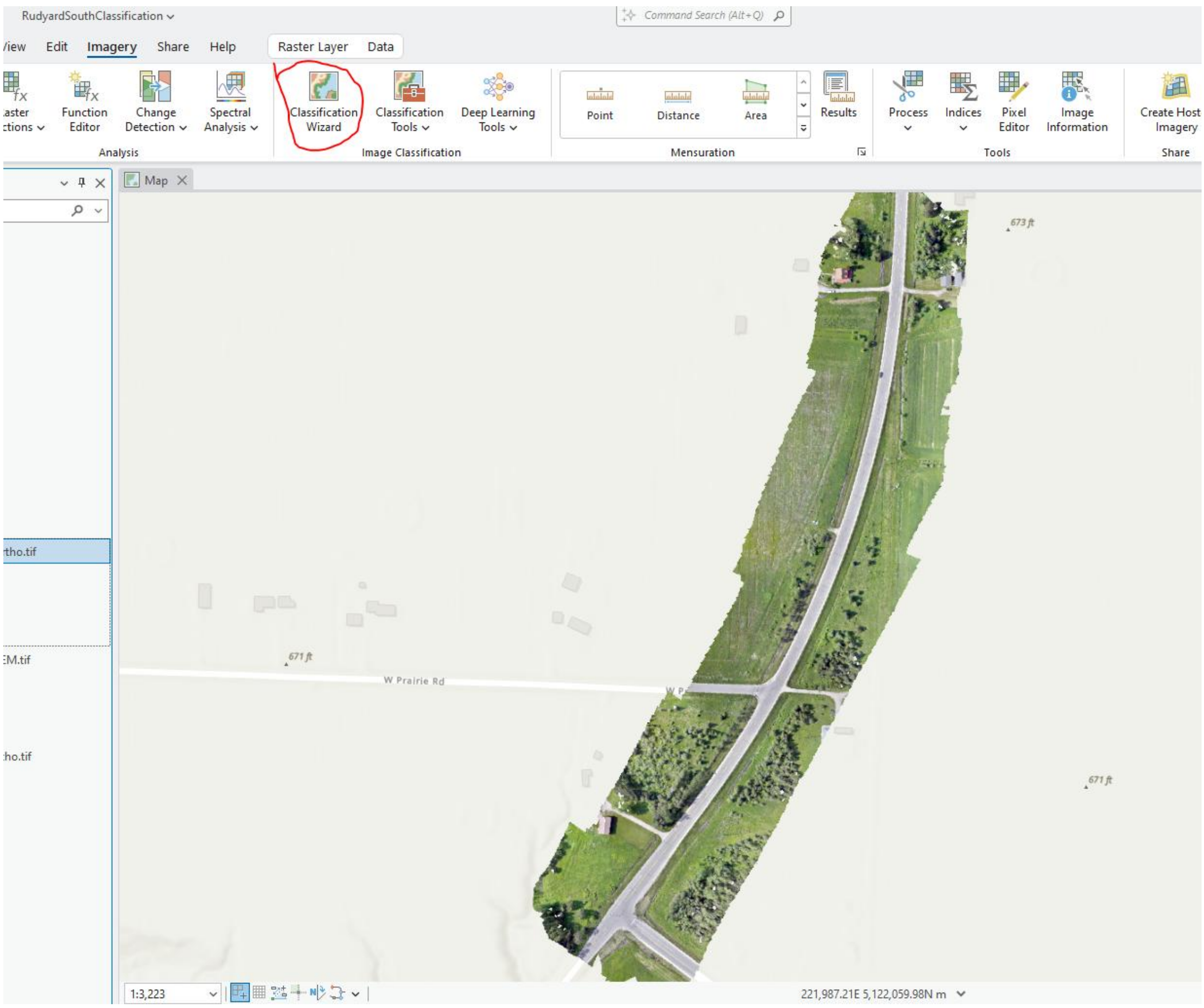

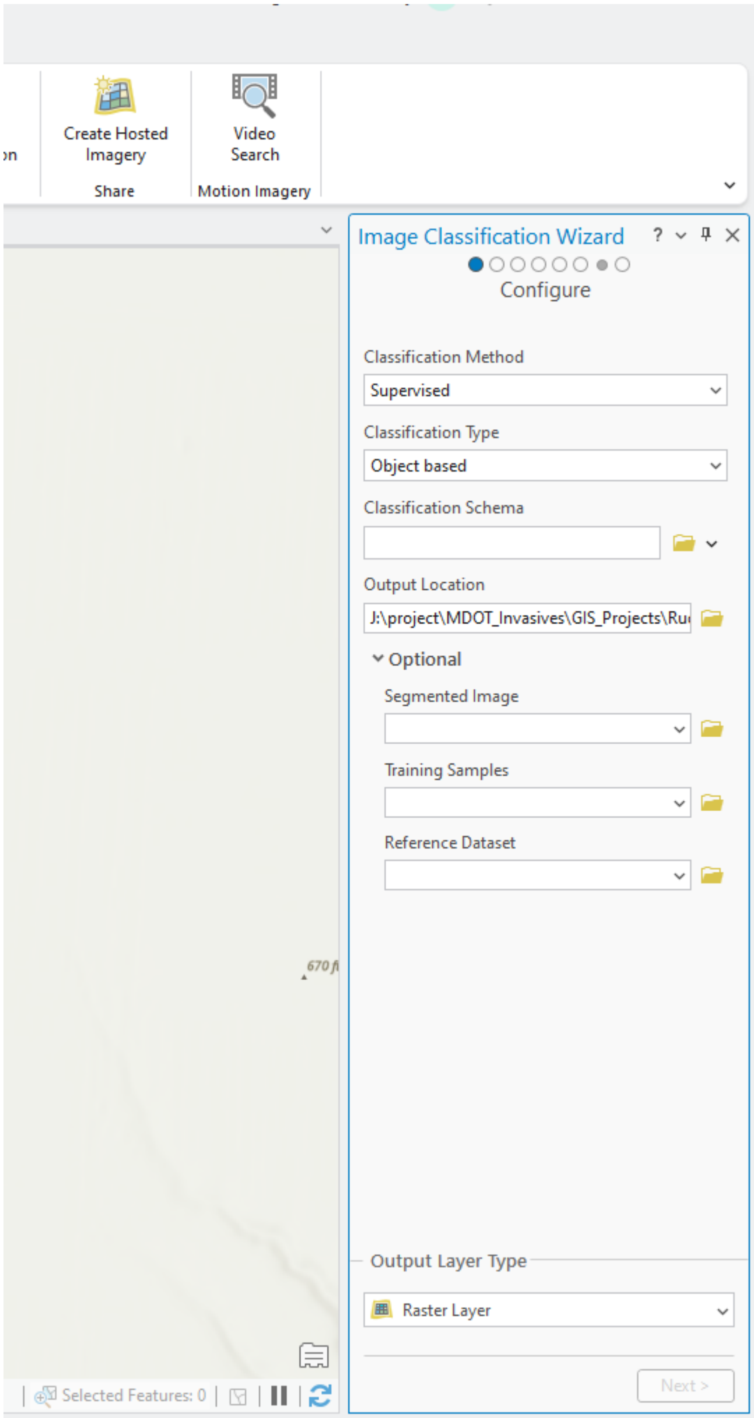

For more complex images, where classes are closer together spectrally, it can be tougher to differentiate with the wizard. In cases such as vegetation classification, it is often necessary to know how to use the individual tools separately, in case steps need to be redone or changed. Below is a step-by-step introduction for how to classify an image using the tools built into ArcGIS Pro.

Step 1. Segmentation. While some software requires a segmentation step to run, ArcGIS Pro makes this step optional. However, the segmentation step is necessary for doing object-based training and classification. The tool also allows you to adjust certain parameters before training data creation. The two parameters that are adjusted in the segmentation step are spatial resolution and spectral resolution. Spatial resolution increases or decreases the fine details in the image, either creating more complex and smaller polygons or less complex larger polygons.

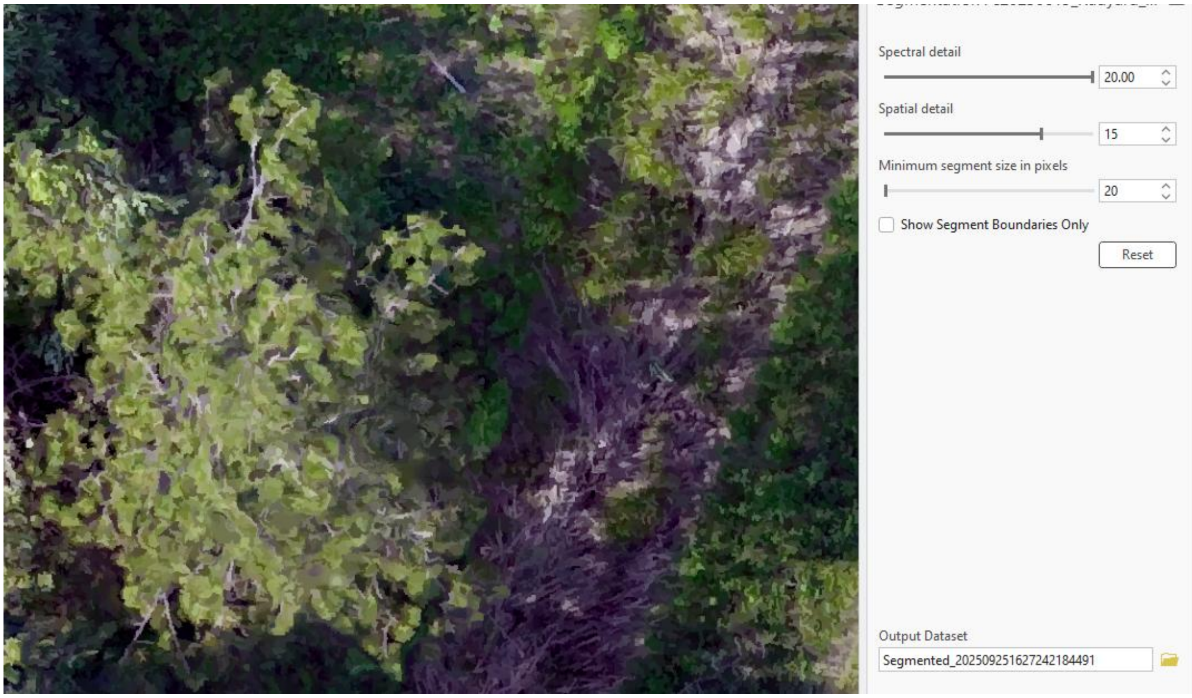

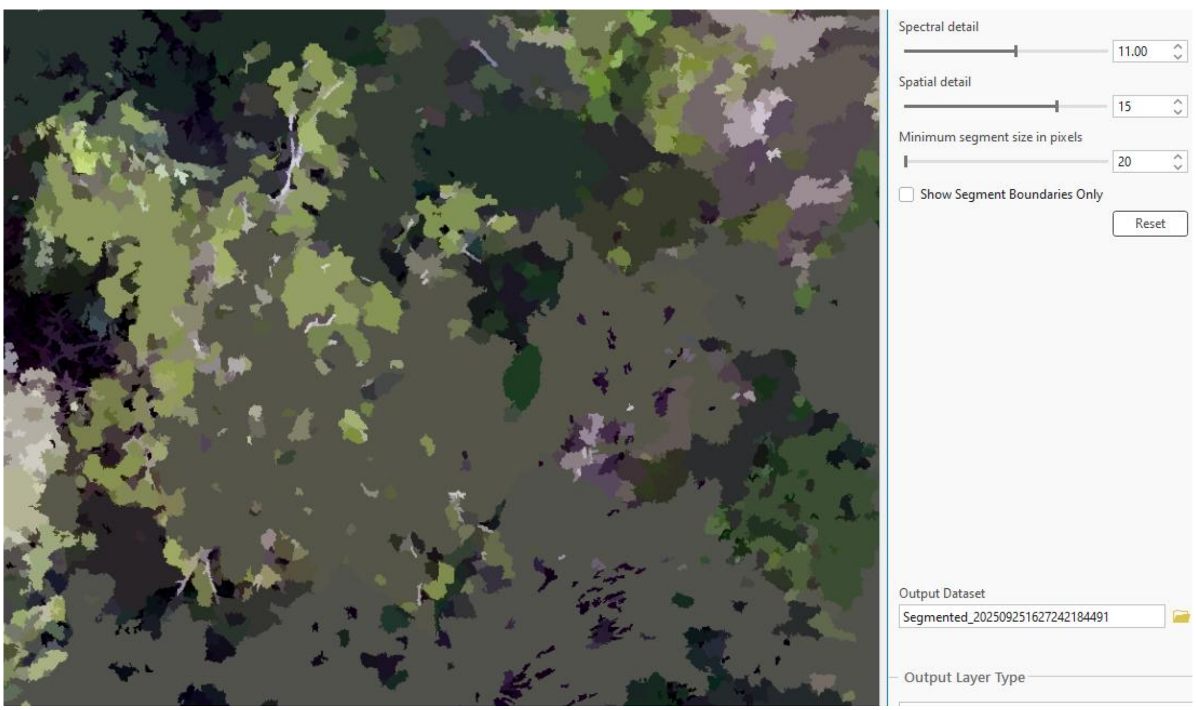

Similarly, spectral resolution increases the number of shades being blended together, creating larger and less complex polygons, or decreases the number of shades being blended together, creating smaller and more complex polygons.

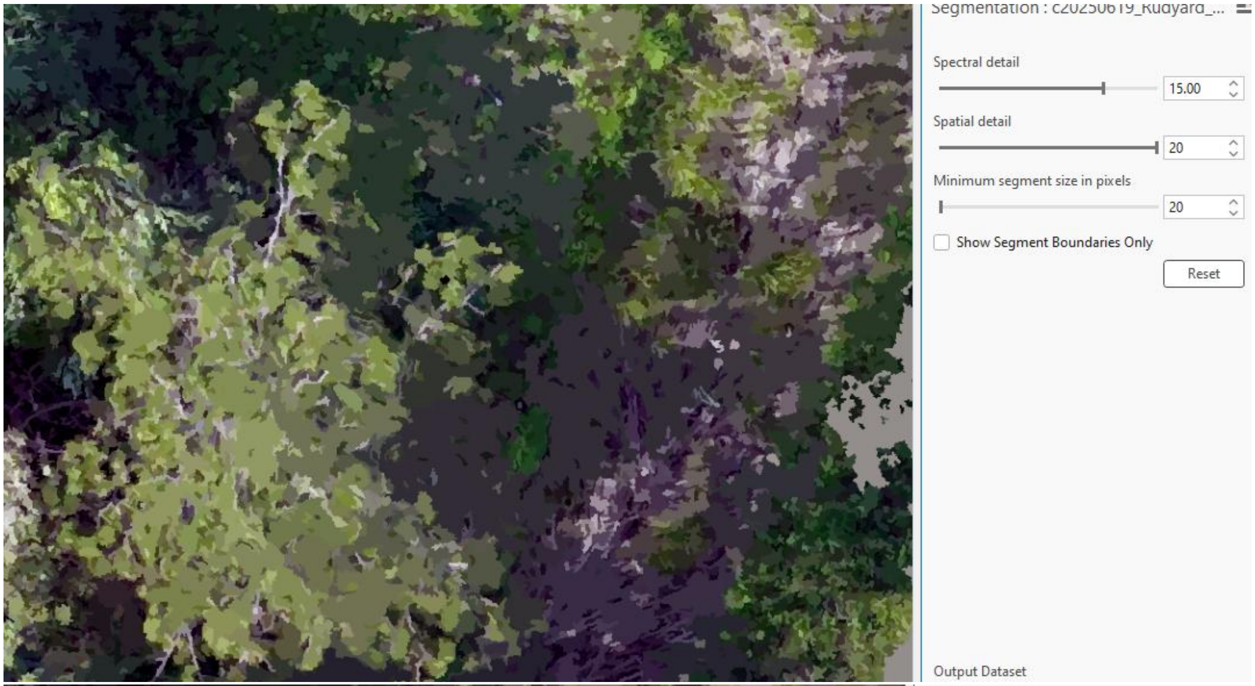

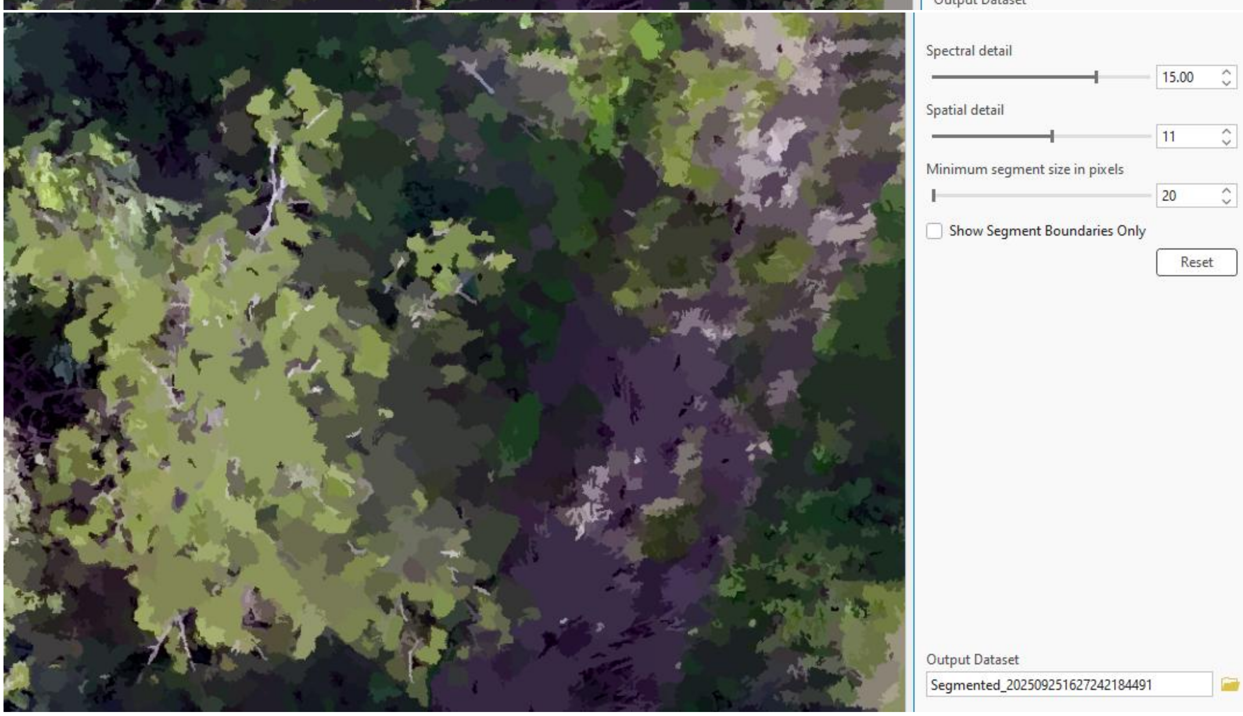

Certain situations will require different levels of each of these parameters, so it is always important to try a few configurations based on some simple questions. I.e. Am I dealing with solitary objects that blend in with their surroundings fairly well? In this case, you may want to decrease spatial resolution while increasing the spectral resolution. Am I dealing with large monocultures? A lower spatial resolution generally helps with monocultures, but the spectral resolution would depend on the surroundings.

Step 2. Choose a classification method. An important choice in the workflow is whether to use a pixel-based or object-based classification. Pixel-based methods rely on the spectral values of individual pixels and extend those values across the image to identify similar features as chosen classes. This approach is common in regional land-cover mapping, where moderate-resolution imagery provides consistent pixel groupings across large areas. Object-based methods classify image segments created during the preprocessing stage. By considering not only spectral information but also shape, size, and spatial context, these methods are often better suited for high-resolution data. For example, object-based classification is frequently used in urban studies to distinguish rooftops, roads, and tree crowns that would be difficult to separate using pixel values alone. In practice, the resolution of the dataset is often the deciding factor, with object-based methods favored for detailed imagery and pixel-based methods applied to broader-scale analyses.

Obj. Based

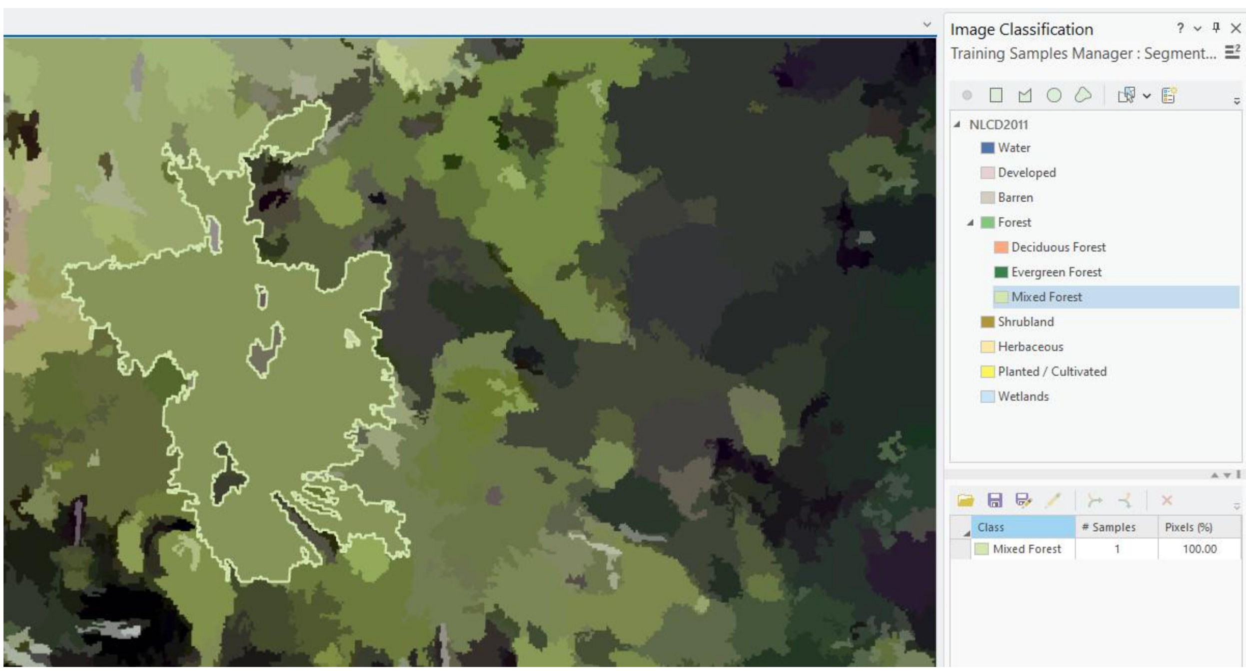

Pix. Based

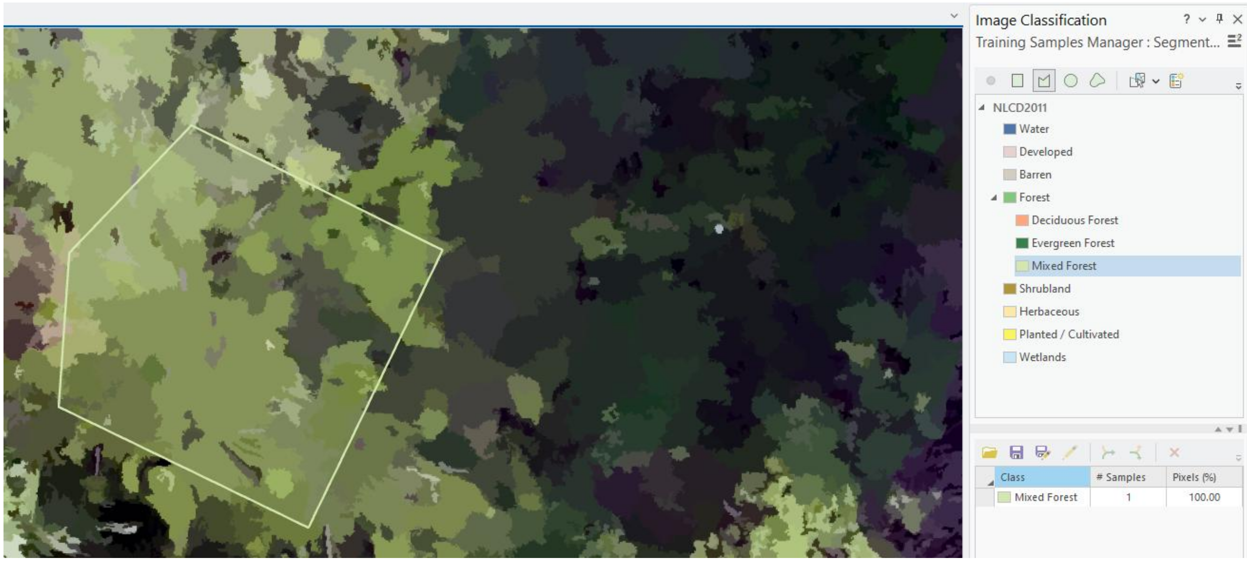

Step 3. Decide on which kind of algorithm to use. ArcGIS provides a set of predefined algorithms for calculating pixel values. While each has a similar framework, some require more user input than others and differ in how they handle complex data. In practice, certain algorithms are better suited to specific applications. For example, maximum likelihood can be effective for well-separated spectral classes, while random forest is often preferred for heterogeneous landscapes. Further details on the available methods are provided in Section 3.6. Once the appropriate algorithm is chosen and the required parameters are defined, the classification tool can be executed.

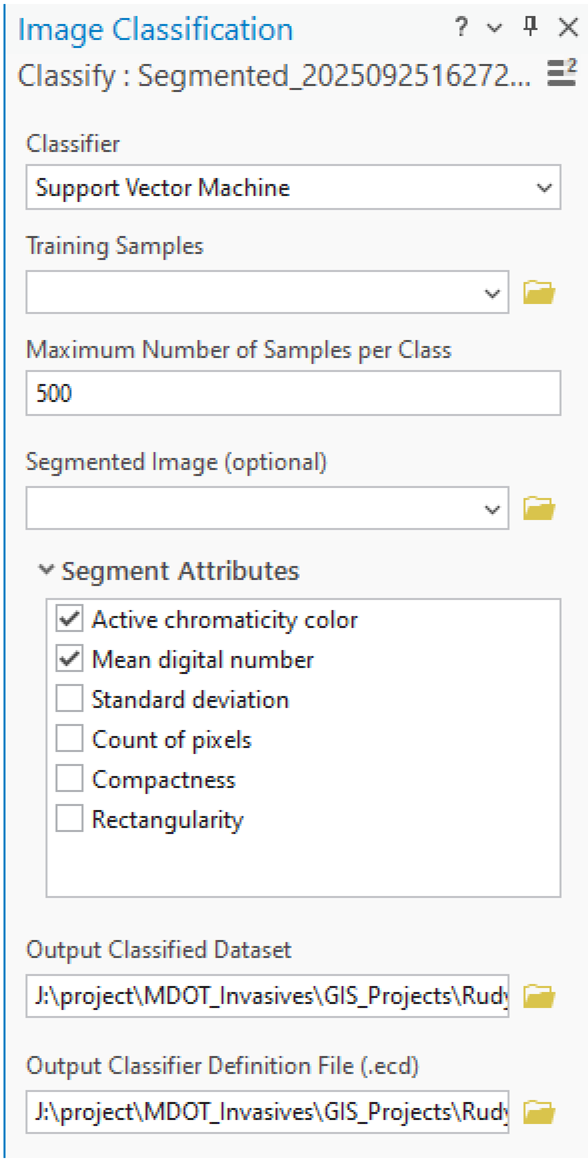
Image Classification
Classify : Segmented_2025092516272...
Classifier
Support Vector Machine
Training Samples
Maximum Number of Samples per Class
500
Segmented Image (optional)
Segment Attributes
Active chromaticity color
Mean digital number
Standard deviation
Count of pixels
Compactness
Rectangularity
Output Classified Dataset
J:\project\MDOT_Invasives\GIS_Projects\Rudy
Output Classifier Definition File (.ecd)
J:\project\MDOT_Invasives\GIS_Projects\Rudy

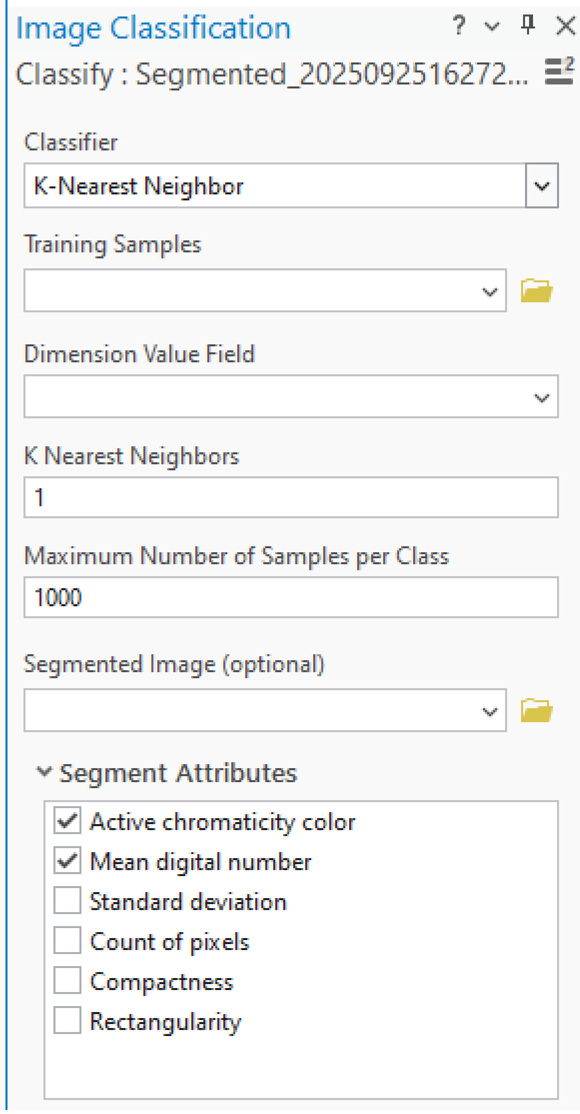
Image Classification
Classify : Segmented_2025092516272...
Classifier
K-Nearest Neighbor
Training Samples
Dimension Value Field
K Nearest Neighbors
1
Maximum Number of Samples per Class
1000
Segmented Image (optional)
Segment Attributes
Active chromaticity color
Mean digital number
Standard deviation
Count of pixels
Compactness
Rectangularity

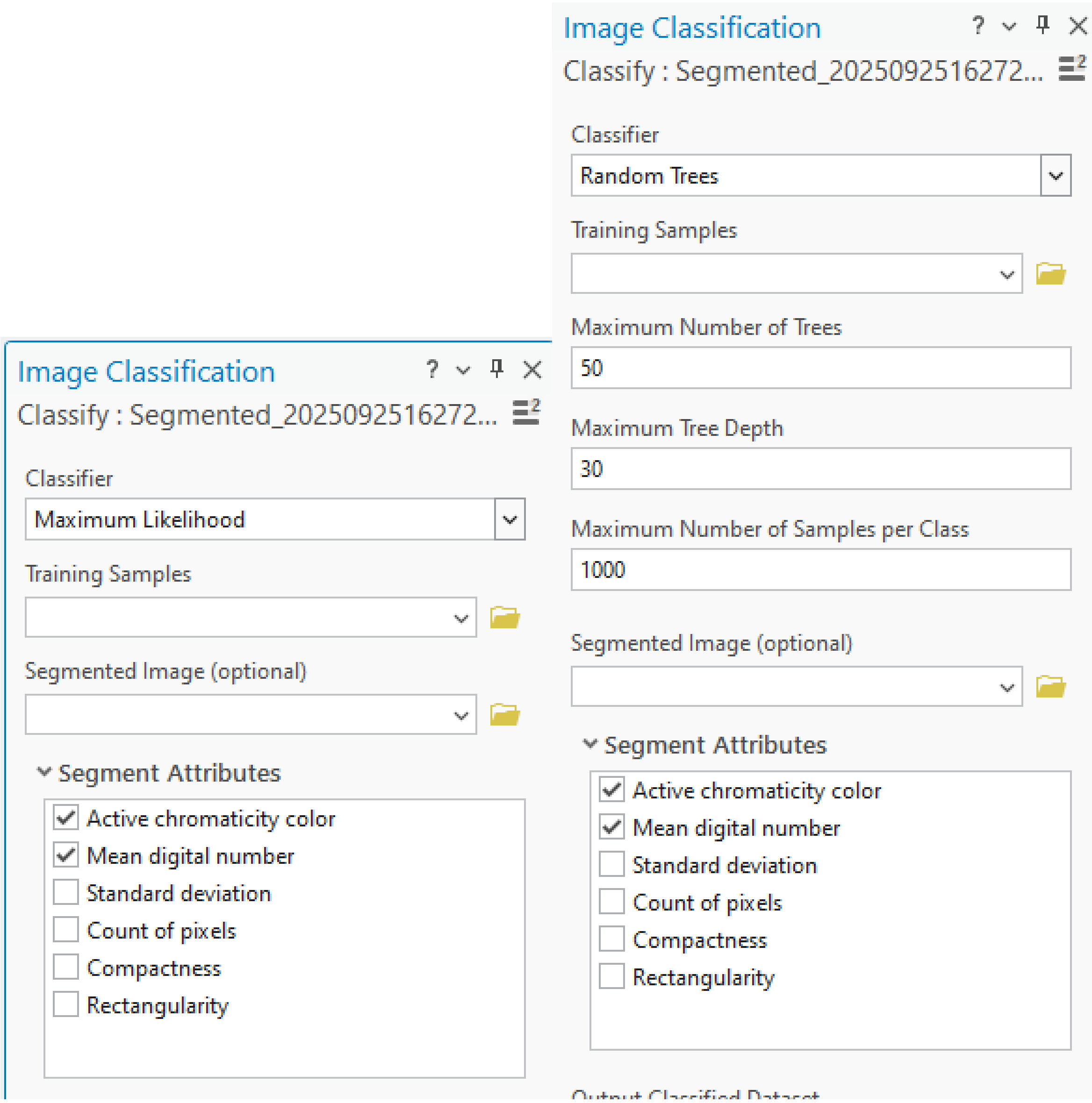

Step 4. Human error. This is an important consideration during the classification process, which is why incorporating ground-truth data from multiple sources within the study area is essential. Early iterations of a classification are often imperfect, and adjustments are usually required. This may involve adding more training samples to address underrepresented classes or removing problematic samples that introduce misclassification. Iterative refinement in this way improves the reliability and accuracy of the final output.

Step 5. Finishing up. Once the classification reaches an acceptable level of accuracy, further refinement can be applied depending on the intended purpose of the dataset. The Reclassify tool is often used to simplify results by consolidating several detailed classes into broader land-cover categories, or to align class values with a standard classification scheme required for reporting. The Merge Classes tool is especially useful when spectrally similar categories are producing confusion, such as combining multiple vegetation subclasses into a single forest class, or grouping different types of developed land into a general urban category. These steps help tailor the output to the analytical or management objectives of the project.

Converting Classification Raster to Shapefile (Optional)

Classification outputs are in a raster format. Here are the steps required to convert the output raster into a shapefile.

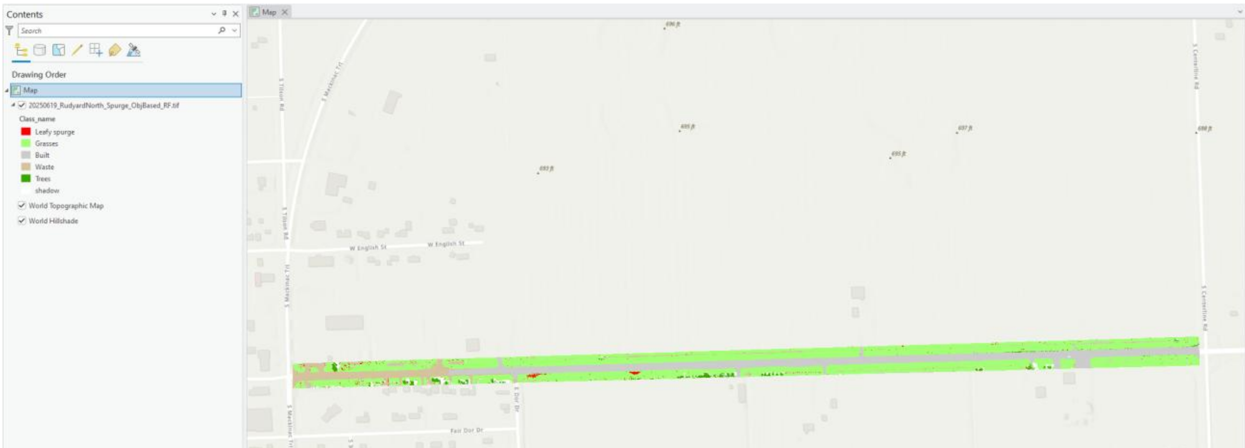

Step 1: In the “Geoprocessing” tab search for the “raster to polygon” tool.

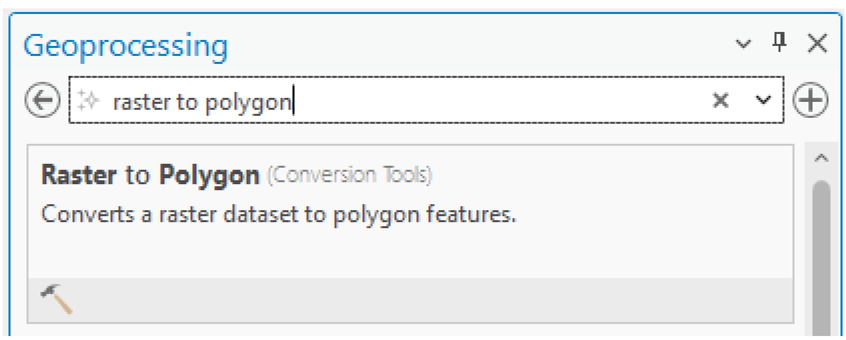

Step 2: Add in your classification raster as the input raster and add the location and name of the desired polygon shapefile output.

- Changing the “Field” parameter allows you to change the value by which the polygon is segmented.
- “Simplify polygons” checked box will create a smooth polygon appearance. If left unchecked, the polygon edges will follow the pixels from the raster.

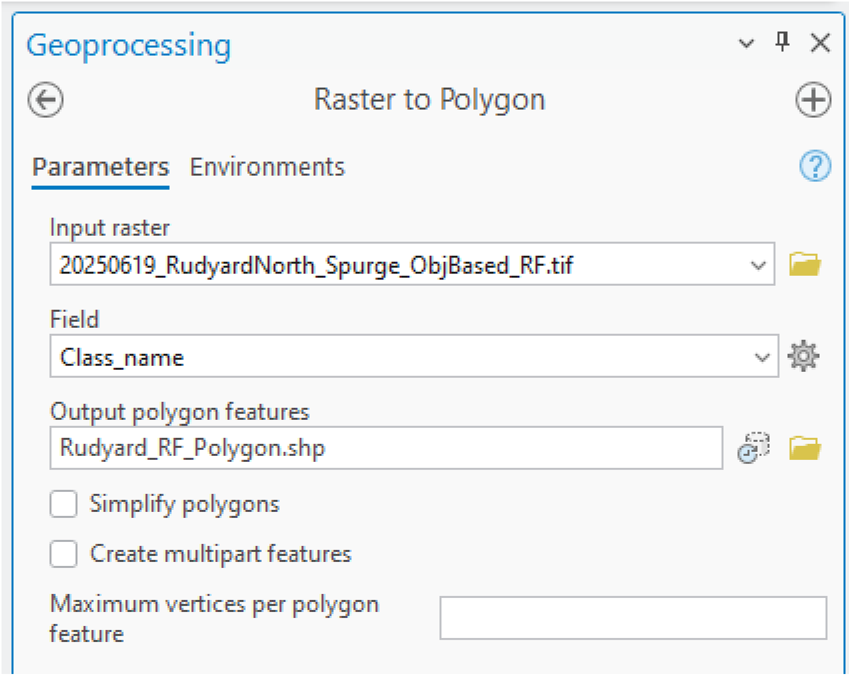

For extracting a polygon of only the target species

Before converting the raster to a shapefile, use the “Extract by Attributes” tool to extract only the class related to the species desired to create a new raster of only the pixels related to the species. This new raster can then be converted into a polygon.

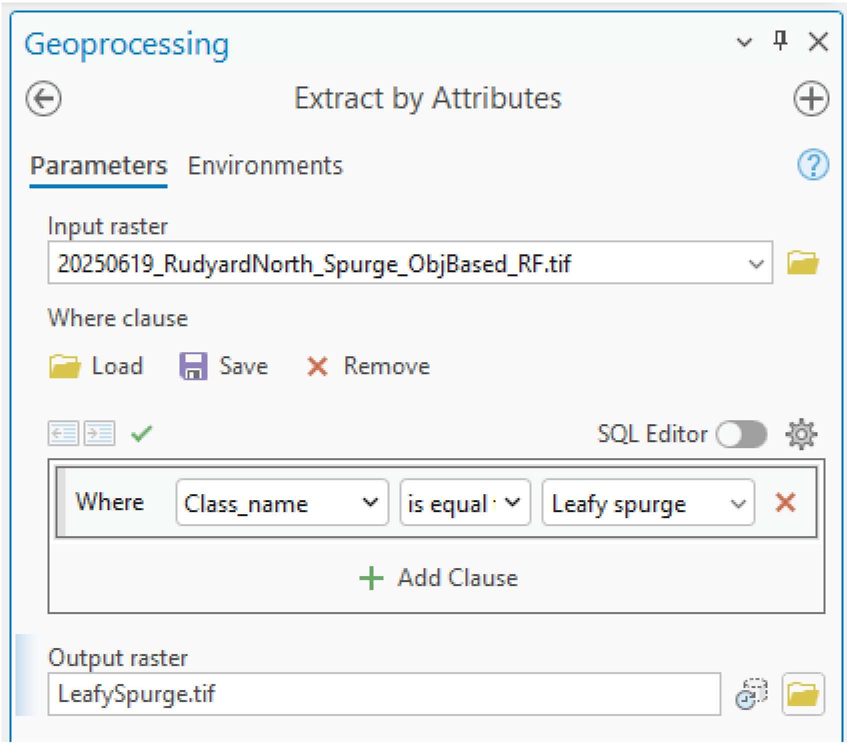

This new raster can then be converted into a polygon. Only red pixels (classified as leafy spurge) are shown below in the new raster.

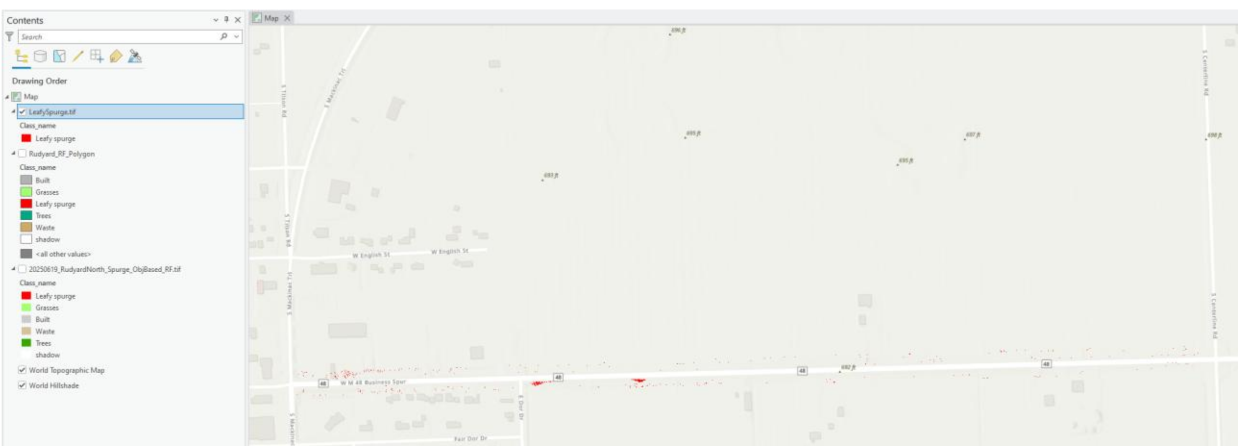

Appendix B

Literature Review

Michigan Department of Transportation

Invasive Species in Right-of-Ways

Literature Review

Michigan Technological Research Institute

Richard J. Dobson, Dr. Colin Brooks, Dorthea Vander Bilt, Chris Cook, Abby Jenkins, and Rebecca Lowe

Date: July 1, 2024

Table of Contents

Introduction

Invasive species can be detrimental to our communities and environment as they cause economic and ecological harm, including harm to humans, animals, and plant health. Additionally, invasive species are notoriously difficult to manage due to their aggressive ability to rapidly spread and outcompete native species, particularly in disturbed areas such as along roadways. This displacement of native species is harmful to Michigan's flora and fauna, and all residents who depend upon or appreciate access to the state's natural resources. Michigan's economy, which depends upon agriculture, logging, hunting, and tourism, necessitates well-maintained natural habitats and safe transportation corridors connecting them. Many problematic invasive plant species thrive in wide-open right-of-ways (ROWs) along transportation corridors maintained by the Michigan Department of Transportation (MDOT). Tall rapidly growing invasive species change road conditions through limiting visibility and dense root systems can alter drainage patterns or clog waterways. Some species also produce compounds toxic to animals and humans that pose safety concerns and have economic implications. MDOT is required to perform control of invasive species if they pose safety concerns to the traveling public, cause operational or maintenance related difficulties, or are regulated by government entities. MDOT manages more than 9,600 miles of road corridors and has surveyed thousands of miles of state and federal roads throughout Michigan for invasive plant species in the ROW environments. However, the threat of invasive species is constantly growing and changing with the introduction of new invasive species, as well as the spreading from existing invasive species populations. Early detection, tracking, and remediation to control these problematic invasive species is essential for the maintenance of these ROWs by MDOT.

Within Michigan's ROW, four invasive plant species of focus were selected to reflect MDOT's priorities, due to the scale and urgency of their current or potential impacts, as well as the species potential for being remotely sensed through characteristics such as texture, height, and color. These species were: common reed (*Phragmites australis)*, Japanese knotweed (*Fallopia japonica),* wild parsnip (*Pastinaca sativa)*, and leafy spurge (*Euphorbia esula)*. Tall and rapidly growing species, such as Phragmites and Japanese knotweed, can quickly change or limit road, sign, or other infrastructure visibility within a right-of-way. Other species, such as wild parsnip and leafy spurge, are highly toxic and pose threats to humans and animals if allowed to spread. This literature review will: 1) provide a brief background on each species, 2) provide an overview of relevant remote sensing platforms and image classification methods, and 3) address the past and present methodology for detecting each target invasive plant species through remote sensing. This information will help MDOT with the ability to identify, locate, monitor, and control invasive plant species along Michigan's ROWs.

Species of Focus

Common Reed (*Phragmites australis)*

Reeds in the *Phragmites* genus form tall grass communities and can be found throughout the temperate and tropical regions of the world (Saltonstall and Meyerson 2016). *Phragmites* *australis* subspecies *americanus,* P. M. Peterson & Soreng, is native to North America and fossil records show it was used by Native Americans for weavings, arrow shafts, musical instruments, cigarettes, among others for over 4,000 years (Figure 1) (Voss and Reznicek 2012, Swearingen and Saltonstall 2010, Saltonstall and Meyerson 2016). *Phragmites australis* (Cav.) Trin ex Steud subsp. *Australis,* also known as Haplotype M, was grown in Europe commercially for thatch, livestock, and is currently decreasing in its native ranges (Figure 1) (Swearingen and Saltonstall 2010). However, this European and Middle Eastern subspecies of *Phragmites australis* has aggressively spread throughout North America (Swearingen and Saltonstall 2010, Saltonstall and Meyerson 2016, Voss and Reznicek 2012). It was introduced to the United States through ballast material in the late 1700s and early 1800s along the Atlantic coast (Saltonstall and Meyerson 2016, Swearingen and Saltonstall 2010). It has since spread throughout the United States and Canada, forming large, dense monocultures that push out other plants (State of Michigan: Phragmites (Common Reed), Swearingen and Saltonstall 2010). Non-native *Phragmites* was first collected in Michigan in 1979, has had its highest concentrations around southeast Michigan (Voss and Reznicek 2012), and continues to spread throughout the Great Lakes region (Bourgeau-Chavez et al. 2013).

Non-native *Phragmites* negatively affect the biodiversity and ecosystem functions of habitats it invades (Voss and Reznicek 2012, Braun et al. 2016, Swearingen and Saltonstall 2010). It is able to spread into a variety of habitats and saline conditions from more urban or disturbed regions (e.g. urban wetlands, ditches, roadways) to lakeshores, tamarack swamps, marshes, fens, and even standing water up to 1.8m (Voss and Reznicek 2012, Michigan Department of Environment, Great Lakes, and Energy). The dense monocultures, growing up to 15 feet tall, crowd out native species, including native *Phragmites,* decreasing habitat, can alter wetland hydrology, and increase fire risk (Swearingen and Saltonstall 2010, Michigan Department of Environment, Great Lakes, and Energy). Non-native *Phragmites* can also have negative economic impacts as it devalues shorelines and reduces recreational or aesthetic benefits. Between 2010 and 2015, over $16 million was spent on researching and mitigating the spread of non-native *Phragmites* in the Great Lakes (Braun et al. 2016). Recommended treatment methods are dependent on stand density, propagule pressure, water levels, and nutrient inputs but often include foliar herbicide treatments followed by mechanical (mowing or burning) removal of standing dead biomass.

Despite the overlap in habitat, non-native *Phragmites australis* and native *Phragmites* subsp. *americanus* can be differentiated through their physical characteristics, though genetic testing is more accurate (Swearingen and Saltonstall 2010, Voss and Reznicek 2012). Non-native *Phragmites* grow in very tall, rigid, dense stands 6-15 feet tall and have standing biomass that persists throughout all seasons. The lower stem internodes are dull yellow to yellow brown with no texture or spots and leaf sheaths persist throughout the winter, hugging closely to the stem (Swearingen and Saltonstall 2010, Voss and Reznicek 2012). Leaves are alternate, entire, and blue-green in color. Native *Phragmites* grow much more sparsely, intermingling with other native species. Its leaves are a lighter yellow green and the leaf sheaths fall off once the plant scenes, exposing a reddish-purple stem internode (Swearingen and Saltonstall 2010, Voss and Reznicek 2012). Stems are delicate, smooth and shiny, often chestnut in color with black spots from a native fungus, and do not always persist through winter. Native *Phragmites* flower 3-4 months after spring growth and have sparse plumes compared to non-native *Phragmites*. Non-native *Phragmites* flower in August and September with large bushy plumes with each plume sourcing 100-1000 seeds a year (Swearingen and Saltonstall 2010). It can also spread asexually and vegetatively through rhizomes (Department of Environment, Great Lakes, and Energy, Swearingen and Saltonstall 2010). The dense network of rhizomes go down several feet and can extend 10-13 feet from the plant in one growing season. Non-native *Phragmites* can also be spread through rhizome fragments floating downstream or being carried on boats or machinery (Swearingen and Saltonstall 2010).

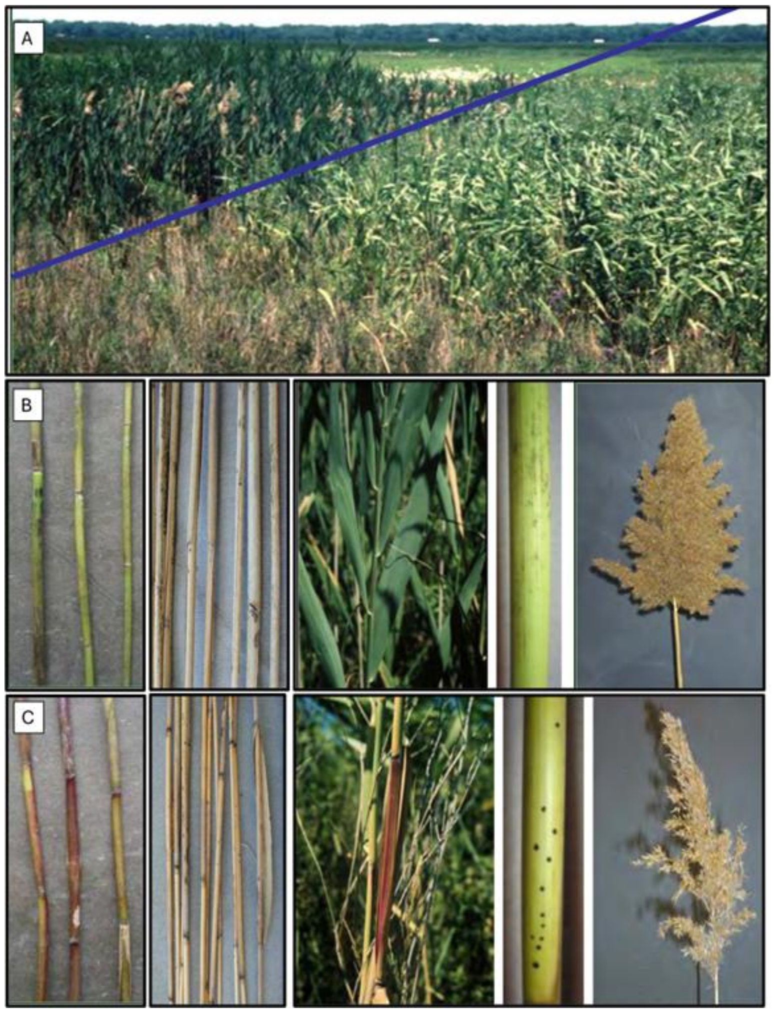

Figure 1. *Phragmites australis* subspecies comparison from Swearingen and Saltonstall 2010. A) comparison of color and stature of non-native (top) and native (bottom) subspecies, B) stems, leaves, and plume from non-native *Phragmites australis,* C) stems, leaves and plume from native *Phragmites australis* subsp. *americanus*.

Japanese Knotweed (*Fallopia japonica)*

Japanese knotweed (*Polygonum cuspidatum* Sieb. & Zucc. or *Fallopia japonica* (Houtt.) Ronse Decr.) is a perennial plant native to east Asia (Voss and Reznicek 2012) that has caused serious biodiversity and human impacts as it spread globally (Figure 2) (Lowe at al 2021, Aguilera et al. 2012, Herben 2004). Due to its showy flowers, Japanese knotweed became a popular garden plant and was widely spread throughout Europe and North America, even winning the most "interesting" plant of the year in 1847 from the Society of Agriculture and Horticulture (Bailey and Conolly 2000, Barney 2006, Townsend 1997). Japanese knotweed was first collected in Michigan in 1919 in Wayne County and has spread rapidly along riverbanks, railroads, roadways, right-of-ways, construction sites and filled grounds, dumps, and ditches (Voss and Reznicek 2012, Smerdu et al 2020). By 2006, Japanese knotweed was found in almost every state in the continental United States and Alaska as well as 9 of the 10 Canadian provinces (Barney 2006).

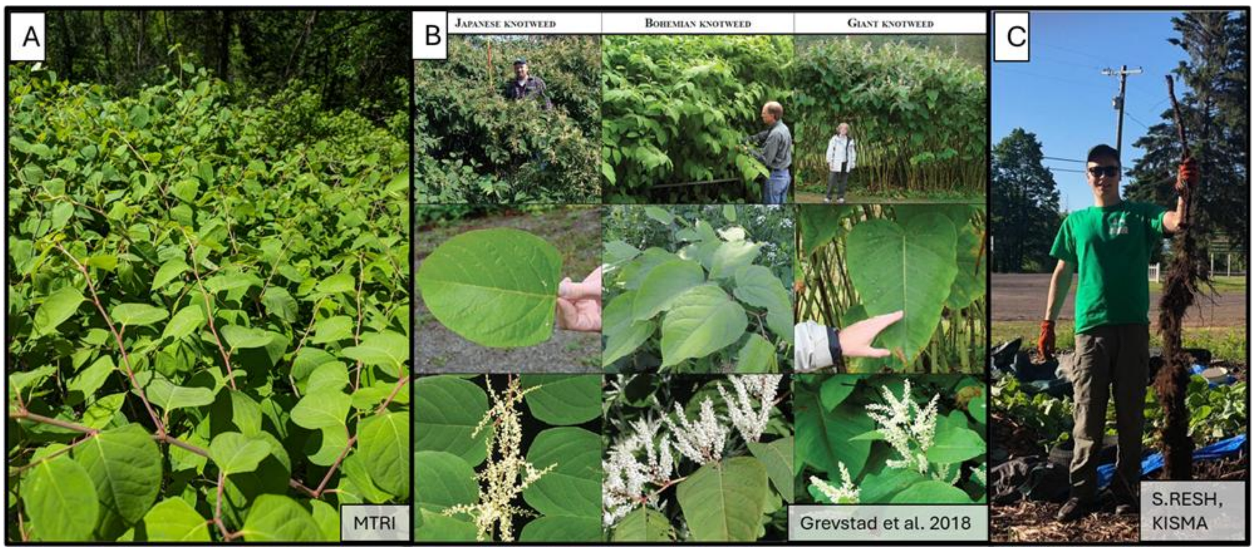

Figure 2. Japanese knotweed characteristic for identification, including: A) leaves and branching red stems, B) Japanese knotweed size, leaves, and flowers compared to other invasive knotweeds, C) deep rhizomes from Japanese knotweed.

Japanese knotweed is typically shade intolerant and requires abundant moisture, leading it to grow abundantly in riparian zones, wetlands, near water bodies and along roadsides with drains (Beerling et al. 1995 and Zhang 2015). In its natural habitat, it is a pioneer species, growing on volcanic slopes (Tezuka 1961, Adachi et al. 1996a) which allows Japanese knotweed's root system to break through pavement, building foundations, walls, and drainage infrastructure (Zhang 2015, Beerling 1991). Japanese knotweed can spread clonally with rhizomatous growth underground as well as sexually through seeds (Oborny et al. 2000, Moola and Vasseur 2009). The rhizomes are dark and knotty with an orange inside and emerge each year from late April to July. Initial sprouts resemble asparagus shoots, but quickly grow into dense thickets greater than 6 feet tall (Shaw et al. 2009, Voss and Reznicek 2012). Stems are tall, hollow, similar to bamboo, and have reddish purple spots (Voss and Reznicek 2012, Barney et al. 2006). The hollow stems help knotweed spread in moving water and have even been observed crossing open seas (Barney et al 2006). Japanese knotweed leaves are alternate, heart shapes, entire, and roughly 2-6 inches across. The leaves remain photosynthetically active throughout the fall until the first frost prompts the leaves to turn a rusty orange. From August through September, Japanese knotweed will produce small creamywhite flowers that grow on long terminal racemes 3-6 inches long (Barney et al. 2006). Japanese knotweed is difficult to remove once it is established and treatment, whether manual or chemical, needs to be sustained for several years in order to remove it (Richards et al 2012). Best management practices for the eradication of Japanese knotweed in Michigan are currently being studied (MISGP Grant #IS20-5003).

Leafy Spurge (*Euphorbia esula*)

Leafy spurge (*Euphorbia esula* L.) is a long-lived perennial originating in cool moist places in Eastern Europe and Russia (Figure 3) (Croizat 1945). It was first recorded in Michigan in 1885 in Ingham County but remained rare in Michigan through the 1930s despite spreading rapidly throughout the continental United States (Voss and Reznicek 2012, Hanson and Rudd 1933). By 1985, leafy spurge was well established as an invasive species across 1 million acres of the United States and Canada (Alley and Messersmith 1985). It is commonly found in rocky slopes and disturbed areas such as along roadsides, railroads, right-of-ways, gravel pits (Voss and Reznicek 2012, Alley and Messersmith 1985) as well as cultivated land, rangeland, meadows, and pastures (Alley and Messersmith 1985**,** Dunn 1979**,** Hanson and Rudd 1933). The invasion of leafy spurge into pasture and rangeland is particularly problematic as it displaces of native foraging plants and more significantly, is toxic to livestock when ingested (Dunn 1979). All parts of the plant produce a sticky white latex sap that causes dermatitis upon contact and can lead to severe illness or death if ingested (Hanson and Rudd 1933, Dunn 1979, Noxious Weed Program 2018).

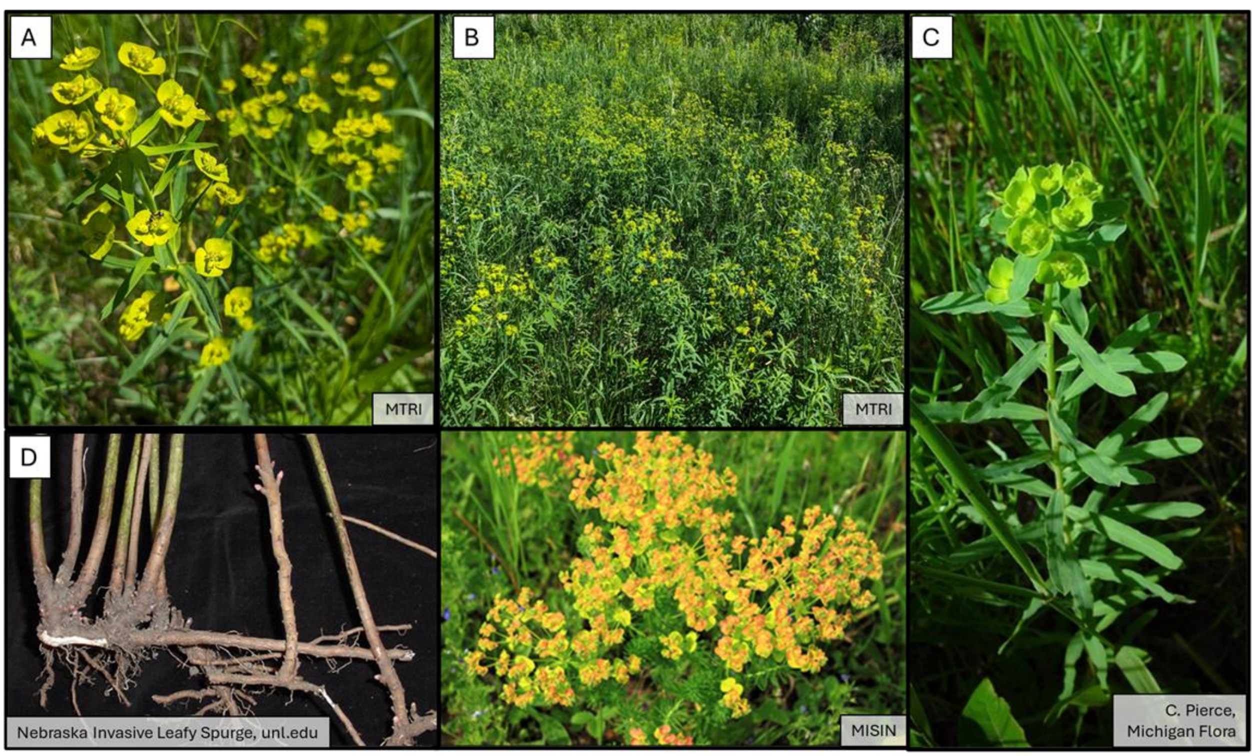

Figure 3. Leafy spurge characteristics for identification, including: A) cup like bracts flowering in early summer, B) dense monocultures formed of leafy spurge replacing native vegetation, C) entire opposite blue-green leaves and D) seeding heads.

Leafy spurge grows from the base with several unbranched stems and distinctive opposite, simple, entire, blue-green color leaves that are weakly veined except for the midrib (Hanson and Rudd, 1933, Noxious Weed Program 2018, Croizat 1945, Voss and Reznicek 2012). The mature plant can grow 14-48 inches tall and become somewhat woody at the base (MISIN 2016, Hanson and Rudd 1933, Noxious Weed Program 2018). Leafy spurge has the ability to propagate vegetatively through root segments and root buds, as well as sexually through seeds (MISIN 2016, Dunn 1979, Hanson and Rudd 1933, Croizat 1945, Alley and Messersmith 1985). Networks of tough woody roots and flexible secondary roots extend from a central tap root and can penetrate 2-8 feet below the ground (Hanson and Rudd 1933). Along these roots are pink root buds that can send up shoots from depths of 8-21 inches, if the above ground plant is removed (Hanson and Rudd 1933, Dunn 1979, MISIN 2016, Alley and Messersmith 1985). Leafy spurge flowers in the early summer starting at the end of May and continuing into June (Hanson and Rudd 1933, Noxious Weed Program 2018, MISIN 2016), though if mowed the flowering may be delayed (Hanson and Rudd 1933). The flowers are small yellow-green with fused cup-like involucre, or bracts, and grow in clusters (Hanson and Rudd 1933, MISIN 2016, Voss and Reznicek 2012). Fruit begins to form mid-July and continues through September, when the plant turns a characteristic yellow or reddish-orange (Hanson and Rudd 1933). Seeds can be launched by the seedpod 13-20 feet away from the parent plant (Noxious Weed Program 2018, Hanson and Rudd 1933) or spread by animals and birds (Hanson and Rudd 1933). Seeds can persist and remain viable in the seed bank (i.e. seeds that are stored in the soil or leaf litter) for up to 8 years (Alley and Messersmith 1985, MISIN 2016).

Current treatment options for leafy spurge involve biocontrols, herbicide, and manual techniques (Alley and Messersmith 1985). Mowing can reduce seed production, however repeat mowing can initially increase density as root buds resprout (Hanson and Rudd 1933, Noxious Weed Program 2018). Therefore, mowing is most beneficial if followed by herbicide treatments on the resprouts. Repeated herbicide during the spring and fall can also reduce spurge populations (Noxious Weed Program 2018).

Wild Parsnip (*Pastinaca sativa*)

Wild parsnip (*Pastinaca sativa* L. Apiales: Apiacea, subspecies Pastinaca sativa ssp. sativa) is a European native herbaceous root vegetable closely related to parsley and carrots (Figure 4) (Kennay et al. 2017, Voss and Reznicek 2012, Baranová 2021). The white tap root on wild parsnip is edible and was eaten in ancient Greece and Rome (Voss and Reznicek 2012, Kennay et al. 2017). Wild parsnip was first recorded in Michigan's Keweenaw, Emmet, and Ingham counties as early as1836 but was not collected until 1871 in Wayne County (Voss and Reznicek 2012). It now is found commonly throughout the United States and Canada, particularly in roadsides, railroads clearings, fields, meadows, pastures and agricultural landscapes (Voss and Reznicek 2012, Cornell University 2017, Baranová 2021, Kennay et al. 2017). Wild parsnip prefers sunny, nutrient rich habitats but can tolerate moist to dry conditions, open forests and thickets, and disturbed landscapes (Voss and Reznicek 2012, Baranová 2021, Cornell University 2017).

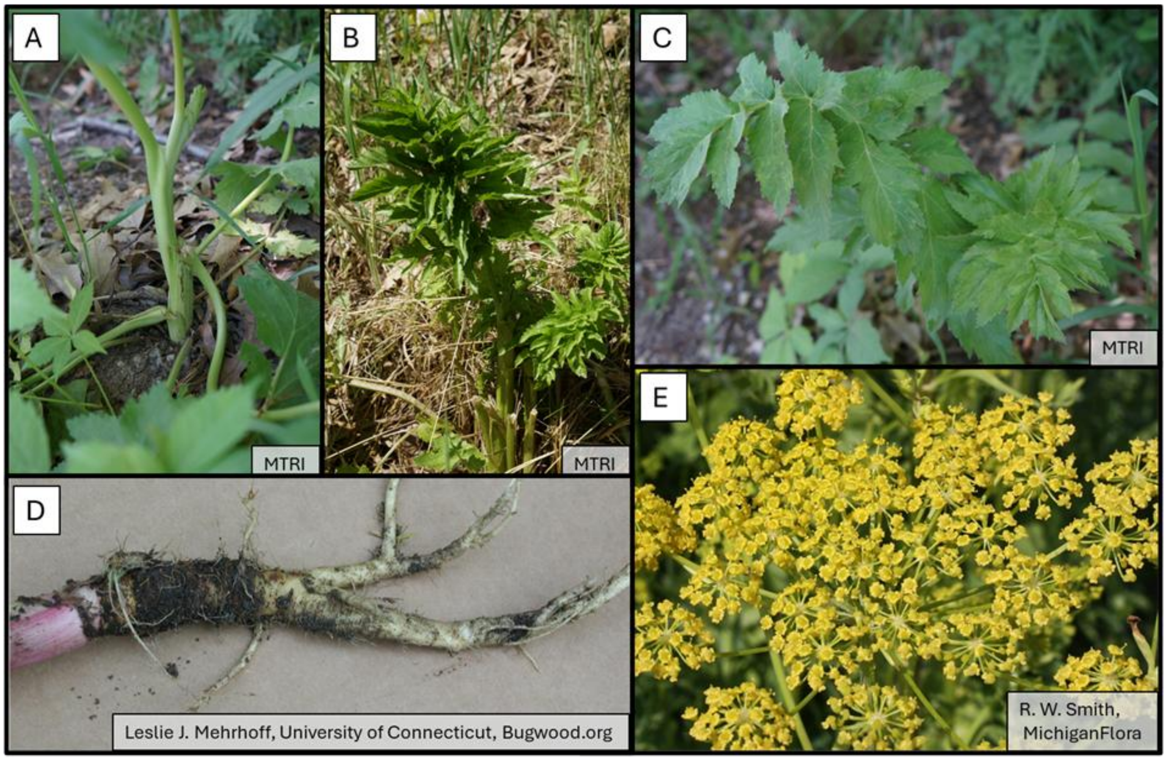

Figure 4. Wild parsnip characteristics for identification, including: A) light green ridged stem, B) leafy first year rosettes, C) toothed leaflets, D) tap root, and C) yellow flowers growing in clustered umbels.

Wild parsnip is most often a biennial, requiring 2 years to mature, but can also behave as a perennial (Kennay et al. 2017, Baskin and Baskin 1979, Gleason and Cronquist 1991). The first year, the plant's energy is put into growing a deep tap root and a basal rosette 5-15 inches tall (Cornell University 2017, Kennay et al. 2017). The second or third year, the same plant will grow much larger, 3-5 ft tall, before flowering and dying (Baranová 2021, Kennay et al. 2017, Cornell University 2017). Wild parsnip has a light yellow-green, deeply grooved stem and alternate pinnately compound leaves (Kennay et al. 2017, Cornell University 2017). Each leaf has 5-15 leaflets, 6-13 inches long, with deep serration or lobes (Gleason and Cronquist 1991, Kennay et al. 2017, Martinson et al. 2021, Cornell University 2017). Wild parsnip can be differentiated from others in its family by its yellow flowers starting as early as June and lasting into September (Kennay et al. 2017, Baranová 2021, Cornell University 2017). Each flower has 5-petals and flowers are clustered in terminal umbels (Kennay et al. 2017, Cornell University 2017). Seeds are smooth with ribbed edges, ¼ in long, bright green then becoming brown. One plant can produce up to 1,000 seeds, which can survive in the soil for 4 years (Cornell University 2017).

The main concern surrounding the spread of wild parsnip is human and livestock exposure to the furanocoumarins chemicals that are produced in the sap of all above ground plant parts (Martinson et al. 2021, Cornell University 2017). These chemicals cause severe burns to the skin that are photosensitive (phytophotodermatitis) and discoloration on the skin can last from 6-months to 2 years (Martinson et al. 2021, Stegelmeier et al. 2019, Walling and Walling 2018, Cornell University 2017). Wild parsnip is most irritating when flowering but remains toxic even when dried and in hay (Martinson et al. 2021). If exposed, it is recommended to immediately cover with a wet cloth and keep away from the sun (Cornell University 2017). The chemicals in wild parsnip can also cause allergies, burns, lesions and sores through the blood vessels under the skin if ingested by livestock, particularly horses and goats (Walling and Walling 2018, Stegelmeier et al. 2019, Martinson et al. 2021).

The recommended management for wild parsnip is to cut or pull the plants before seeding (Kennay et al. 2017). Mowing and burning can increase sunlight, promoting native species to outcompete wild parsnip, however doing so at the wrong time can also increase the number of seedlings and the success of maturing for wild parsnip by the same mechanism (Kennay et al. 2017). Chemical treatment can be applied in the shoulder seasons (March-May and Aug-Oct) to the basal rosettes and herbaceous plants before they become woody (Martinson et al. 2021, Kennay et al. 2017). Biocontrols, such as the parsnip webworm, can severely damage individual plants but have not successfully eradicated wild parsnip stands (Kennay et al. 2017).

Remote Sensing Platforms and Image Classification

Remote Sensing Platforms

Remote sensing for vegetation detection and identification has been an invaluable method of applied research for several decades. While satellite remote sensing was initially developed primarily for defense-oriented purposes in the 1950s and 60s, the use of satellite remote sensing for earth observation started with the launch of Landsat-1 (Campbell, 2011). The NASA Landsat series of satellites has been observing the Earth since 1972: Landsat-1 (1972), -2 (1975), -3 (1978), -4 (1982), -5 (1984), -7 (1999), -8 (2013), -9 (2021), and -Next (expected 2031). The Landsat series is the world's longest running system of satellites for moderate-resolution optical and multi-spectral remote sensing for land, coastal areas, and shallow waters. Other satellite missions primarily mentioned in the literature for this review include passive sensors: NASA Hyperion (hyperspectral), MAXAR Digitalglobe Worldview-1 through 3 (high-resolution multispectral), Planet Labs PlanetScope constellation (high resolution multispectral), European Space Agency (ESA) Sentinel-2 through 3 (multispectral), and NASA Landsat (multispectral), as well as active radar sensors: Japan Aerospace Exploration Agency (JAXA) PALSAR and PALSAR-2 (L-band radar), Canadian Space Agency RADARSAT and RADARSAT-2 (C-band radar).

Passive sensor satellites vary in their onboard sensors and data that they collect, but can include the capture of optical (red-green-blue bands), thermal, multispectral (3-36 bands), and hyperspectral (36+ bands) imagery. Multispectral and hyperspectral imagery are useful for distinguishing vegetation types based on cellular level interactions with leaf chlorophyll and water content that can lead to distinct spectral signatures for plants. Comparisons of species unique spectral curves can be used to inform the best bands to use in order to target different species. Additionally, combinations of multispectral bands have made satellites like Landsat and Sentinel very useful for the estimate of band-specific indices like Normalized Difference Vegetation Index (NDVI) and Enhanced Vegetation Index (EVI). Measurements of vegetation properties like greenness using these indices allow for normalized and relative but robust comparisons of vegetation across an image or series of images. The use of such indices have shown utility for measuring crop, and tree crown health, and identifying invasive species.

Active sensors such as radar, multi-frequency synthetic aperture radar (SAR) and light detection and ranging (LiDAR), emit pulses of energy at different wavelengths which can detect feature characteristics such as structure or moisture (Table 1). In addition to satellite sensors, aerial systems (mounted and flown as payload on airplanes) and drone-based sensors were also surveyed.

Table 1. Summary of passive and active sensors and their characteristics frequently used for natural resource earth observations, such as plant species and functional type mapping.

Satellite / System	Spatial Resolution	Sensor / Spectral Bands	Temporal Revisit	Years of Operation	Accessibility	Utility for Mapping Invasive Species	Source
Landsat-7	15-30m	Multispectral - 8 bands	16 days	1999-2022	Openly Available	Moderate	NASA/USGS
Landsat-8	15-30m	Multispectral - 11 bands	16 days	2013-current	Openly Available	Moderate	NASA/USGS
Landsat-9	15-30m	Multispectral - 11 bands	16 days	2021-current	Openly Available	Moderate	NASA/USGS
Landsat-Next	10-20m	Multispectral - 26 bands	6 days	Launch in 2031	N/A	High	NASA/USGS
NAIP	0.6-1m	Multispectral - 4 bands	1x 3 years	2003-current	Openly Available	High	USDA
PlanetScope	3m	Multispectral - 8 bands	daily	2016-current	Moderate	High	Planet Labs
SEMCOG	~1m	Multispectral - 4 bands, LiDAR	1x 5 years	1949-current	Available from counties	High	Michigan Counties
Sentinel-2	10-20m	Multispectral - 13 bands	5-10 days	2015-current	Openly Available	High	ESA
Sentinel-3	10-20m	Multispectral - 21 bands	13-27 days	2016-current	Openly Available	High	ESA
SPOT 7	6m	Multispectral - 5 bands	daily	2014-2023	Limited	Moderate	ESA
Worldview-2	1.8m	Multispectral - 8 bands	1-3 days	2009-current	Expensive	Very High	Maxar
Worldview-3	1-4m	Multispectral - 29 bands	1-3 days	2014-current	Expensive	Very High	Maxar
AVIRIS	20m	Hyperspectral - 224 bands	N/A	2006-current	Openly Available	High	NASA/JPL
CASI	1m	Hyperspectral - 288 bands	N/A	2007- current	Limited	High	NASA/Others
Hyperion (EO-1)	10-30m	Hyperspectral - 220 bands	16 days	2000-2017	Openly Available	High	NASA
HySpex Mjolnir	<1m - 10m	Hyperspectral - 400-700 bands	N/A	1995-Current	Very Limited	High	HySpex
PALSAR	3m	L-Band Radar, Dual- or Quadpol	46 days	2006-2011	Openly Available	Moderate	JAXA
PALSAR-2	3-10m	L-Band Radar, Dual- or Quadpol	14 days	2014-current	Openly Available	High	JAXA
RADARSAT	5-100m	C-Band Radar, Dual- or Quadpol	24 days	1995-2008	Openly Available	Moderate	ESA
RADARSAT-2	5-100m	C-Band Radar, Dual- or Quadpol	24 days	2008-present	Openly Available	Moderate	ESA
Sentinel-1	5-20m	C-Band Radar, Dualpol	6-12 days	2014-current	Openly Available	Moderate	ESA

In this of this literature review, it was found that multispectral imagery from Sentinel-2, Worldview-2, and PlanetScope, which have a greater spectral, spatial, and temporal resolution, were often used for a more detailed view of invasive plant species over Landsat. Sentinel-2, launched by The European Space Agency (ESA) in 2015, has two satellites in orbit with high-resolution multispectral images and has been 83-90% successful in identifying Japanese knotweed with a support vector machine (SVM) algorithm as seen in the research (Smerdu et al., 2020) and *Phragmites*, especially in buffer areas like the MDOT's right-of-way. While Sentinel-2 allows for the classification of large regions and has high temporal resolution, the 10-meter spatial resolution may not be sufficient for all mapping applications, such as identifying individual plants or small patches of invasive species.

High-resolution commercial satellites like the Worldview constellation, which have a greater spatial resolution than Sentinel-2, can be costly to acquire and are more limited in their collection timing and footprints, and thus challenging to scale to large regions. PlanetScope "smallsat" imagery is a larger constellation of low-cost satellites, which greatly improve temporal resolution, but can still be costly for large areas to acquire imagery. SPOT 7 (Satellite Pour l'Observation de la Terre), from Airbus Defence and Space (originally CNES – the French space agency), has been used to detect dense patches of the yellow-green leafy spurge bracts in Colorado with 5 spectral bands (panchromatic, red (625–695 nm), green (530–590 nm), blue (450–520 nm), and near infrared (NIR, 760–890 nm)), a 6m spatial resolution, and a temporal resolution of 26 days (European Space Agency, 2022) (Mattilio, 2023).

Hyperspectral satellites and/or airborne platforms, like Hyperion (EO-1), AVIRIS, CASI, and HySpex, provide near continuous spectral data across the visual and infrared spectrum (wavelengths between 400-900 nm for VNIR and wavelengths between 900-2500 nm for SWIR) that allows for identification of unique spectral signatures of plants at a high spatial resolution (Papp et al., 2021). These data, when not made available by agencies like NASA or NOAA, are spatially limited and procuring this data can be prohibitively expensive. Data collected by plane or uncrewed aerial system (UAS or "drone") (e.g., AVIRIS, CASI, HySpex) are usually very limited in geographic scope, and freely available data are not likely to coincide with regions outside of NASA's funded research. Hyperion, a NASA satellite that collected data at moderate resolution (30m cell size) and 16 day revisit time from 2000-2017, is one of very few hyperspectral satellite systems with openly available data. Hyperion hyperspectral imagery has shown utility for mapping invasive species in Hawaiian rainforests (Somers, 2013), in addition to mapping invasive Phragmites in coastal wetlands. AVIRIS, in combination with advanced image classification algorithms like Random Forest (RF) and Support Vector Machines (SVM), has been used to locate leafy spurge with highest accuracies in the spring (74% accuracy) (Royimani et al., 2019), and has even been successful in detecting small infestations (Glenn et al., 2005).

Synthetic aperture radar (SAR) data acquired by satellites have demonstrated utility for species mapping efforts. The primary advantage for SAR is that it is an active sensor and can provide images day or night as well as penetrate through clouds ("NASA - Earthdata - PALSAR," 2024.). The intensity and polarization (e.g. wave direction, horizontal or vertical) of the returned energy allows for the differentiation of vegetation structure, biomass and moisture/inundation. In addition, the energy pulse can penetrate clouds and haze, which is an advantage in cloudy regions such as the Great Lakes. The frequency or wavelength of the radar allows for the differentiation of feature size with C-band data (5cm) penetrating dense emergent vegetation and sparse shrubs and L-band data (24cm) allowing for penetration of forested or dense shrub wetlands (Bourgeau-

Chavez et al. 2015). Other SAR bands include X-band (3cm) which provides high spatial resolution and does not penetrate vegetation and P-band (100cm) which can be used for vegetation mapping (Figure 5). Additionally, the scattering mechanism (volumetric, surface, or double bounce) based on the polarization of the energy helps differentiate if an area is vegetated, determine its relative density, and if there is also water present. This ability enables SAR sensors to be particularly useful in detecting inundated vegetation and vegetation with large biomass. SAR is also useful for measuring vegetation structure and density which is valuable for invasive species mapping and classification.

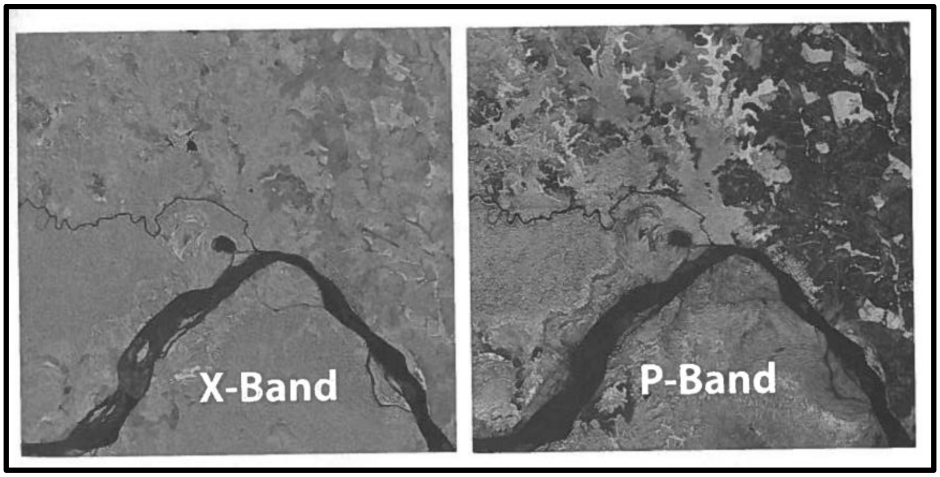

Figure 5: Comparison of X-Band (~3cm wavelength) and P-Band (~100cm wavelength) SAR imagery of Colombia. P-band achieves penetration through tree canopies to the vegetation and ground surface below, revealing flooding or land clearance, while X-Band interacts solely with the vegetation canopy. Image from Campbell, 2011.

Multi-frequency SAR has repeatedly been shown by MTRI research teams to accurately differentiate vegetation species (such as *Phragmites australis*, *Schoenoplectus* spp. and *Typha* spp.) from other wetland species based on the unique capabilities of the data (Battaglia et al. 2021, Bourgeau-Chavez et al. 2015, Ahern et al. 2022). Phased array SAR such as the L-band satellite PALSAR combined with multispectral Landsat imagery has been used for detection of phragmites (Bourgeau-Chavez et al., 2015) around the Great Lakes but found better results with larger stands. Use of the multispectral imagery allows for visualization and measurements of basic plant phenology and the chlorophyll of the plant, while the SAR is sensitive to the plant biomass and the moisture.

In addition to satellite-based remote sensing, there is also the use of manned aircraft and UAS/drones to collect aerial imagery. Aerial imagery, typically collected using airplanes or helicopters, can be useful for collecting moderate resolution (on the scale of 0.3m (12in)) imagery over a relatively large area. Aerial imagery available through NAIP and the Southeast Michigan Council of Governments (SEMCOG) is typically free to download, with most states recollecting NAIP imagery every 2-3 years (SEMCOG collects every 5 years). The Michigan Statewide Authoritative Imagery and LiDAR (MiSAIL) program also provides aerial imagery with 8 to 30cm (3 inch to 12 inch) resolution for every Michigan county every few years, and has been available for MDOT research programs. While NAIP, MiSAIL, and SEMCOG products provide an near infrared (IR) image band, their spectral resolution is limited relative to drone-based multispectral imagery. In addition, NAIP collections are typically performed during mid-summer to capture 'leaf-on' imagery, which limits the available data to periods not associated with plant senescence.

Previous and ongoing research efforts have worked to combine various satellite, aerial, and other imagery sources for the purpose of improved land cover classification. One example, the AllenAI (Bastani, 2024) remote sensing dataset, consists of aligned NAIP, Sentinel-2, Sentinel-1, Landsat 8/9, OpenStreetMap, and WorldCover imagery (Figure 6). This combination provides valuable information in a single data layer, including high resolution optical imagery (NAIP), multispectral imagery (Sentinel-2 and Landsat sources), radar images (Sentinel-1), building and road shapefile data (OpenStreetMap), and recent land cover information (WorldCover). MTRI has also used sensor fusion for various applications, including previously mentioned work in the Great Lakes using Landsat multispectral and PALSAR radar data (Bougeau-Chavez, 2015). Additionally, MTRI has shown the utility of using RADARSAT-2 radar and high-resolution WorldView-2 imagery for wetland type delineation, wetland gain and loss, and the classification of wetland plant species (Battaglia, 2021). The fusion of these data types allows for the input of more information into the image classifier providing improved classification results.

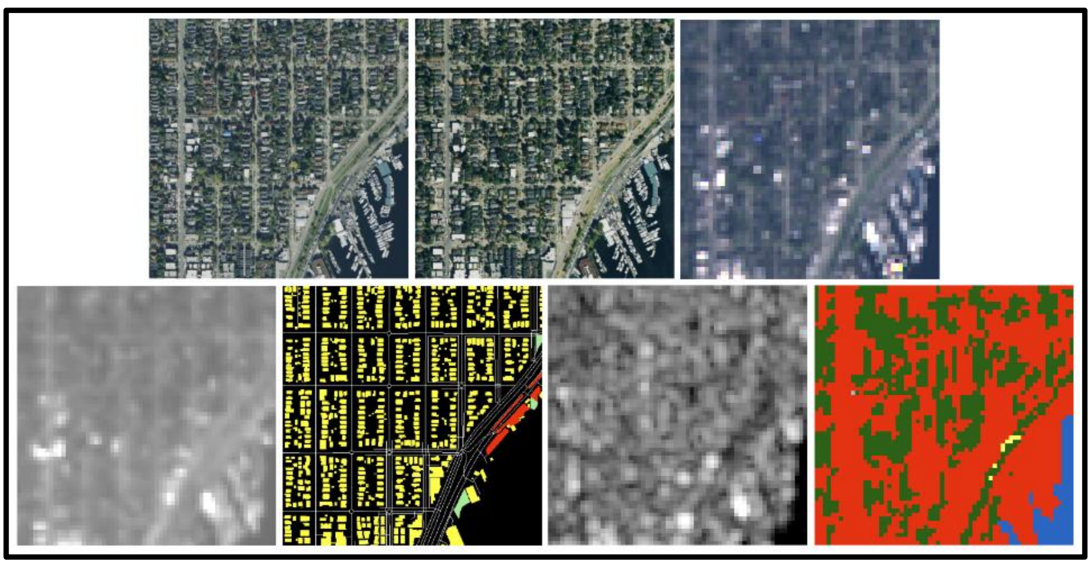

Figure 6: Example of imagery and data types in the AllenAI co-aligned dataset. Top-Left to Bottom-right, in order: Old NAIP (2015-2018), new NAIP (2019-2022), Sentinel-2 RGB, Landsat 8/9 spectral band, OpenStreetMap GeoJSON layer of land use and cover, Sentinel-1 radar image, and WorldCover land cover (Image from Bastani, 2024).

UAS have become increasingly used for mapping and research purposes (Figure 7) (Nex, 2022). Flying at lower altitudes and oftentimes with narrower fields of view, this results in higher resolution of imagery to be captured, or increased ground sample distance (GSD) on the resulting maps. In other words, the pixel footprint of data collected will be smaller and finer for sensors that are deployed closer to the target. For this reason, many studies have explored comparing UAS and satellite imagery for remote sensing of vegetation, or using only UAS imagery. Furthermore, the high resolution of UAS data may be more desirable in some situations because imagery captured will have lower GSD and therefore produce higher accuracy classifications. The tradeoff with this improved GSD of other platforms is that UAS is often reduced to mapping smaller areas when compared to manned aircraft or satellites. UAS can also be flexibly deployed as needed multiple times a year, if the drone platform and pilot are available.

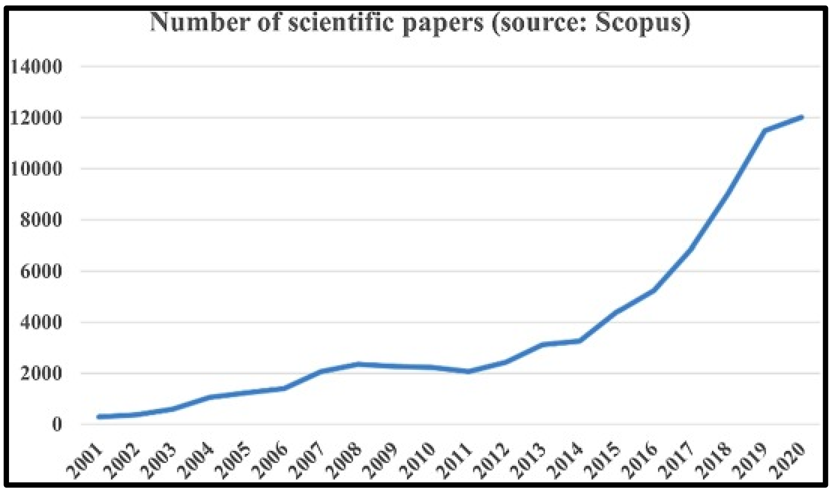

Figure 7: Trend line showing the number of scientific papers published in the last 20 years using 'UAV', 'UAS', 'drone' or 'RPAS' as a keyword or in the title. Image and caption from Nex, 2022.

Several studies have been conducted to utilize UAS to identify and map invasive species (Martin et al., 2018; Zhang, 2015; Abeysinghe et al., 2019; Sathishkumar Samiappan et al., 2017; Brooks et al., 2021; Liu et al., 2021). Photogrammetric methods also allow for UAS images to be processed into 3D models that "highlight the structure of vegetation", which can be incorporated into the analysis to improve classifications of vegetation like Knotweed (Martin et al., 2018). LiDAR (Light Detection and Ranging) is an active sensor that can be mounted on UAS (among other platforms), which results in a very accurate and dense 3D point cloud. These are typically more expensive than optical UAS sensors but provide robust datasets and have accuracy on a three-dimensional plane (Martin et al., 2018). The downside of UAS is the limited amount of data that is captured over smaller swaths of land when compared to satellite imagery. However, satellite imagery may not have a high enough resolution for identifying small single patches and early growth (Brooks et al., 2015). Using UAS in combination with satellite imagery may be a desirable method for larger sites and regions that are being studied to provide the most effective plant species identification.

Classification Overview and Methods

At its simplest, a classification algorithm can be considered a decision tree for labeling an input set of unknown items based on a set of known, "field data", categorical training data or natural splits within the data (Figure 8). While humans are effective classifiers themselves, capable of differentiating very subtle changes within an image by eye through photo-interpretation, this process is time consuming and impossible to perform for large datasets or with high temporal frequency. This difficulty necessitates the use of digital images, computer processing, and algorithms for performing quantitative analyses of imagery such as classification tasks (Tan, 2021).

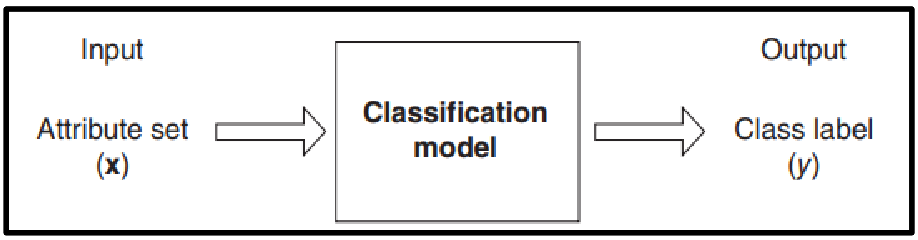

Figure 8. A schematic representation of a classification algorithm or process. Image from Tan, 2021.

Data being used for training and as input to the classification algorithm is typically the intensity of each of the image color (spectral) bands (e.g., red, green, blue, red-edge, near-infrared, etc.), and relationships between bands. Classification processes can be customized to rely on a number of parameters, but typically involve the use of nearest neighbor algorithms operating on the spectral properties of the selected training samples. Comparisons between image bands in a multispectral space provides the statistical information necessary to create the algorithm for grouping input data into the desired classes (Figure 9). The developed algorithm then applies statistical analysis (e.g., maximum likelihood or nearest neighbor classifiers) to determine the best label to apply to each input data. For multi-spectral imagery (images with multiple spectral bands), classification can be considered a method used to attach labels to pixels based upon their spectral characteristics (Richards, 2005).

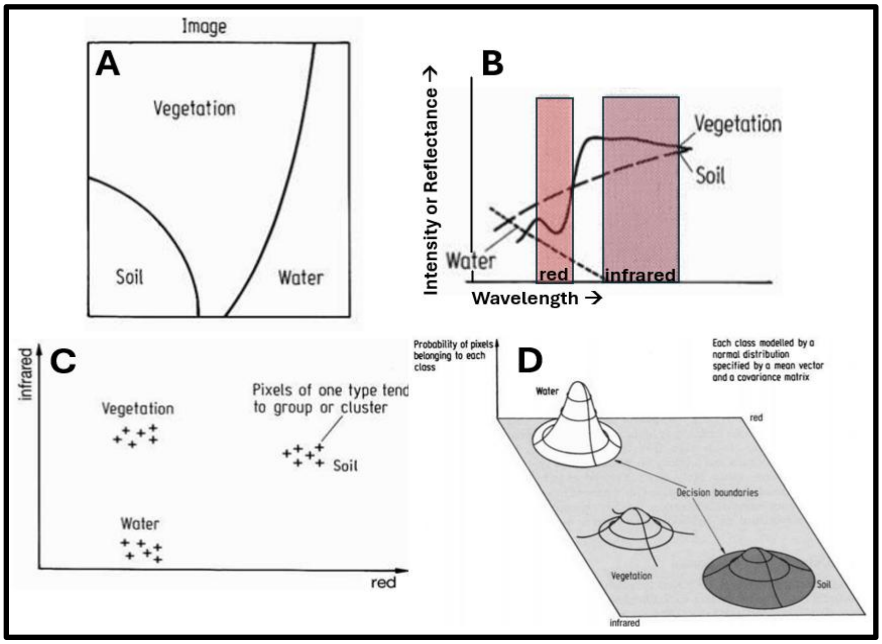

Figure 9: Overview of the process behind image classification of multispectral images. A) Example simplified land cover image containing three land cover types, B) general differences in spectral characteristics for the three example land cover types, C) samples of each cover type plotted by comparison of two spectral image bands in vector space, and D) same image space as shown in 'C', now with each class displayed as gaussian probability distributions indicating the strength of the relationship for a given class. Image adapted from figures in Richards, 2005.

When classifying an image at the pixel level, each individual pixel is assessed for its similarity to the pixels associated with the training dataset. Alternatively, classifying or applying algorithms to images at the pixel level, images can first be parsed into semi-homogeneous "objects" using spatial and similarity-based segmentation algorithms (Figure 10) prior to classification. This classification procedure is called object-based classification or object-based image analysis (OBIA) (Blaschke, 2010). There are both benefits and drawbacks to the use of OBIA relative to pixel-based classification. First, the integration of similar neighboring pixels into objects reduces the 'salt and pepper' appearance of a classification. More importantly these objects and their associated properties can provide additional spatial (e.g., position, adjacency and distance to other classes), textural (e.g., color and shadow, color mixtures), and contextual (e.g., shape, size, found within) information useful for classification purposes (Liu, 2009, Baatz, 2004). These properties of segmented image objects provide additional information unavailable at the pixel-level and can be used in a rule-based classification process (Baatz, 2004, Blaschke 2010). One drawback to OBIA is the requirement of a large amount of computer memory for the calculation of relationships between objects, which increases with the addition of more spectral bands and improved image resolution (Hay, 2006).

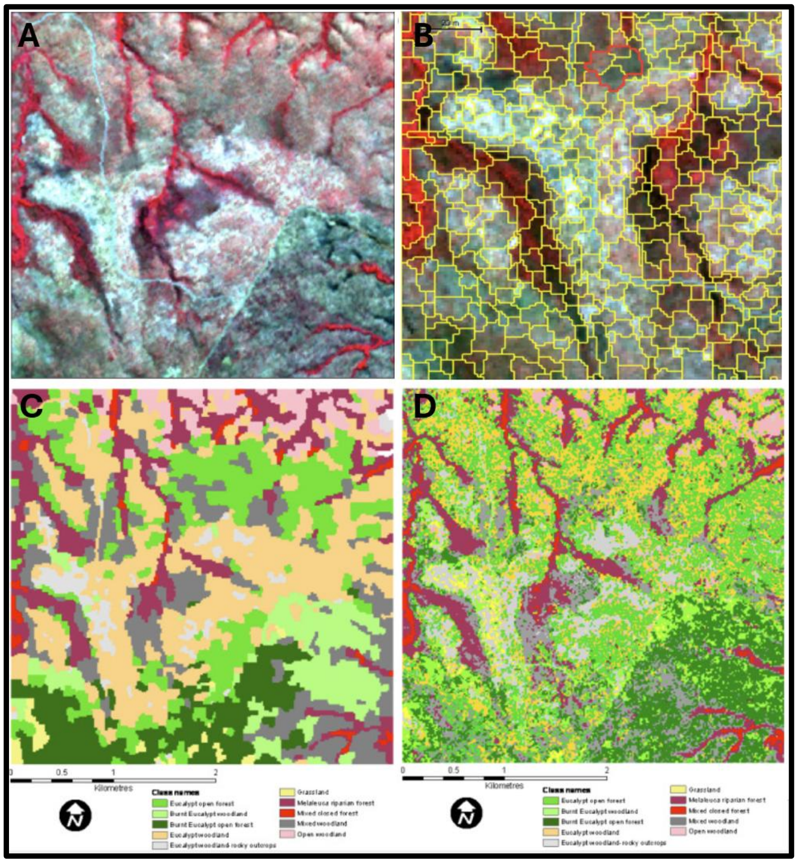

Figure 10: Example multispectral image, segmentation, and classifications. A) ASTER multispectral image shown in false color composite for a savanna area in NW Australia. B) Zoom of image in 'A' showing resultant image objects following image segmentation, C) object-based classification result using segments in 'B', and D) pixel-based classification result. Image adapted from figures in Whiteside, 2011.

There are numerous software packages available for performing pixel- and object based image classification. Both ESRI ArcGIS Pro (commonly used by state agencies, license-based GIS software) and QGIS (open-source, freely available GIS software) are software packages that have image classification techniques available for use on various types of imagery. More specialized image processing software, such as Trimble's eCognition (Figure 11), provide additional features and capabilities for performing more fine-tuned image analysis, including the use of spatial and topological parameters in object-based image analysis (Baatz, 2004). Additional softwares frequently used for image classification and multi- or hyperspectral image analysis include Erdas Imagine, NV5 Geospatial's ENVI (more focused on multi- and hyperspectral image analysis), and various image classification tool boxes and packages available in Matlab or R-studio.

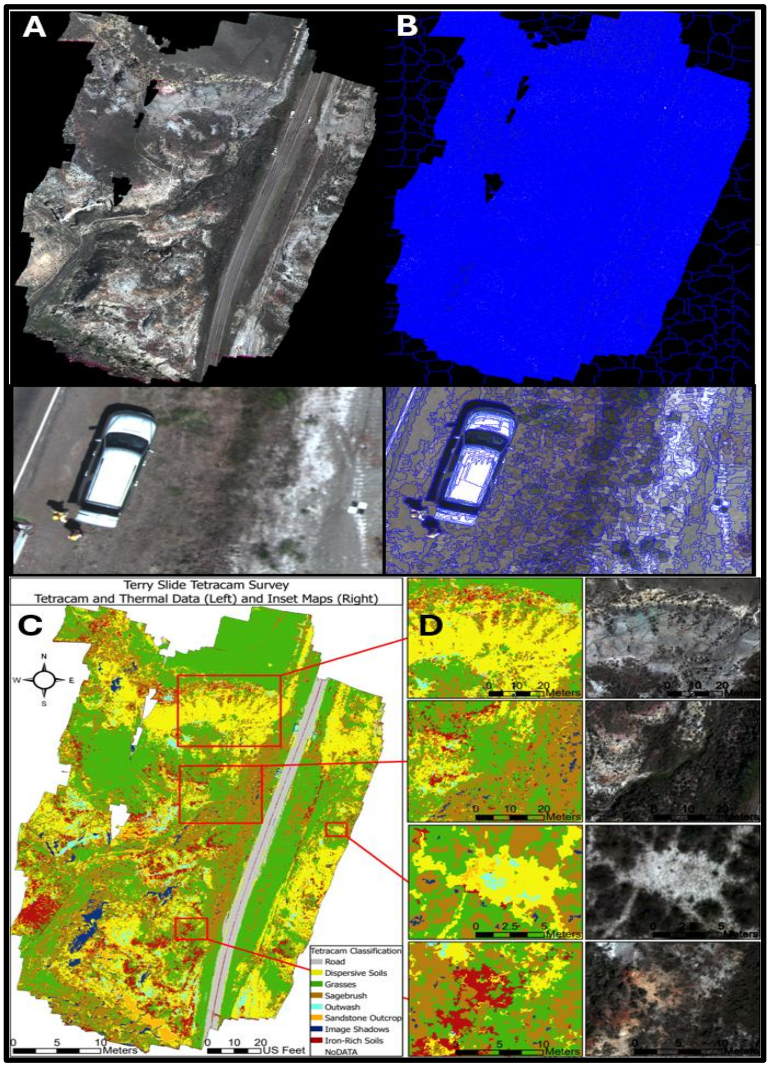

Figure 11: Example object-based image classification of soil types using Trimble eCognition. A) 7-band multispectral imagery, with zoom, and B) segmenting of objects at a high resolution, with zoom. C) Output image classification, with D) zoom showing side-by-side comparison of classification (left) and true-color image composite (right). Image selected from previous analysis performed by MTRI.

In remote sensing, classification of imagery can be performed using two general methods: supervised and unsupervised classification. The examples provided up to this point have shown supervised classification methods, where the user provides training to the classification model by manually grouping a subset of the image data based on their knowledge of the imaged area or other ground-truth information. In unsupervised classification pixels, or image objects, are clustered together into natural groups based solely upon their spectral similarity, spectral distance, and a number of clusters provided by the user (Figure 12): unsupervised classification uses no ground-truth information (Parece, 2023, Campbell, 2011). While difficult to visualize intuitively or by eye, remotely sensed images are generally made up of relatively uniform and distinct spectral classes of cover types (e.g., urban, water, grassland, forest), and this property is exploitable through unsupervised classification (Lillesand, 1994).

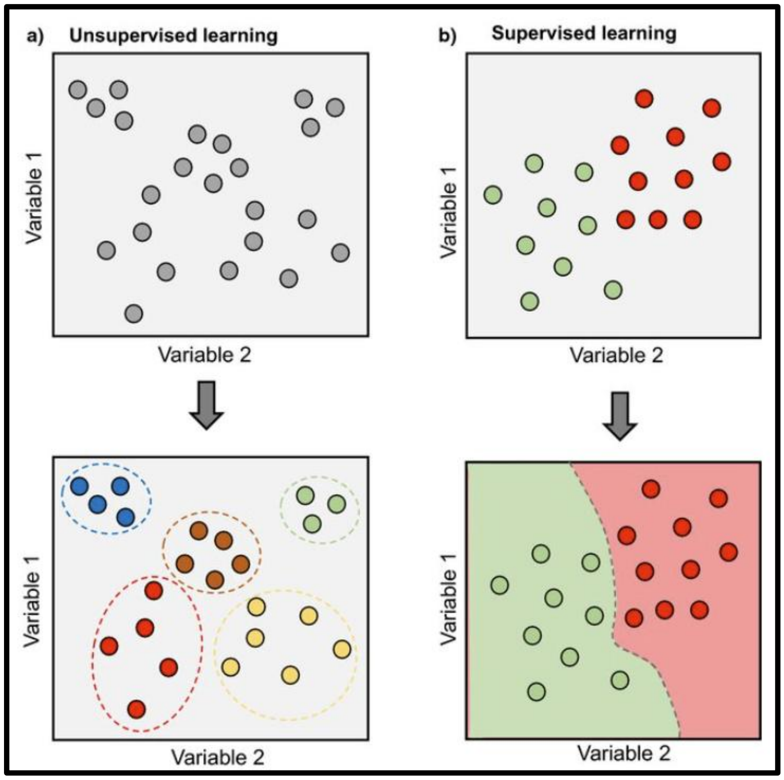

Figure 12: Visual comparison of unsupervised and supervised classifications. a: Unsupervised learning uses no input ground-truth information, unlike supervised classification (b) which is reliant upon ground-truth input from the user (color coding, top-right). Unsupervised learning uses clustering algorithms to identify distinct classes, while supervised learning uses the supplied ground-truth information to classify input data. Image from Morimoto, 2021.

Unsupervised classification has both advantages and disadvantages. One major advantage, as discussed previously, is that no extensive prior knowledge of the imaged region is required of the user for the classification. Knowledge of the imaged region is required, however, for interpretation of the results produced by the unsupervised classification process (Campbell, 2011). Because unsupervised classification is based solely on the natural groupings of the image values, the classes that result from unsupervised classification can be considered ‘spectral classes’ (Lillesand, 1994). These homogenous spectral classes may not necessarily correspond to informational classes of interest to the image analyst and are likely to change over time (e.g., a ‘vegetation’ spectral class that changes color over time due to senescence), making it difficult or impossible to apply informational and spectral class relationships between images (Campbell, 2011).

For the specific purposes of invasive species identification, supervised classification algorithms can be trained to locate pixels or objects in the imagery that are known patches of the species of interest, then locate other pixels or objects in the imagery that "match" values to the spectral properties of the training data. Most of the surveyed literature has involved machine learning-based supervised classification to help identify objects and features in imagery. The most commonly used supervised classification techniques included Random Forest (RF), Support Vector Machines (SVM), and artificial neural networks (ANN) (Zagajewski et al., 2021). For example, hyperspectral and/or high resolution images and SVM algorithms have been shown to produce accurate results for detection of invasive species (Liu et al., 2021). Both RF and SVM are supervised machine learning algorithms, and while RF has historically been used for remote sensing image classification because of its high accuracy, SVM has been shown to produce similar classification accuracy (Raczko, 2017, Zagajewski, 2021).

As an example of the development of a semi-automated classification workflow, MTRI has previously produced a pixel-based approach for ingesting georeferenced image data, creating additional image features (NDVI, Hue, etc), and building predictive machine learning models (e.g. Random Forests, XGBoost) based on training data from both field sites and well defined elements of image interpretation (Olson, 1960) to create classification maps. This pipeline has been developed through previously funded mapping efforts throughout North America (Brooks et al. 2021, Bourgeau-Chavez et al. 2019, GLARS 2021 & 2022, Bourgeau-Chavez et al. 2015, French et al. 2022), many of which included the differentiation of specific wetland vegetation from one another (e.g. *Phragmites australis*, *Typha* spp., *Schoenoplectus*, floating aquatic, submerged aquatic, wet meadow, marsh, fen, bog) as well as from broader land cover classes (e.g. developed, agriculture, barren, forest).

Classifications of invasive species require assessments of their accuracy and error to determine the ability of different imagery types (and their combinations), and classification methods, to produce accurate maps of a given plant species. Assessments of map accuracy require determining positional accuracy as well as species accuracy of the output products. Accuracy assessment techniques can include the creation and evaluation of an error matrix or Kappa analysis, with field data collected (separate of that used for classification training) according to various randomized sampling regimes (Congalton & Green, 2019). The error matrix, sometimes referred to as a confusion matrix or contingency table, compares the reference ground-truth data with the corresponding results of the classification (Lillesand, 1994) (Table 2). Errors are explored in this table, with non diagonal numbers representing errors of omission (exclusion) in non diagonal column elements and commission (inclusion) in non diagonal row elements. Overall accuracy is calculated as the total number of correctly classified pixels (diagonal column) divided by the total number of reference pixels. Producer's accuracy indicates how well training set samples of a cover type are classified, and is the number of correctly classified pixels for a cover type divided by the number of training pixels used for the category. User's accuracy provides an estimate of commission error and the probability that a classified pixel in a given category truly represents what was measured in ground-truth. Classifications are not complete without an assessment of their accuracy (Campbell, 2011).

Table 2: Example error matrix comparing ground truth and classification results (scanned from Lillesand, 1994).

Classification Data	Training Set Data (Known Cover Types)[a] W	S	F	U	C	H	Row Total
W	480	0	5	0	0	0	485
S	0	52	0	20	0	0	72
F	0	0	313	40	0	0	353
U	0	16	0	126	0	0	142
C	0	0	0	38	342	79	459
H	0	0	38	24	60	359	481
Column total	480	68	356	248	402	438	1992

Producer's Accuracy	User's Accuracy
W = 480/480 = 100%	W = 480/485 = 99%
S = 052/068 = 76%	S = 052/072 = 72%
F = 313/356 = 88%	F = 313/353 = 87%
U = 126/248 = 51%	U = 126/142 = 89%
C = 342/402 = 85%	C = 342/459 = 74%
H = 359/438 = 82%	H = 359/481 = 75%

Overall accuracy = (480 + 52 + 313 + 126 + 342 + 359)/1992 = 84%

[a]W, water; S, sand; F, forest; U, urban; C, corn; H, hay.

Methods Used for Target Species

Common Reed (*Phragmites australis*)

Phragmites is prevalent in many wetlands ecosystems, but is often found in wet, low-lying areas like roadside ditches. This can mean that the species can be found in mixed ecosystems or in monoculture stands, depending on the landscape. Furthermore, smaller stands and early growth of the invasive species is important to capture in mapping efforts, since preventing dense monocultures is ideal. Several studies showed the use of satellite imagery from Landsat, Worldview 2 and 3, and Sentinel-2 to map areas of Phragmites. Eight-band Worldview 2 imagery with extra near-infrared bands and 2-meter spatial resolution was compared to a four-band subset in both object- and pixel-based classifications of Phragmites in a study by Lantz and Wang in 2013. The wetlands imagery was processed with pan-sharpening methods, to increase spatial resolution to 0.5m, and the Normalized Difference Vegetation Index (NDVI) and Normalized Difference Water Index (NDWI) were calculated. In this study, object-based classification with six classes was conducted in eCognition Definiens eCognition 8.0.1, then maximum likelihood pixel-based classification with training data was done to evaluate the accuracy of the object-based results. The eight-band Worldview imagery with object-based classification had the greatest overall accuracy when identifying the species, which was 93.2%, compared to 90.8% for the four-band object-based classification accuracy. The pixel-based classifications were considerably lower in accuracy.

Worldview 2 and 3 have higher costs than other satellite sources, but it can be used to identify smaller stands of Phragmites due to its higher resolution. Sentinel-2 has no cost, is available for easy download, and is useful for detecting larger stands with the lower, limited resolution. Both satellite imagery sources were used by Rupasinghe and Chow-Fraser in 2021 to identify Phragmites in wetlands. Imagery was processed with mixture-tuned matched filtering (MTMF), and classified with either support vector machine (SVM) or maximum likelihood (ML). Worldview 3 performed better than Worldview 2 and Worldview 2 performed better than Sentinel-2. The best accuracy obtained was 93.1% for Worldview 3 imagery with ML classification. Both Worldview 2/3 were able to identify “small patches (percentage cover ≥ 20%; shoots ≥ 1 m tall; stem counts ≥ 25) with accuracy ≥ 80%”. The results allowed for sparse Phragmites stands to be found, in addition to larger monocultures (Chow-Fraser in 2021).

Hyperspectral satellite imagery, from the Hyperion sensor, has a greater number of bands than previously mentioned sources. A study in Green Bay took imagery from Hyperion, with 30-meter spatial resolution, that contained Phragmites monocultures and applied a Spectral Correlation Mapper (SCM) algorithm that used the pure Phragmites pixels in the hyperspectral data as the reference and applied it to the entire site (Pengra et al., 2007). A similarity metric from zero to one was generated in the raster results. The species could be delineated and quantified from this method, and a validation process from previous field data found a 81.4% overall accuracy. Due to the larger spatial resolution of Hyperion, the smaller stands of Phragmites were harder to identify, as well as linear groups of the species along shorelines. The reason for this is due to mixed pixel values where more than just Phragmites were present and there was a low count of pure pixels that was required for the reference model.

With improving UAS sensor capabilities and the lower cost of acquisition, this method of acquiring imagery of invasive species has proven desirable in more recent studies using object- or pixel-based classification methods. One study compared the four-band Sequoia multispectral (G, R, RE, NIR) UAV-flown imagery of a Phragmites-invaded estuary (Abeysinghe et al., 2019). Imagery was classified with machine learning (ML) techniques: neural net (NN), k-nearest neighbors (kNN), and support vector machine (SVM) algorithms. They also tested the parametric maximum likelihood classifier (MLC). Multispectral data was classified with the addition of the Normalized Difference Vegetation Index (NDVI) and LiDAR-derived canopy height models (CHM) (digital surface model (DSM) - digital terrain model (DTM)). Band indice calculations, texture analysis, principal component analysis (PCA), and the canopy height model (CHM) were done prior to classifications in order to supply more information in the classifier and improve accuracy (Figure 13). Object- and pixel-based methods were used for classifications with Trimble eCognition Developer 9 and ENVI 5.4, respectively. The best results for mapping Phragmites were from the machine learning pixel-based neural net (NN) method, “with an overall accuracy of 94.80% and the lowest error of omission of 1.59%”. The study also found that the best method for identifying small patches of the species with UAS was to use a “stratified random sampling design with multi-pixels as a sampling unit”, and that NDVI and CHM were more important to the classification accuracy than the texture analysis and the PCA analysis. The machine learning algorithms (NN, SVM, and kNN) and maximum likelihood classifier (MLC) were found to have similar results, but ML was slightly better. Overall, this study found that machine learning and maximum likelihood methods achieve high accuracy for the classification of invasive species in comparison to object-based classification.

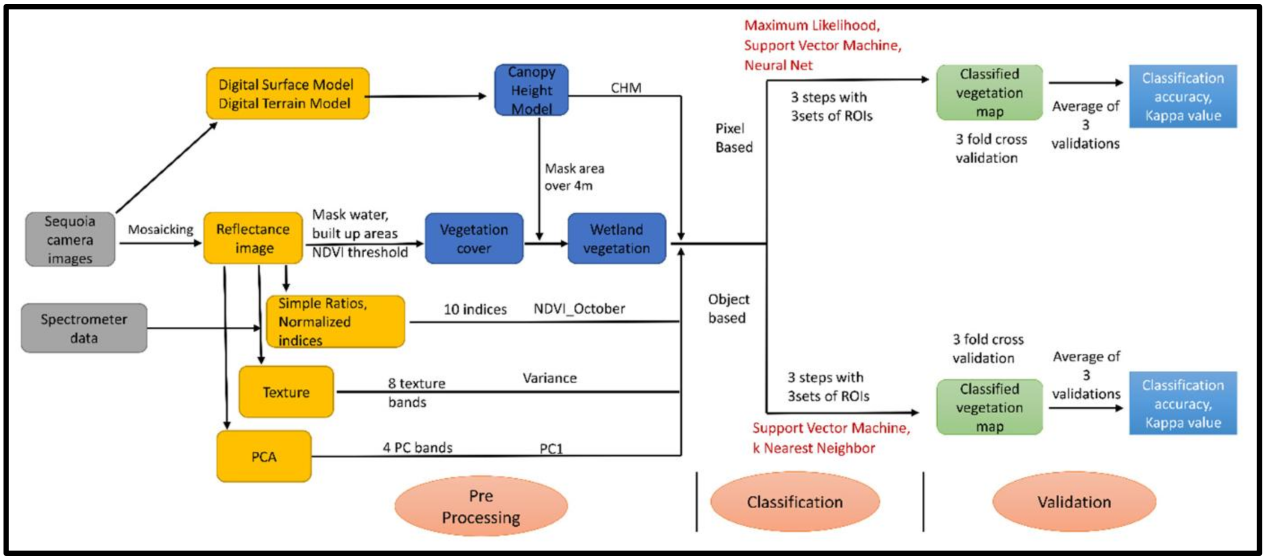

Figure 13. Workflow for comparing machine learning algorithms and remote sensing methods of UAV imagery to identify invasive Phragmites (Abeysinghe et al., 2019).

While texture analysis was ineffective at increasing accuracy in the previous study, a texture method proposed by Samiappan et al. using RGB UAS imagery achieved reasonable accuracy (2016). Four wetland sites in Louisiana were flown with an RGB camera only and analyzed with "Gabor filters (GF), (2) gray level co-occurrence matrix (GLCM)-based texture features, (3) segmentation-based fractal texture analysis (SFTA), and (4) wavelet texture analysis (WTA)" following image mosaicking in Agisoft Photoscan. Visual validation was done following the classification process done with a support vector machine (SVM) informed by the texture features and spectral bands. Ground patches were also used for validation of classification results. These methods achieved an "average accuracy of 85%, [and] an average kappa accuracy of 70%", which indicated that texture can be useful in Phragmites object-based classification using UAV imagery. The study also showed that RGB UAV imagery can be sufficient for identifying Phragmites.

Another study investigated the use of optical and near-infrared bands captured by UAS for identifying Phragmites in wetlands of the Great Lakes region (Brooks et al., 2021). A mosaicked optical image for each site was created in the photogrammetry software Agisoft Metashape and used for texture analysis, which were included as layers in object-based classification. The classification process was done with four classes in Trimble eCognition. Near-infrared bands were also collected by a mounted sensor for vegetation indice calculations. A digital surface model was created and added as a layer in the classification scheme to help identify and differentiate the height of Phragmites stands from surrounding vegetation, and for change analysis. Further calculations included the Visible Atmospherically Resistant Index (VARI) and NDVI, which helped inform the classifier. The classifications from only optical data achieved 91.7% overall accuracy, which was assessed with visual inspections of the classifications compared to optical imagery. For near-infrared data collected and used in the classifications, some sites achieved greater accuracy than RGB only. The study concluded that RGB imagery flown by UAS can capture Phragmites stands greater than 0.1 hectares (¼ acre) and they cannot be underneath tree canopy.

SAR, specifically the ALOS L-band PALSAR satellite, combined with multispectral Landsat 5 imagery has been used for detection of Phragmites (Bourgeau-Chavez et al., 2015) around the Great Lakes, with the highest accuracy results for larger stands of the species. The advantage of SAR is that it can provide images day or night, and the L-band is less affected by weather disturbances. In the study by Bourgeau-Chavez et al., early growth, peak growth, and senescing periods were targeted for imagery of wetlands in the Great Lakes. Atmospheric corrections and NDVI calculations from Landsat 5 were done and included in the classifications. Single and dual channel modes were included for PALSAR. For classification, the following methods were considered: "hierarchical classification, object-based image analysis (OBIA with eCognition), maximum likelihood (Erdas Imagine) classification of optical and SAR data separately and then recombination of the classes and Random Forests (in the software R)". Random Forests was chosen for this analysis in which training polygons were generated by researchers to inform the decision tree algorithm. Accuracy assessment was performed by setting aside training polygons from field sites as validation polygons and then verified for accuracy in the classification. Overall, the wetland map achieved 94% overall accuracy and 84% user's accuracy for Phragmites. In conclusion, SAR is a viable option for the mapping of invasive Phragmites.

Japanese Knotweed (*Fallopia japonica)*

Since its dispersal as an invasive species, researchers around the globe have been looking into ways to accurately map Japanese knotweed, including the application of remote sensing technology. Studies have frequently listed UAS-collected, or other aerial imagery with high spatial resolution as the most effective way to classify knotweed (Smerdu et al., 2020; Jones et al., 2011). Other studies have found that there are highly accurate ways to utilize satellite-based imagery, despite the lower spatial resolution making it much more difficult to classify features correctly (Smerdu et al., 2020; Martin et al., 2018). One study that utilized both satellite-based and UAS imagery is the 2020 Smerdu study, "Automatic detection of Japanese knotweed in urban areas from aerial and satellite data".

This 2020 study took place in the Slovenian capital of Ljubljana and looked at the dispersal of Japanese knotweed around the 275 km^2 city. Researchers used two separate sources of data: high spatial resolution aerial images and satellite data. The high spatial resolution data was obtained in the form of 64 orthophotos from the Surveying and Mapping Authority of the Republic of Slovenia (Smerdu et al., 2020). These orthophotos each covered 6.75 km^2, and utilized four bands: red, green, blue and near infrared. While the spatial resolution of these orthophotos was high at 0.5 meters, the imagery was only captured on a single day in April 2018. The satellite data was obtained from Sentinel-2, which has a GSD of 10 meters and a revisit time of every 5 days, is easy to track phenological changes over time. They used bands 2, 3, 4, and 8 which are blue, green, red, and near infrared and were used to produce RGB images, as well as NDVI and EVI indices (Smerdu et al., 2020).

In addition to remotely sensed data, sets of field data were used as both a form of validation data and as a training model for the Support Vector Machine (SVM) classification. Orthophotos and positive samples were fed through the processes. The first step of the process was segmentation, in which the researchers manipulated the scale of fragmentation and the level of merging between segments. The study settled on a 40% scale level and a 85% merge through empirical means. Two sets of the images were separated; one process consisted solely of the RGB and texture layers of the orthophotos, while the used RGB and the infrared band (Smerdu et al., 2020). These two sets were put through a One-Class SVM with radial basis function kernel, following a 2014 study that suggested it would "...provide the best overall results for green urban areas extraction" (Smerdu et al., 2020).

After the One-Class SVM, the study applied a K-means algorithm to improve the inlier versus outlier data on the RGB=IR sample and then the products were merged. Ultimately, this methodology concluded with the orthophoto classification resulting in a 83% accuracy. While this number is lower than other such studies, the study acknowledged that the phenology of the shrub when the orthophotos were produced may have been an issue.

The satellite data was also classified using RGB data. The RGB image and indices were all stacked with the training data and put through the One-Class SVM to determine the inliers and outliers. The researchers then used the same radial basis function kernel that was used on the orthophotos. Finally, a mask was applied to filter out forested land and agricultural land. The results of this part of the study vary depending on the season and phenology of the Japanese Knotweed, but an overall accuracy of 90% was stated with stands larger than 100 m^2 (Smerdu et al., 2020).

Another study that used both satellite (Pleiades 1B PMS images with 0.5m GSD, RGB+NIR) and UAV (DS6 hexacopter with a Sony Alpha 7 with 24.3 Megapixels Full Frame Exmor CMOS Sensor and a Sonnar T* FE 35mm f/2.8 Zeiss lens) was the 2018 study "Using Single- and Multi-Date UAV and Satellite Imagery to Accurately Monitor Invasive Knotweed Species". This study took place over multiple seasons in two different locations (Anse site, and Serrières site) along the floodplain of two major rivers in France (Martin et al., 2018). These sites were selected because of the difference in species composition, landscape coverage, and how severe the knotweed invasion was. Two cameras were utilized in this study, one of which collected RGB imagery, and the other was modified to collect the near infrared (NIR) band. After images were collected by the drone, they were processed in Agisoft Metashape to create Digital Terrain Models (DTMs), Digital Surface Models (DSMs), and orthoimages of the study sites with subcentimeter GSD (Martin et al., 2018). Single-date and multi-date imagery with and without variables mentioned below were compared to determine which method excelled at identifying Japanese knotweed.

Due to computational limitations, the study limited additional variables to Bi-Temporal Band Ratios (BTBRs: multi-date information) and Canopy Height Models (CHMs: single- and/or multi-date information) (Martin et al., 2018). The researchers in this study chose to use an object-based classification over pixel-based, as they wanted more contextual information to be taken into account during the processing. Classification was separated into three different classes, Knotweed, cut knotweed, and other, then was processed using the machine learning algorithm Random Forests (RF) within eCognition Developer. Since using multi-date sources of data can introduce its own set of errors, this study utilized a "buffer" to stretch the boundaries around knotweed predictions. These buffers were two sizes, 2-pixels and 10-pixels which represented 16 cm and 80 cm, and 1 m and 5 m for the UAV and the Pleiades images, respectively. These Buffers proved to be exceptionally important, as the accuracies of all results improved greatly regardless of season. While the results of the Pléiades imagery classifications had lower accuracy, only reaching 61/34 for the producer's accuracy and users accuracy respectively, the UAS data showed more promise, with accuracies reaching as high as 86/80. The results of this study showed that Japanese knotweed could be mapped by UAVs using MBTBRs and CHMs, if the species is not under trees or freshly cut (Martin et al., 2018).

An example of the literature available on strictly UAV-based approaches to detecting knotweed can be seen in the 2016 article, "Mapping of riparian invasive species with supervised classification of Unmanned Aerial System (UAS) imagery". This study set out to define an easily reproducible methodological framework for mapping three different species: *Impatiens glandulifera*, *Heracleum mantegazzianum*, and Japanese knotweed (*Fallopia sachalinensis*, *Fallopia japonica* and hybrids). This study took place in two riparian zones in Wallonia, the Berwinne valley and the Oreneau valleys respectively. Using a Gatewing X100 UAS with two pre-calibrated Ricoh GR3 cameras (10 megapixel; focal length of 6 mm), researchers performed a total of seven flights, and utilized a 75% overlap on all imagery taken. Researchers then performed photogrammetric surveys with Agisoft Photoscan and generated orthophotos using the "Mosaic" blending mode with color correction (Michez et al., 2016). The orthophotos were then processed in eCognition with a multi-resolution image segmentation algorithm with four different scale parameters being tested: 10, 30, 45, and 60. Additionally, the three spectral bands were equally balanced in the segmentation parameter (Michez et al., 2016). The supervised classification processes based on the RF algorithm were used to identify invasive plant species segments versus non-invasive plant species by applying 20% of the training sets to 80% of the evaluations sets to determine accuracy. The RF model was repeated a total of 50 times in order to generate statistics such as standard deviations of the accuracies (Figure 14). Unfortunately, the accuracies that were achieved by this study were not high enough for operational application, being only 68%. Regardless of the outcome, the authors were positive about the results, as they acknowledge that these results were achieved with both a light training set and very budget friendly equipment.

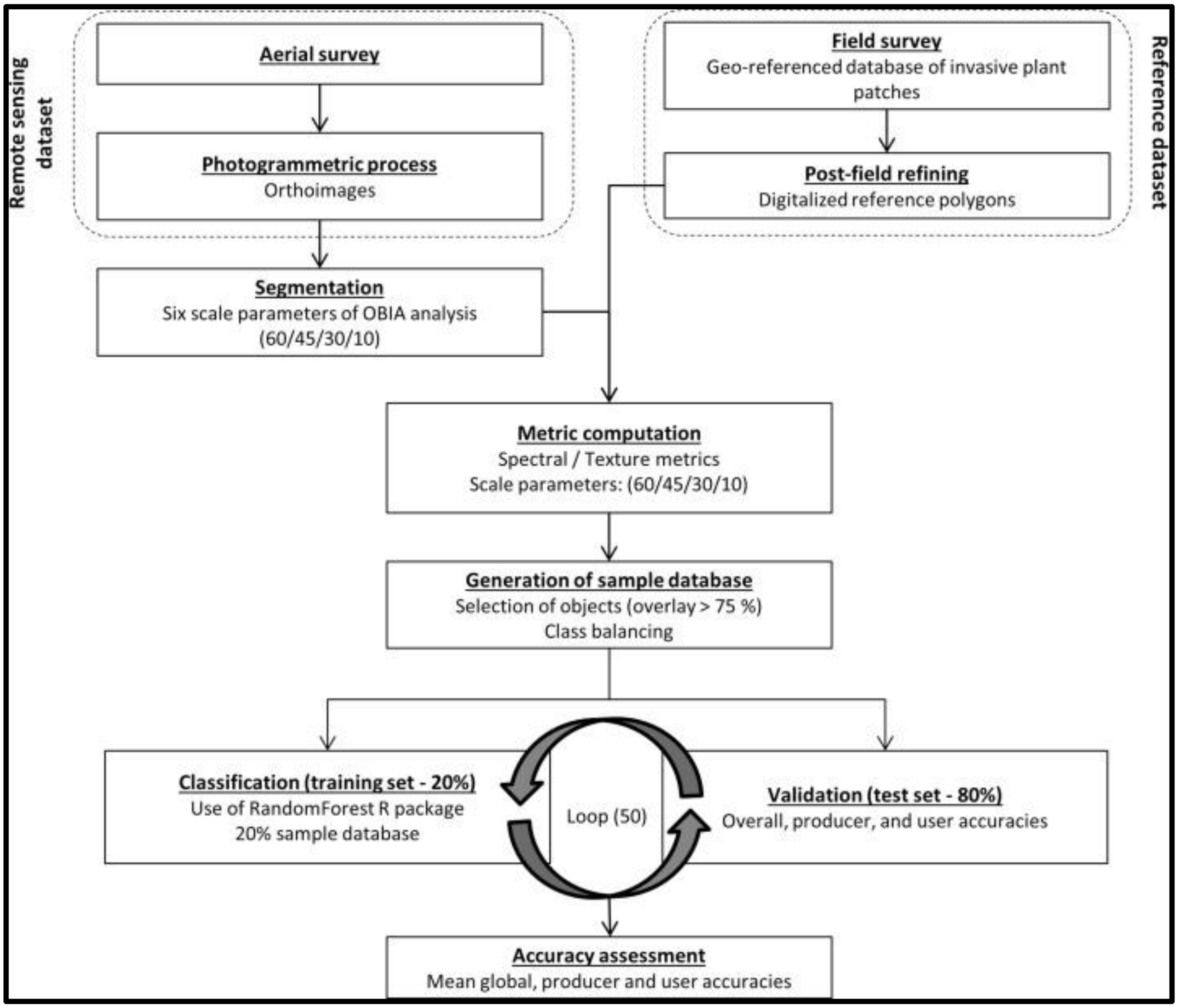

Figure 14: Workflow defined in "Mapping of riparian invasive species with supervised classification of Unmanned Aerial System (UAS) imagery" showing how they gathered and processed the data related to identifying their target species.

Leafy Spurge (*Euphorbia esula)*

The persistent invasive leafy spurge is often identified with multispectral or hyperspectral imagery, especially in spring when the bracts appear. One of the most cited studies for identification of leafy spurge was done in Theodore Roosevelt National Park in 1999. Ground-level and plant spectral data, 325-2500 nm with a GER2600 spectrometer with a 23^{0} field-of-view, was collected along with differential GPS locations with a Trimble GPS Unit. Four flight lines, with four scenes, were gathered from the high-altitude Airborne Visible and Infrared Imaging Spectrometer (AVIRIS) (O'Neill, 2000). Homogeneous plant stands were identified and used as training polygons for image analysis based on accessibility, extent, and relative density. Spectral measurements were made from approximately one meter above the vegetation, producing a 0.40 m diameter GSD. For every ground target, five different replicate spectra were measured and averaged, equaling a total of 2,514 individual spectra for 475 ground targets (O'Neill, 2000). Some common plants in the park, like silver sage, snowberry, juniper, native grasses, and sweet clover spectra were obtained along with an asphalt parking lot as a calibration site (Figure 15). Linear unmixing of the field spectra data was applied and then analyzed using UC Davis Spectra Analysis and Management System (SAMS) and then uploaded to the ENVI software. The Principle Components Analysis (PCA) and Spectral Angle Mapper (SAM) algorithms were performed in ENVI and applied to the field spectra. AVIRIS image processing was conducted in ENVI, except for the calibration to reflectance (O'Neill, 2000). The calibration to reflectance was processed in a modified version of MODTRAN, calibration site field spectra, and perl scripts (O'Neill, 2000).

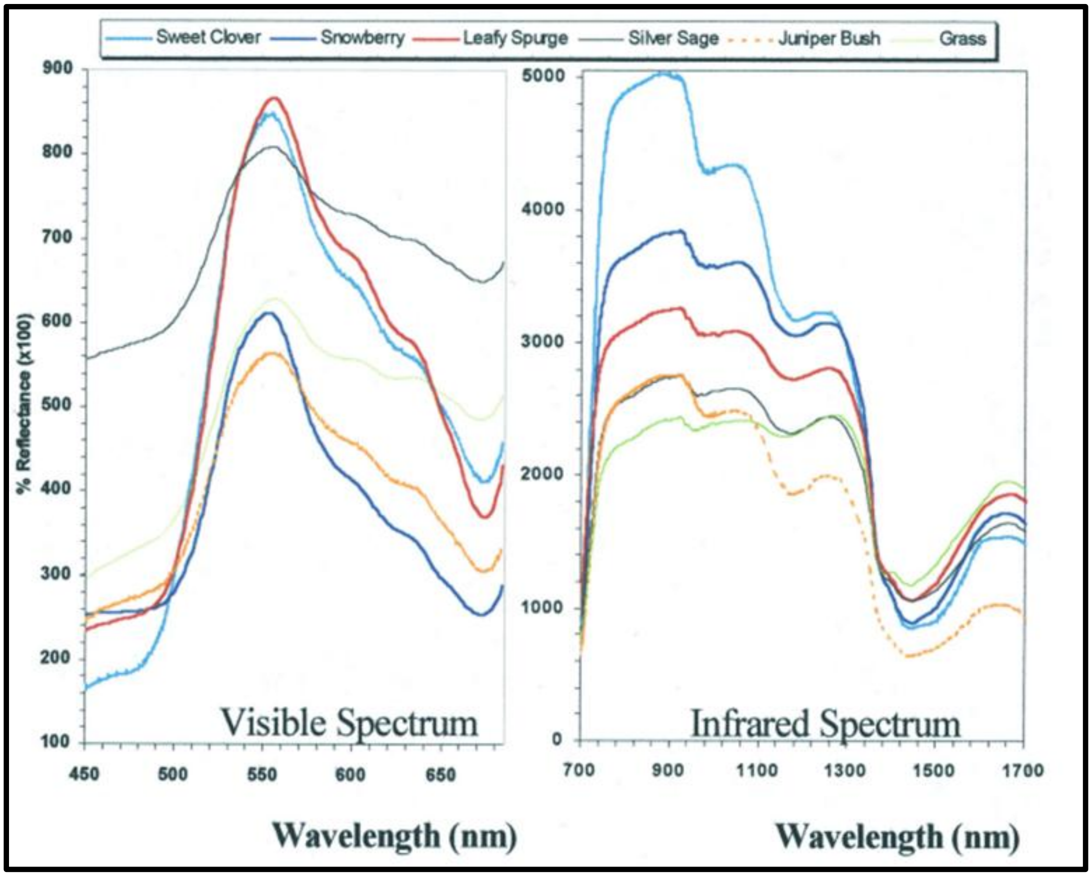

Figure 15: Spectral Differences among different species in areas infested with leafy spurge at Theodore Roosevelt National Park (O'Neill, 2000).

The image analysis methods tried were: the common multispectral transformations, NDVI, simple vegetation index (VI), and chlorophyll region slope (O'Neill, 2000). Besides these transformations, the SAM algorithm was applied to the original reflectance data as well as Principal Components (PCA) and Minimum Noise Fraction (MNF) transformations of the data. Applying SAM to the raw reflectance data, both the full set of bands, and a subset of eleven bands that captured the general behavior of the spectra, were used and eleven bands were for the following wavelengths: 478, 557, 606, 636, 683, 779, 1020, 1200, 1510, 1660, 2210 nm (O'Neill, 2000). The linear unmixing was used on the field spectra but not used on the AVIRIS data with several species' endmembers not found in imagery (O'Neill, 2000).

Two classifications attempts were performed:

Tier 1: Eight leafy spurge training sets were chosen based upon the criteria: 1) Personal knowledge of some locations of Leafy Spurge; 2) The NPS 1993 Map of Leafy Spurge; 3) NDVI values above 0.65; and 4). A qualitative understanding of leafy spurge spectra, and those became the eight Regions Of Interest (ROI), >150 pixels, leafy spurge training sets (O'Neill, 2000). A mean spectrum of the eight sets was then used as an endmember for the SAM algorithm producing a one rule image for each endmember (O'Neill, 2000). SAM was applied to the original reflectance data and the PCA and MNF transformations. Only the MNF bands 3 through 17 of the combined rule image were used as input to the SAM algorithm to establish the threshold of capture for the leafy spurge of 500 digital numbers (DN) as the highest leafy spurge pixel in the image. This first classification was a conservative estimate of the distribution of leafy spurge in the park (O'Neill, 2000).

Tier 2: The second attempt of classification to identify more leafy spurge had a lower confidence because larger pixels were accepted as a match while masking all pixels with a DN of values ≥700 with a low pass 3x3 filter applied (O'Neill, 2000).

The upper and lower threshold values were then established. Then the georeferenced rule image was masked and re-thresholded in ENVI using the UTM projection, NAD83 datum, 17.5 m pixels, nearest neighbor interpolation, and triangulation warping parameters. The classification validation was performed in ESRI Arc/Info GIS along with the 1993 vector map of leafy spurge that was converted to raster with 17.5 m cells (O'Neill, 2000). The Tier 1 and Tier 2 classifications were exported from ENVI to Arc/Info. Twelve validation zones were identified and then the cells were counted for Tier 1 and Tier 2 classifications, along with ground truth (O'Neill, 2000). Then the ratios of classification to ground truth cell counts were calculated for each validation zone (O'Neill, 2000). The GER field spectra was not used in the image analysis, but did help establish other plants similar to leafy spurge and that remote sensing can detect leafy spurge with the right conditions (O'Neill, 2000). Other multispectral transformations were tested: NDVI, NVI, and the slope across the chlorophyll region. None of these methods were noteworthy (O'Neill, 2000). After comparison of the 1993 map of TRNP, the ground truth, and the AVIRIS data, the spatial registration errors in both the AVIRIS data and the vector map could not support a more detailed accuracy assessment (O'Neill, 2000). In 2001, the study of the leafy spurge infestation in TRNP continued with NASA's EO-1 Hyperion, AVIRIS (2001) hyperspectral data, and AVIRIS (1999) data from the prior article (Root, 2002). The prior study classifications and SAM algorithm from O'Neill, 2000 were applied to the new data sets (Root, 2002). The results supported that the different platforms and classification types could separate leafy spurge from similar vegetation types, but the calculation of red edge spectral parameters from the hyperspectral data is more responsive to foliar chlorophyll pigment levels and compares well with the other classification methods (Root, 2002).

In a more recent article, "Advancements in satellite remote sensing for mapping and monitoring of alien invasive plant species (AIPs)" in 2019, authors agreed with the abilities of hyperspectral sensors quality in differentiating plant spectral variations to better identify and map invasive plant species with satellites like AVIRIS and EO-1 Hyperion that have better spectral resolution (Royimani, 2019). They also supported classification algorithms like RF, SVM, ANN and vegetation indices that have improved the capabilities of hyperspectral data in the detection and mapping (Royimani, 2019). The downside of hyperspectral data is that it is not a long-term or fix-all solution that can be costly (Royimani, 2019). The ability to fuse the hyperspectral data with some multispectral sensors like Landsat ETM and SPOT-4 could improve the accuracy of detection, especially with new and improved multi-sensors like Sentinel-2 and more advanced algorithms that might be attainable in more remote and larger areas of interest. (Royimani, 2019).

Another study from 2005 supported the use of HyMap (126 bands between 0.45 μm and 2.5 μm with a pixel size of 3.5 m and bandwidths ranging from 15 μm in the visible and near infrared to 20 μm in the shortwave infrared) hyperspectral imagery that was classified with a Mixture Tuned Matched Filtering (MTMF) algorithm to detect small infestations in southeastern Idaho (Glenn, 2005). They used a Trimble GeoXT unit for correct GPS locations and an Analytical Spectra Device spectroradiometer for the spectral plant data (Glenn, 2005). The imagery used was non-georeferenced mosaicked imagery from 2002 and 2003, and then processed using Environment for Visualizing Images (ENVI) (Glenn, 2005). The MNF transformed reflectance data was classified using the MTMF algorithm (Glenn, 2005). The accuracy of the hyperspectral sensors in detecting leafy spurge was 70% producer's accuracy and 84% user's accuracy, even for small infestations in a riparian or steppe environment. Methods were considered repeatable if the leafy spurge cover was over 40% per 3.5 pixel (Glenn, 2005).

With the technological improvements over time, the multispectral satellite imagery has improved. In 2019, there was a study that mapped leafy spurge in northwestern Colorado along the Yampa River and up into the highlands surrounding (Mattilio, 2023). Multispectral imagery from SPOT-7 was obtained, along with ground truth mapping of the infestation, land cover data, canopy cover, and vegetation types in the region (Mattilio, 2023). These data were brought into ESRI Desktop ArcMap (Mattilio, 2023). RF was used for classification in Program R, producing a binary classification with a probabilistic scale from 0 to 1 (Mattilio, 2023). These were: "leafy spurge (1)" and "not leafy spurge (0)" classes (Mattilio, 2023). The accuracy assessment of the RF classification had an overall accuracy of 90.7% (Mattilio, 2023). Authors recommended the use of multispectral imagery with a larger NIR band for greater vegetative spectral detail (Mattilio, 2023).

Wild Parsnip (*Pastinaca sativa*)

Identifying wild parsnip has been challenging due to the small size and common yellow colored flower. Not many studies have focused on identification of wild parsnip with remote sensing. However, in 2016, a study at Lemoine Point Conservation Area in Kingston, Ontario used ultra-high resolution (UHR) images, taken on July 27, 2016, from a UAV were shown to provide enough detail for locating smaller outcrops of wild parsnip (Liu et al., 2021). In this study, it was noted that infrared bands, along with the RGB bands, would improve the ability of identification (Liu et al., 2021). Processing (see Fig. 16) started with ortho-rectification of the images, then creating DSMs and DTMs and mosaicking the images (Liu et al., 2021). Both object- and pixel-based classification methods were performed using classifiers like SVM, RF, and maximum likelihood with RGB imagery, then using RGB, texture features, and vegetation indices as input variables (Liu et al., 2021). These extra datasets compensated for the lack of infrared bands (Liu et al., 2021).

Canopy Height Model (CHM) representations were then used to filter out the taller vegetation (trees, bushes, etc.) from the DSM and used as a mask for the classification (Liu et al., 2021).

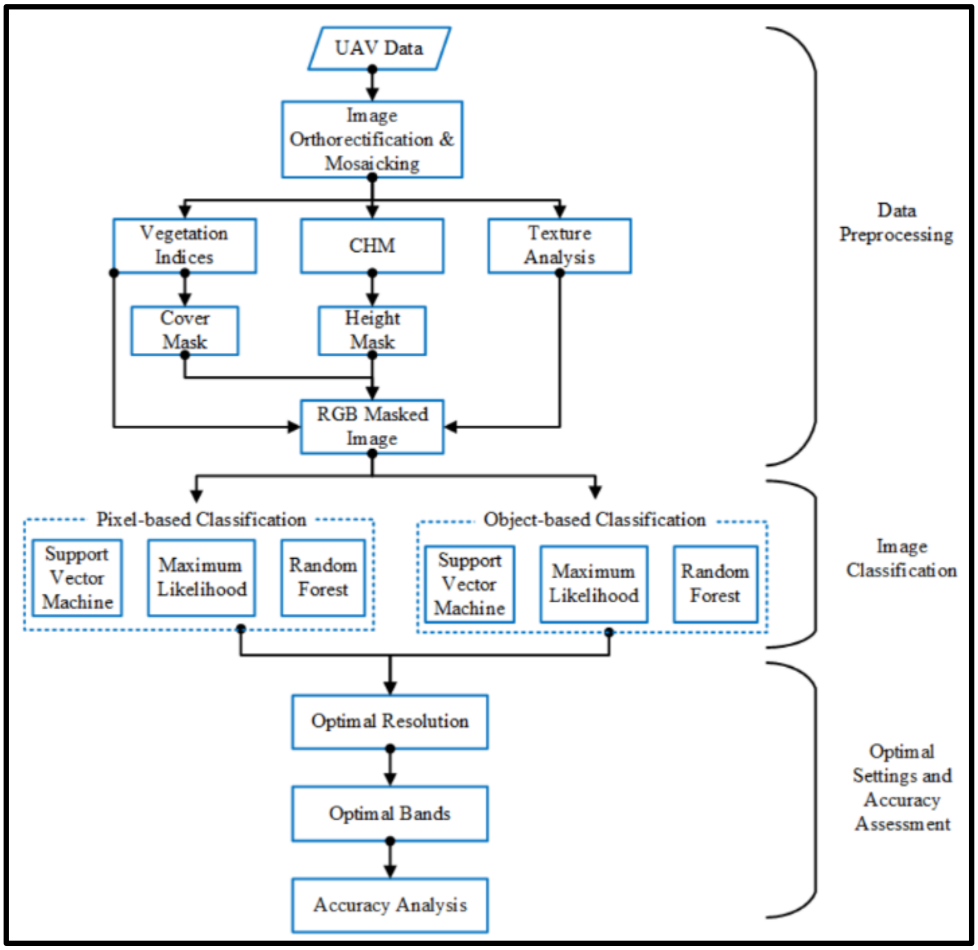

Figure 16: Workflow of distinguishing wild parsnip (Liu et al., 2021).

Three vegetation indices were tested to identify wild parsnip from other vegetation: Normalized Green-Blue Difference Index (NGBDI), Excess Green (EXG), and Vegetation (VEG), which were calculated using ENVI 5.2 software (Liu et al., 2021). The EXG showed a higher value for wild parsnip in the higher resolution, but the NGBDI had the most significant difference when the resolution became lower (Liu et al., 2021). The texture features mean, variance, and entropy based on a 3x3 window size were added as ancillary bands and were best for identifying wild parsnip from other vegetation (Liu et al., 2021). The object-based classification provided a higher overall accuracy of 95.2% with a SVM classifier compared to the pixel-based method of 86.45% that had shorter processing time (Liu et al., 2021). The input variables of EXG and mean worked best with the lower resolution (lower than 0.03 meters), while NGBDI and EXG worked best with the higher resolutions (larger than 0.03 meters). In conclusion, the study found that the workflow of masking out large vegetation and using the object-based SVM classifier with 0.02-meter resolution RGB imagery worked the best for classifying wild parsnip as long as other small, yellow colored flowers were not in the area of interest.

Conclusions

With how destructive and hazardous invasive species can be on the natural environment there has been great interest in mapping the extent of their spread. A variety of remote sensing methods have been developed for this purpose ranging in complexity and ease of implementation. Satellite imagery offers the ability to map large areas on the scale of an entire state with freely available platforms like Landsat and Sentinel. The disadvantage to these platforms is a lower spatial resolution, which typically makes at least freely available satellite imagery such as Landsat and Sentinel most appropriate for mapping larger patches. Commercial satellites such as WorldView and Planetscope offer greater spatial resolution to map smaller patches of invasive plants, but they can be cost prohibitive depending on the scale of the areas to be mapped, and frequency of needed imagery. Satellite imagery has been shown to be able to accurately map Phragmites and Japanese Knotweed over areas as large as the Great Lakes Basin. This could be useful to map the extent and spread of large patches of these species along freeway corridors within Michigan.

UAS (drone) platforms offer the greatest utility in their ability to collect imagery on demand and with a spatial resolution which can aid in the identification of individual plants (depending on flight altitude and camera specifications). This does come at the tradeoff of being able to map limited areas in a typical field day of deployment. Drones are best suited for mapping specific segmentation along a road corridor or other areas on the scale of less than 100 acres (40ha) down to patches as small as ¼ acre (0.1 ha). The literature shows that UAS have been used to map all four target species with high accuracy. There is a wide variety of drones available, with both integrated RGB and multispectral cameras. Larger drones offer the ability to mount custom sensors such as larger high resolution DSLR (Nikon D850 for example) type cameras, multispectral cameras (Micasense RedEdge-MX or RedEdge-P), and even hyperspectral systems (Headwall Nano-HP VNIR and SWIR). Smaller drones provide flexibility in deployment and can come with four-band multispectral cameras or be mounted with them. Changing federal and state rules may affect which UAS can be deployed for vegetation mapping in the future.

Image classification can be performed in a variety of ways through the use of software such as ArcGIS, ERDAS, eCognition, R, and many others. Object oriented classification tends to have better results than pixel based methods, but requires special software and more computational resources. Advances in machine learning techniques such as Random Forest, SVM, and XGBoost offer alternatives which have shown to be more accurate than traditional software packages in some situations. A mix of capabilities will allow for greater versatility for classification with different remote sensing sources and environmental conditions.

For the implementation of invasive species mapping methods, it can be advantageous to select more than one remote sensing source and analysis method for a species. This enables a customized approach based on the size of the area to be mapped and the size and density expected of the species in a region. This project will use the literature review to guide implementation of remote sensing methods for practical use by MDOT to identify and monitor priority invasive plants in their ROW.

Acronyms

ANN - Artificial Neural Network

AVIRIS - Airborne Visible / Infrared Imaging Spectrometer

CASI - Compact Airborne Spectrographic Imager

CHM - Canopy Height Model

CMOS - Complementary Metal-Oxide Semiconductor

DEM - Digital Elevation Model

DSM - Digital Surface Model

DTM - Digital Terrain Model

ESA - European Space Agency

ETM - Enhanced Thematic Mapper

EVI - Enhanced Vegetation Index

GIS - Geographic Information Systems

GSD - Ground Sample Distance

JAXA - Japan Aerospace Exploration Agency

kNN - k-Nearest Neighbors

LiDAR - Light Detection and Ranging

MISGP - Michigan Invasive Species Grant Program

MISIN - Midwest Invasive Species Network

ML - Machine Learning

MLC - Maximum Likelihood Classifier

MP (or mp) - Megapixels

MTU - Michigan Technological University

MTRI - Michigan Tech Research Institute

NAIP - National Agriculture Imagery Program

NASA - National Aeronautics and Space Administration

NIR - Near Infrared

NDVI - Normalized Difference Vegetation Index

NDWI - Normalized Difference Water Index

NN - Neural Network

OBIA - Object-Based Image Analysis

PC or PCA - Principal Component (Analysis)

RGB - Red, Green, Blue

RF - Random Forest

ROW - Right-Of-Way

RPAS - Remotely Piloted Aircraft Systems

SAR - Synthetic Aperture Radar

SEMCOG - Southeastern Michigan Council of Governments

SPOT - Satellite Pour l'Observation de la Terre

SVM - Support Vector Machine

SWIR - Shortwave Infrared

UAS - Uncrewed Aerial Systems

UAV - Uninhabited Airborne Vehicle

VARI - Visible Atmospherically Resistant Index

VNIR - Visible and Near Infrared

Bibliography

Abeysinghe, Tharindu, Anita Simic Milas, Kristin Arend, Breann Hohman, Patrick Reil, Andrew Gregory, and Angélica Vázquez-Ortega. "Mapping Invasive Phragmites Australis in the Old Woman Creek Estuary Using UAV Remote Sensing and Machine Learning Classifiers." Remote Sensing 11, no. 11 (June 10, 2019): 1380. https://doi.org/10.3390/rs11111380.

Adachi, N., Terashima, I. and Takahashi, M. 1996a. Central die-back of monoclonal stands of Reynoutria japonica in an early stage of primary succession on Mt. Fuji. Ann. Bot. (Lond.) 77: 477–486.

Aguilera, A.G., Alpert, P., Dukes, J.S. (2009). Impacts of the invasive plant Fallopia

japonica (Houtt.) on plant communities and ecosystem processes. Biological Invasions.

12, 1243–1252

Ahern, F.J., Brisco, B., Battaglia, M.J., Bourgeau-Chavez, L.L., Atwood, D., & Murnaghan, K.P. (2022). SAR Polarimetric Phase Differences in Wetlands: Information and

Mis-Information. Canadian Journal of Remote Sensing, 48, 703 - 721

Alley, H. P. and C. G. Messersmith. (1985). Chemical control of leafy spurge, pp. 65-78. In Watson, A.K. (ed.). Leafy Spurge. Monograph No. 3, Weed Science Society of America, Champaign, Illinois, USA.

Baatz, M., Benz, U., Dehghani, S., Heynen, M., Höltje, A., Hofmann, P., Lingenfelder, I., Mimler, M., Sohlbach, M., Weber, M., & Willhauck, G. (2004). eCognition Elements 4.0 User Guide. Definiens Imaging, Munich, 22(3), 14-27. https://www.irfanakar.com/GIS_Remote_Sensing_files/eCognition%20Definiens/Elementd%204.0%20User%20Guide.pdf

Bailey, J.P., Conolly, A.P. (2000). Prize-winners to pariahs -- a history of Japanese

knotweed s.l. (Polygonaceae) in the British Isles. Watsonia. 23, 93–110.

Baranová, B. (2021). On the occurrence of the wild parsnip (Pastinaca sativa L.) within the Prešov city urban greenery. *Biodiversity & Environment*, *13*(2), 36–40.

Barney, J. N., (2006). North American history of two invasive plant species:

photogeographic distribution, dispersal vectors, and multiple introductions. Biological

Invasions. 8, 703-717.

Barney, J.N., Tharayil, N., DiTommaso, A., Bhowmik, P.C. The biology of invasive alien plants in Canada. 5. Polygonum cuspidatum Sieb. & Zucc. [= Fallopia japonica (Houtt.) Ronse Decr.]. Can. J. Plant Sci. (2006), 86, 887–905.

Baskin, J. M. and C. M. Baskin. (1979). Studies on the autecology and population biology of the weedy monocarpic perennial, Pastinaca sativa. J.Ecol. 67:601–610.

Bastani, Favyen. (2024). Satlas: Open AI-Generated Geospatial Data. https://github.com/allenai/satlas

Battaglia, Michael J., Sarah Banks, Amir Behnamian, Laura Bourgeau-Chavez, Brian Brisco, Jennifer Corcoran, Zhaohua Chen, et al. “Multi-Source EO for Dynamic Wetland Mapping and Monitoring in the Great Lakes Basin.” Remote Sensing 13, no. 4 (February 8, 2021): 599. https://doi.org/10.3390/rs13040599.

Beaury, Evelyn M., Catherine S. Jarnevich, Ian Pearse, Annette E. Evans, Nathan Teich, Peder Engelstad, Jillian LaRoe, and Bethany A. Bradley. “Modeling Habitat Suitability across Different Levels of Invasive Plant Abundance.” Biological Invasions 25, no. 11 (November 2023): 3471–83. https://doi.org/10.1007/s10530-023-03118-z.

Beerling, D. J. (1991). The testing of cellular concrete revetment blocks resistant to growths of Reynoutria japonica Houtt.(Japanese knotweed). Water Res. Ox. 25: 495–498.

Beerling, D.J., Huntley, B., Bailey, J.P. (1995). Climate and the distribution of Fallopia japonica: use of an introduced species to test the predictive capacity of response surfaces. Journal of Vegetation Science. 6: 269-282.

Blaschke, T. (2010). Object based image analysis for remote sensing. ISPRS Journal of Photogrammetry and Remote Sensing. Volume 65, Issue 1, Pages 2-16. ISSN 0924-2716, https://doi.org/10.1016/j.isprsjprs.2009.06.004.

Bourgeau-Chavez et al. 2013) - Bourgeau-Chavez L, Kowalski KP, Carlson Mazur ML, Scarbrough KA, Powell RB, Brooks CN et al (2013) Mapping invasive *Phragmites australis* in the coastal Great Lakes with ALOS PALSAR satellite imagery for decision support. J Gt Lakes Res 39:65–77

Bourgeau-Chavez, Laura, Sarah Endres, Michael Battaglia, Mary Miller, Elizabeth Banda, Zachary Laubach, Phyllis Higman, Pat Chow-Fraser, and James Marcaccio. “Development of a Bi-National Great Lakes Coastal Wetland and Land Use Map Using Three-Season PALSAR and Landsat Imagery.” Remote Sensing 7, no. 7 (July 9, 2015): 8655–82. https://doi.org/10.3390/rs70708655.

Bourgeau-Chavez, Laura L., Kurt P. Kowalski, Martha L. Carlson Mazur, Kirk A. Scarbrough, Richard B. Powell, Colin N. Brooks, Brian Huberty, Liza K. Jenkins, Elizabeth C. Banda, David M. Galbraith, Zachary M. Laubach, Kevin Riordan. “Mapping Invasive Phragmites Australis in the Coastal Great Lakes with ALOS PALSAR Satellite Imagery for Decision Support.” Journal of Great Lakes Research 39 (2013): 65–77. https://doi.org/10.1016/j.jglr.2012.11.001.

Bradley, Bethany A. “Remote Detection of Invasive Plants: A Review of Spectral, Textural and Phenological Approaches.” Biological Invasions 16, no. 7 (July 2014): 1411–25. https://doi.org/10.1007/s10530-013-0578-9.

Braun HA, Kowalski KP, Hollins K (2016) Applying the collective impact approach to address non-native species: a case study of the Great Lakes Phragmites Collaborative. Biol Invasions. doi:10.1007/s10530-016-1142-1

Brooks, Colin, Laura Bourgeau-Chavez, Eleanor Serocki, Amanda Grimm, and Sarah Endres. “Implementing Practical Field and Remote Sensing Methods to Inform Adaptive Management of Non-Native Phragmites Australis in the Midwest.” MTU, December (2015). chrome-extension://efaidnbmnnnibpcajpcglclefindmkaj/https://www.mtu.edu/mtri/research/project-areas/environmental/wetlands/treatment-phragmites/adaptive-management-report.pdf.

Brooks, Colin, Amanda Grimm, Amy M. Marcarelli, Nicholas P. Marion, Robert Shuchman, and Michael Sayers. “Classification of Eurasian Watermilfoil (Myriophyllum Spicatum) Using Drone-Enabled Multispectral Imagery Analysis.” Remote Sensing 14, no. 10 (May 12, 2022): 2336. https://doi.org/10.3390/rs14102336.

Brooks, Colin N., Amanda G. Grimm, Amy M. Marcarelli, and Richard J. Dobson. “Multiscale Collection and Analysis of Submerged Aquatic Vegetation Spectral Profiles for Eurasian Watermilfoil Detection.” Journal of Applied Remote Sensing 13, no. 03 (August 27, 2019): 1. https://doi.org/10.1117/1.JRS.13.037501.

Brooks, Colin, Charlotte Weinstein, Andrew Poley, Amanda Grimm, Nicholas Marion, Laura Bourgeau-Chavez, Dana Hansen, and Kurt Kowalski. “Using Uncrewed Aerial Vehicles for Identifying the Extent of Invasive Phragmites Australis in Treatment Areas Enrolled in an Adaptive Management Program.” Remote Sensing 13, no. 10 (May 12, 2021): 1895. https://doi.org/10.3390/rs13101895.

Bzdęga, Katarzyna, Adrian Zarychta, Alina Urbisz, Sylwia Szporak-Wasilewska, Michał Ludynia, Barbara Fojcik, and Barbara Tokarska-Guzik. “Geostatistical Models with the Use of Hyperspectral Data and Seasonal Variation – A New Approach for Evaluating the Risk Posed by Invasive Plants.” Ecological Indicators 121 (February 2021): 107204. https://doi.org/10.1016/j.ecolind.2020.107204.

Campbell, James B., Wynne, Randolph H. 2011. Introduction to Remote Sensing: Fifth Edition. Ch.12: Image Classification (pp. 339-347). The Guilford Press. ISBN 978-1-60918-176-5

Chowdhury, Md. Sharafat. “Comparison of Accuracy and Reliability of Random Forest, Support Vector Machine, Artificial Neural Network and Maximum Likelihood Method in Land Use/Cover Classification of Urban Setting.” Environmental Challenges 14 (January 2024): 100800. https://doi.org/10.1016/j.envc.2023.100800.

Congalton, R., Green, K. (2019). “Assessing the Accuracy of Remotely Sensed Data Principles and Practices”, Third Edition. Taylor and Francis Group. ISBN 978-1-4987-7666-0

Cornell University. (2017). *Wild Parsnip*. Cornell Weed Identification, Agricultural Weed ID for New York State. https://blogs.cornell.edu/weedid/wild-parsnip/

Croizat, L. (1945). “Euphorbia Esula” in North America. *The American Midland Naturalist*, *33*(1), 231–243. https://doi.org/10.2307/2421329

De Castro, Ana, Jorge Torres-Sánchez, Jose Peña, Francisco Jiménez-Brenes, Ovidiu Csillik, and Francisca López-Granados. “An Automatic Random Forest-OBIA Algorithm for Early Weed Mapping between and within Crop Rows Using UAV Imagery.” Remote Sensing 10, no. 3 (February 12, 2018): 285. https://doi.org/10.3390/rs10020285.

Dunn, P. H. (1979). The Distribution of Leafy Spurge (Euphorbia esula) and Other Weedy Euphorbia spp. in the United States. *Weed Science*, *27*(5), 509–516. https://doi.org/10.1017/S0043174500044507

"Environment, Great Lakes, and Energy (EGLE) - Water Resources, Wetlands, Phragmites," n.d. https://www.michigan.gov/egle/about/organization/Water-Resources/Wetlands/phragmites.

European Space Agency. (2022, December 6). SPOT Overview. Earth Online. https://earth.esa.int/eogateway/missions/spot/description

Feng, Quanlong, Jiantao Liu, and Jianhua Gong. "UAV Remote Sensing for Urban Vegetation Mapping Using Random Forest and Texture Analysis." Remote Sensing 7, no. 1 (January 19, 2015): 1074–94. https://doi.org/10.3390/rs70101074.

Gholizadeh, Hamed, Michael S. Friedman, Nicholas A. McMillan, William M. Hammond, Kianoosh Hassani, Aisha V. Sams, Makyla D. Charles, et al. "Mapping Invasive Alien Species in Grassland Ecosystems Using Airborne Imaging Spectroscopy and Remotely Observable Vegetation Functional Traits." Remote Sensing of Environment 271 (March 2022): 112887. https://doi.org/10.1016/j.rse.2022.112887.

Glenn, Nancy F., Jacob T. Mundt, Keith T. Weber, Timothy S. Prather, Lawrence W. Lass, and Jeffrey Pettingill. "Hyperspectral Data Processing for Repeat Detection of Small Infestations of Leafy Spurge." Remote Sensing of Environment 95, no. 3 (2005): 399–412. https://doi.org/10.1016/j.rse.2005.01.003.

Hay, G.J., Castilla, G. 2006. Object-Based Image Analysis: Strengths, Weaknesses, Opportunities and Threats. The International Archives of the Photogrammetry, Remote Sensing and Spatial Information Sciences. Commission VI, WG VI/4.

Hanson, H. C. and Rudd, V. E. 1933. Leafy spurge, Life history and habits. N. D. Agric. Exp. Stn. Fargo, Bull. 266, 24 pp.

Herben, T. (2004). Physiological integration affects growth form and competitive ability

in clonal plants. Evolutionary Ecology. 18, 493–520.

Holroyd, Pablo J. Zarco-Tejada and R. Root and S. L. Ustin and C. Pinilla and Raymond Kokaly and G. Anderson and K. Brown and K. Dudek and S. Hager and E. Comparison of AVIRIS and EO-1 Hyperion for Classification and Mapping of Invasive Leafy Spurge in Theodore Roosevelt National, 2002.

Huang, Cho-ying, and Gregory Asner. "Applications of Remote Sensing to Alien Invasive Plant Studies." Sensors 9, no. 6 (June 19, 2009): 4869–89. https://doi.org/10.3390/s90604869.

Huylenbroeck, Leo, Marianne Laslier, Simon Dufour, Blandine Georges, Philippe Lejeune, and Adrien Michez. "Using Remote Sensing to Characterize Riparian Vegetation: A Review of Available Tools and Perspectives for Managers." Journal of Environmental Management 267 (August 2020): 110652. https://doi.org/10.1016/j.jenvman.2020.110652.

Japanese knotweed – Fallopia japonica - Plant & Pest Diagnostics. Plant & Pest Diagnostics. https://www.canr.msu.edu/resources/japanese-knotweed-fallopia-japonica

Jones, Daniel, Stephen Pike, Malcolm Thomas, and Denis Murphy. "Object-Based Image Analysis for Detection of Japanese Knotweed s.l. Taxa (Polygonaceae) in Wales (UK)." Remote Sensing 3, no. 2 (February 16, 2011): 319–42. https://doi.org/10.3390/rs3020319.

Jorgensen, Niels, and Mark Renz. "Assessing the Performance and Accuracy of Invasive Plant Habitat Suitability Models in Detecting New Observations in Wisconsin." Invasive Plant Science and Management 14, no. 4 (December 2021): 214–22. https://doi.org/10.1017/inp.2021.27.

Kennay, J., Fell, G., & Edgin, B. (2017). Vegetation Management Guideline Wild Parsnip (Pastinaca sativa L.). Illinois Nature Preserves Commission. Vol. 1, No. 26 https://dnr.illinois.gov/content/dam/soi/en/web/dnr/inpc/documents/vmg/vmg-26-wild-parsnip-revised-2017.pdf

Landsat NASA. (2024, April 4). LandsAt 7 | Landsat Science. Landsat Science | a Joint NASA/USGS Earth Observation Program. https://landsat.gsfc.nasa.gov/satellites/landsat-7/

Landsat NASA. (2023, January 12). LandsAt 8 | Landsat Science. Landsat Science | a Joint NASA/USGS Earth Observation Program. https://landsat.gsfc.nasa.gov/satellites/landsat-8/

Lantz, Nicholas J., and Jinfei Wang. "Object-Based Classification of Worldview-2 Imagery for Mapping Invasive Common Reed, Phragmites Australis." Canadian Journal of Remote Sensing 39, no. 4 (October 30, 2013): 328–40. https://doi.org/10.5589/m13-041.

Leafy Spurge | Minnesota Department of Agriculture. https://www.mda.state.mn.us/plants/pestmanagement/weedcontrol/noxiouslist/leafyspurge

Lillesand, T.M., Kiefer, R.W. (1994). Remote Sensing and Image Interpretation: Third Edition.Ch.7: Digital Image Processing - Unsupervised Classification (pp. 604-608). John Wiley & Sons. ISBN 0-471-57783-9.

Liu, D., & Xia, F. (2010). Assessing object-based classification: advantages and limitations. Remote Sensing Letters, 1(4), 187–194. https://doi.org/10.1080/01431161003743173

Liu, J., M. D. Hossain, and D. Chen. "A PROCEDURE FOR IDENTIFYING INVASIVE WILD PARSNIP PLANTS BASED ON VISIBLE BANDS FROM UAV IMAGES." The International Archives of the Photogrammetry, Remote Sensing and Spatial Information Sciences XLIII-B1-2021 (June 28, 2021): 173–81. https://doi.org/10.5194/isprs-archives-XLIII-B1-2021-173-2021.

Lowe, S. M., Browne, S. B., de Poorter, M. (2001). 100 of the World's Worst Invasive

Alien Species, a selection from the Global Invasive Species Database. IUCN-ISSG,

Auckland, New Zealand.

Martin, François-Marie, Jana Müllerová, Laurent Borgniet, Fanny Dommanget, Vincent Breton, and André Evette. "Using Single- and Multi-Date UAV and Satellite Imagery to Accurately Monitor Invasive Knotweed Species." Remote Sensing 10, no. 10 (October 20, 2018): 1662. https://doi.org/10.3390/rs10101662.

Martin, F.-M., Müllerová, J., Borgniet, L., Dommanget, F., Breton, V., & Evette, A. (2018). Using Single- and Multi-Date UAV and Satellite Imagery to Accurately Monitor Invasive Knotweed Species. Remote Sensing, 10(10), 1662. https://doi.org/10.3390/rs10101662

Martinson, K., Hovda, L., & Murphy, M. (2021). *Wild parsnip: problem plant in hay and pastures*. University of Minnesota Extension. https://extension.umn.edu/horse-pastures-and-facilities/wild-parsnip

Mattilio, Chloe M., Daniel R. Tekiela, and Urszula Norton. "Remote Mapping of Leafy Spurge (Euphorbia Esula, L.) in Northwestern Colorado." Frontiers in Remote Sensing 4 (January 18, 2023): 1086085. https://doi.org/10.3389/frsen.2023.1086085.

Michez, Adrien, Hervé Piégay, Lisein Jonathan, Hugues Claessens, and Philippe Lejeune. "Mapping of Riparian Invasive Species with Supervised Classification of Unmanned Aerial System (UAS) Imagery." International Journal of Applied Earth Observation and Geoinformation 44 (February 2016): 88–94. https://doi.org/10.1016/j.jag.2015.06.014.

Michigan Coastal Zone Management Program, Office of the Great Lakes, Department of Environmental Quality, National Coastal Zone Management Program, National Oceanic and Atmospheric Administration, & U.S. Department of Commerce. (2014). A guide to the control and management of Invasive phragmites. https://www.michigan.gov/-/media/Project/Websites/invasives/Documents/Response/Status/egle-ais-guide-phragmites.pdf?rev=99773b1ab927407ba5cd7e4532a3ad4d

MISIN - Midwest Invasive Species Information Network (2016). *Leafy spurge (Euphorbia virgata)*. Published by Michigan State University. Accessed through: https://www.misin.msu.edu/facts/detail/?project=misin&id=27

Michigan Department of Agriculture and Rural Development, Michigan Department of Environmental Quality, Michigan Department of Natural Resources, & Michigan Department of Transportation. (2017). Michigan's Terrestrial Invasive Species State Management Plan [Report]. https://www.michigan.gov/-/media/Project/Websites/dnr/Documents/PublicLands/Terrestrial_invasivesp_plan.pdf?rev=5c725bbe55844139b67655df722ed18c#:~:text=Michigan's%20Terrestrial%20Invasive%20Species%20State%20Management%20Plan%20provides%20a%20strategy,often%20have%20irreversible%20ecological%20effects.

Moola, F.M., Vasseur, L. (2009). The importance of clonal growth to the recovery of Gaultheria procumbens L., (Ericaceae) after forest disturbance. Plant Ecology. 201, 319–337.

Morimoto, J., Ponton, F. (2021) Virtual reality in biology: could we become virtual naturalists? Evolution: Educ Outreach 14(1):7

Müllerová, Jana, Giuseppe Brundu, André Große-Stoltenberg, Teja Kattenborn, and David M. Richardson. “Pattern to Process, Research to Practice: Remote Sensing of Plant Invasions.” Biological Invasions 25, no. 12 (December 2023): 3651–76. https://doi.org/10.1007/s10530-023-03150-z.

Nasa, E. S. D. S. (2024, January 5). PALSAR | EarthData. Earthdata. https://www.earthdata.nasa.gov/sensors/palsar

Nex, F., Armenakis, C., Cramer, M., Cucci, D.A., Gerke, M., et al. (2022). UAV in the advent of the twenties: Where we stand and what is next. ISPRS Journal of Photogrammetry and Remote Sensing. Vol 184 (pp. 215-242), ISSN 0924-2716. https://doi.org/10.1016/j.isprsjprs.2021.12.006.

Noxious Weed Program, Minnesota Department of Agriculture. (2018). Leafy spurge. https://www.mda.state.mn.us/plants/pestmanagement/weedcontrol/noxiouslist/leafyspurge

Oborny, B., Kun, A., Czaran, T., Bokros, S. (2000). The effect of clonal integration on

plant competition for mosaic habitat space. Ecology. 81(12), 3291-3304.

Olson, Charles. (1960). Elements of Photographic Interpretation Common to Several Sensors. Photogrammetric Engineering.

O’Neill, Michael, Susan Ustin, Steve Hager, and Ralph Root. “Mapping The Distribution of Leafy Spurge at Theodore Roosevelt National Park Using Aviris.” NASA, n.d. chrome-extension://efaidnbmnnnibpcajpcglclefindmkaj/https://aviris.jpl.nasa.gov/proceedings/workshops/00_docs/ONeill_web.pdf.

Papp, Levente, Boudewijn Van Leeuwen, Péter Szilassi, Zalán Tobak, József Szatmári, Mátyás Árvai, János Mészáros, and László Pásztor. “Monitoring Invasive Plant Species Using Hyperspectral Remote Sensing Data.” Land 10, no. 1 (January 1, 2021): 29. https://doi.org/10.3390/land10010029.

Parece, T.E., McGee III, J.A. 2023. Remote Sensing with ArcGIS Pro, Second Edition. VirginiaView. ISBN: 9798854833301

Pengra, B., Johnston, C.A., Loveland, T. (2007). Mapping an invasive plant, Phragmites australis, in coastal wetlands using the EO-1 Hyperion hyperspectral sensor. Elsevier. Remote Sensing of Environment. Vol. 108, Issue 1, pp. 74-81. https://doi.org/10.1016/j.rse.2006.11.002

Qian, Wanqiang, Yiqi Huang, Qi Liu, Wei Fan, Zhongyu Sun, Hui Dong, Fanghao Wan, and Xi Qiao. “UAV and a Deep Convolutional Neural Network for Monitoring Invasive Alien Plants in the Wild.”

Computers and Electronics in Agriculture 174 (July 2020): 105519. https://doi.org/10.1016/j.compag.2020.105519.

Rajah, Perushan, John Odindi, Onisimo Mutanga, and Zolo Kiala. “The Utility of Sentinel-2 Vegetation Indices (VIs) and Sentinel-1 Synthetic Aperture Radar (SAR) for Invasive Alien Species Detection and Mapping.” Nature Conservation 35 (June 14, 2019): 41–61. https://doi.org/10.3897/natureconservation.35.29588.

Raczko, E., & Zagajewski, B. (2017). Comparison of support vector machine, random forest and neural network classifiers for tree species classification on airborne hyperspectral APEX images. European Journal of Remote Sensing, 50(1), 144–154. https://doi.org/10.1080/22797254.2017.1299557

Richards, John, Xuiping, Jia. (2005). The Interpretation of Digital Image Data. Fourth Edition, Remote Sensing Digital Image Analysis - An Introduction (Ch. 3, pp. 67-75). Springer. ISBN: 3540251286

Richards, C.L., Schrey, A.W., Pigliucci, M. (2012). Invasion of diverse habitats by few Japanese knotweed genotypes are correlated with epigenetic differentiation. Ecology Letters. 15:1016–1025.

Royimani, Lwando, Onisimo Mutanga, John Odindi, Timothy Dube, and Trylee Nyasha Matongera. “Advancements in Satellite Remote Sensing for Mapping and Monitoring of Alien Invasive Plant Species (AIPs).” Physics and Chemistry of the Earth, Parts A/B/C 112 (2019): 237–45. https://doi.org/10.1016/j.pce.2018.12.004.

Rupasinghe, Prabha Amali, and Patricia Chow-Fraser. “Mapping Phragmites Cover Using WorldView 2/3 and Sentinel 2 Images at Lake Erie Wetlands, Canada.” Biological Invasions 23, no. 4 (April 2021): 1231–47. https://doi.org/10.1007/s10530-020-02432-0.

Sabat-Tomala, Anita, Edwin Raczko, and Bogdan Zagajewski. “Mapping Invasive Plant Species with Hyperspectral Data Based on Iterative Accuracy Assessment Techniques.” Remote Sensing 14, no. 1 (December 23, 2021): 64. https://doi.org/10.3390/rs14010064.

Saltonstall, K., & Meyerson, L. A. (2016). Phragmites australis: From genes to ecosystems. *Biological Invasions*, *18*(9), 2415–2420. https://doi.org/10.1007/s10530-016-1240-0

Samiappan, Sathishkumar, Gray Turnage, Lee Hathcock, Luan Casagrande, Preston Stinson, and Robert Moorhead. “Using Unmanned Aerial Vehicles for High-Resolution Remote Sensing to Map Invasive Phragmites Australis in Coastal Wetlands.” International Journal of Remote Sensing 38, no. 8–10 (May 19, 2017): 2199–2217. https://doi.org/10.1080/01431161.2016.1239288.

Shaw, R.H., Bryner, S., Tanner, R. (2009). The life history and host range of the Japanese knotweed psyllid, Aphalara itadori Shinji: potentially the first classical biological weed control agent for the European union. Biological Control. 49:105–113.

Smerdu, Ana, Urša Kanjir, and Žiga Kokalj. "Automatic Detection of Japanese Knotweed in Urban Areas from Aerial and Satellite Data." Management of Biological Invasions 11, no. 4 (2020): 661–76. https://doi.org/10.3391/mbi.2020.11.4.03.

Somers, Ben & Asner, Gregory. (2013). Invasive Species Mapping in Hawaiian Rainforests Using Multi-Temporal Hyperion Spaceborne Imaging Spectroscopy. Selected Topics in Applied Earth Observations and Remote Sensing, IEEE Journal of. 6. 351-359. 10.1109/JSTARS.2012.2203796.

State of Michigan. Invasive Species: Phragmites (common reed). Michigan Invasive Species. https://www.michigan.gov/invasives/id-report/plants/grass/phragmites-common-reed

Stegelmeier, B. L., Colegate, S. M., Knoppel, E. L., Rood, K. A., & Collett, M. G. (2019). Wild parsnip (Pastinaca sativa)-induced photosensitization. *Toxicon*, *167*, 60-66.

Swearingen, J. and K. Saltonstall. 2010. Phragmites Field Guide: Distinguishing Native and Exotic Forms of Common Reed (Phragmites australis) in the United States. Plant Conservation Alliance, Weeds Gone Wild. http://www.nps.gov/plants/alien/pubs/index.htm

Tan, PN., Steinbach, M., Kumar, V. (2021). Classification: Basic Concepts and Techniques. Second Edition, Introduction to Data Mining (Ch. 3, pp. 1-2). Pearson. ISBN: 0133128903.

Townsend, A. 1997. Japanese knotweed: A reputation lost. Arnoldia (Jam. Plain) 57: 13–19.

"The European Space Agency - Sentinel-2," n.d. https://www.esa.int/Applications/Observing_the_Earth/Copernicus/Sentinel-2.

U.S. Geological Survey | Landsat Enhanced Vegetation Index. n.d. https://www.usgs.gov/landsat-missions/landsat-enhanced-vegetation-index

U.S. Geological Survey | Landsat normalized difference Vegetation Index. n.d. https://www.usgs.gov/landsat-missions/landsat-normalized-difference-vegetation-index

Walling, A.L., Walling, H.W., (2018). Phytophotodermatitis induced by wild parsnip.

Dermatol. Online J. 24 (2)

Whiteside, Timothy G.,Boggs, Guy S.,Maier, Stefan W. (2011). Comparing object-based and pixel-based classifications for mapping savannas. International Journal of Applied Earth Observation and Geoinformation, Volume 13, Issue 6, Pages 884-893. ISSN 1569-8432. https://doi.org/10.1016/j.jag.2011.06.008.

Zagajewski, Bogdan, Marcin Kluczek, Edwin Raczko, Ajda Njegovec, Anca Dabija, and Marlena Kycko. “Comparison of Random Forest, Support Vector Machines, and Neural Networks for Post-Disaster Forest Species Mapping of the Krkonoše/Karkonosze Transboundary Biosphere Reserve.” Remote Sensing 13, no. 13 (July 1, 2021): 2581. https://doi.org/10.3390/rs13132581.

Zhang, Jiazhen, "Spatial Analysis of Distributions and Habitat Conditions of Fallopia japonica (Japanese Knotweed) Invasive Species Applying Unmanned Helicopter Remote Sensing" (2015). Great Lakes Center Masters Theses. 1.
https://digitalcommons.buffalostate.edu/greatlakes_theses/1

Zhu, Z., Wilder, M., Roy, D., Woodcock, C., Hansen, M., et al. (2019). Benefits of the free and open Landsat data policy. Remote Sensing of Environment. Vol. 224 (pp. 382-385). ISSN 0034-4257. https://doi.org/10.1016/j.rse.2019.02.016.